Invited review

The Renazzo-like carbonaceous chondrites as resources to understand the origin, evolution, and exploration of the Solar System

N. M. Abreu[a*], J. C. Aponte[2b,c], E. A. Cloutis[d], A. N. Nguyen[e]

[a]Earth Science, Pennsylvania State University – DuBois Campus, DuBois, PA, 15801, USA

[b]Solar System Exploration Division, Code 691, NASA Goddard Space Flight Center, Greenbelt, Maryland 20771, USA.

[c]Department of Chemistry, Catholic University of America, Washington, DC 20064, USA.

[d]Department of Geography, University of Winnipeg, 515 Portage Avenue, Winnipeg, MB R3B 2E9, Canada.

[e]Jacobs Engineering Group Inc., NASA Johnson Space Center, Houston, Texas 77058, USA

*Corresponding author.

E-mail address: abreu@psu.edu (N. M. Abreu).

ABSTRACT

We present here a review of the characteristics of CR carbonaceous chondrite meteorites. Over the past three decades, our knowledge and understanding of the scientific value of the CR chondrites have increased dramatically, as more samples from cold and hot deserts have become available for analysis. Based on a variety of compositional, mineralogical, isotopic, and spectroscopic studies, we have come to understand that CR chondrites are excellent samples of asteroidal meteorites to look for virtually unaltered solar nebula material and to observe asteroidal processes in progress. This paper summarizes these investigations, their similarities, and differences with other chondritic groups, their relationships to asteroids, and the questions yet to be addressed.

1. Introduction

Carbonaceous chondrites are undifferentiated meteorites. Their principal constituents, namely chondrules, Fe-Ni metal, sulfides, matrix material, and refractory inclusions, accreted from the solar nebula 4.56 billion years ago to form asteroids (e.g., Weisberg et al., 1993; Zolensky et al., 1993). Chondrules are millimeter-sized spherical silicate droplets. Between the chondrules, there is dark, fine-grained, silicate-rich, opaque-bearing assemblage. In addition to these materials, matrices contain dust particles that originated in the gaseous outflows or ejecta of dying stars, as well as a wide variety of organic materials.

Residence in asteroids modified the texture, composition, and mineralogy of chondritic components through aqueous alteration, thermal, and impact metamorphism. However, not all chondrite groups underwent the same level of processing while residing in their parent asteroids. The abundance and origin of alteration products are codified in the petrologic sequence (i.e., Van Schmus and Wood, 1967; Weisberg et al. 2006), in which chondrites that have not been affected by asteroidal processes are assigned type 3.0. Petrologic types 1–2 denote increasing replacements of solar nebula mineral and organic assemblages via aqueous alteration. Water, as a solvent and mass transport agent, is the primary source of low-temperature chemical alteration in some carbonaceous

chondrites. Secondary phases in carbonaceous chondrites formed by aqueous alteration include layered silicates (e.g., serpentine), sulfide-hydroxide (tochilinite), sulfates, oxides, carbonates, and hydroxides, which initially replace matrix materials and eventually affect coarser-grained components (e.g., Zolensky et al., 2018 and references therein). Increasing effects of thermal metamorphism are assigned increasing petrologic types 3-6. The consequences of thermal metamorphism are textural, compositional, and mineralogical homogenization and loss of volatiles.

The abundance variations and chemical compositions of presolar silicates can be used to infer the degree of processing on the parent body. While some presolar phases are resilient to secondary processing, presolar silicates are susceptible to alteration or destruction by radiation, shock, collisions in the interstellar medium (ISM), and by asteroidal processes (Bringa et al., 2007; Floss and Haenecour, 2016a; Jones and Nuth, 2011; Jones et al., 1994; Tielens et al., 1994; van Dishoeck, 2004). Parent body aqueous alteration can destroy presolar silicates, giving rise to abundance variations among chondrites. Other presolar phases, such as SiC and oxides, are not destroyed by aqueous alteration, and the abundance variations of these phases likely point to the heterogeneous distribution of presolar grains in the early solar nebula (Leitner et al., 2012a; Davidson et al., 2014a). Alternatively, these distributions may reflect destruction by significant thermal alteration. Thermal metamorphism can destroy presolar silicate grains and also alter their chemical compositions, particularly their Fe contents (Floss and Stadermann, 2012; Nguyen et al., 2016; Nguyen and Zinner, 2004).

CR chondrites, in particular, are comprised of abundant chondrules, small and few refractory inclusions, and a variety of fine-grained materials (e.g., Fig. 1). In average CRs, chondrules occupy ~64.6 area%, fine-grained materials ~35 area% (including matrix and dark inclusions), and refractory inclusions ~0.4 area% (Schrader et al., 2011). Fe-Ni metal grains are commonly associated with chondrules (e.g., Kong and Palme, 1999; Krot et al., 2002). These grains are more abundant than in other hydrated chondrites, which led investigators to group these meteorites with the admittedly much more metal-rich CB and the CH chondrites as part of the CR clan (e.g., Weisberg et al., 1995; Krot et al., 2002). These authors noted that, despite their petrologic differences, metal-rich carbonaceous chondrites shared depletions in moderately volatile elements,

bulk O and N isotope trends, and similar matrix mineral assemblages.

Multiple lines of evidence indicate that most CR chondrites preserve a wealth of records from solar nebular processes (e.g., Kong and Palme, 1999; Krot et al., 2002; Floss et al., 2014; Schrader et al., 2015). CR chondrites have solar abundances for all but the most volatile elements, which are extremely depleted (e.g., Krot et al., 2002). They contain a variety of presolar phases of diverse origins (e.g., Davidson et al., 2014a; Zhao et al., 2013; Floss and Stadermann, 2009a,b). Preservation of presolar materials is consistent with our understanding that the CR group is particularly pristine. CR chondrites record all stages of aqueous alteration, but essentially no evidence of thermal metamorphism (e.g., Harju et al., 2014; Schrader et al., 2015; Abreu, 2016a).

Here, we summarize the characteristics of all components of CR chondrites, their formational histories, intra- and inter-group relationships, the effect that residence in asteroidal parent bodies and terrestrial environments have had on these materials, and how to identify CR parent bodies via spectroscopic analysis.

2. Survey and provenance of CR chondrites

2.1. Falls

There are only two CR observed falls, the type meteorite for the group – Renazzo – and an anomalous (e.g., unusually matrix-rich) chondrite, Al Rais (Table 1). Renazzo was the second carbonaceous chondrite observed to fall (Mason, 1962). It was collected near Ferrara (Italy) on January 15, 1824 (Cordier, 1827). Renazzo is made up of several stones, of which at least three were recovered (Mason, 1962). The largest Renazzo fragment was reported to weigh ~5 kg, but only ~1.1 kg of this mass was in museum collections by 1962. The main mass is located at the University of Bologna (Mason, 1962). Early workers recognized the importance of this meteorite in elucidating hypotheses about carbonaceous chondrites (e.g., Urey and Craig, 1953; Wiik, 1956; Mason, 1960a,b, 1962; Mason and Wiik, 1962; Wood, 1962, 1963a,b). Wood (1962) suggested that Renazzo was more pristine than CI chondrites. These early descriptions

identified the predominant minerals (i.e., olivine, clino and orthopyroxenes, serpentine, Fe-Ni metal, Fe-sulfides, magnetite, and chromite). Based on its high abundance of metallic Fe, Renazzo was initially thought to be an intermediate between the carbonaceous and the enstatite chondrites (Mason and Wiik, 1962; Mason, 1971). Later authors grouped Renazzo with the CV chondrites, because they have chondrules of similar diameters, but noted its unusual characteristics (e.g., McSween, 1977a). As more extensive studies were conducted and more CR chondrites became available, it became evident that Renazzo belonged to a different, new group of carbonaceous chondrites (e.g., McSween, 1979a; Weisberg et al., 1993; Zolensky et al., 1993). The second CR fall, Al Rais, was observed to fall near Medina (Saudi Arabia) on December 10, 1957. The main mass of this meteorite was originally 162 g. Other stones were reported to exist (Mason, 1962). Starting with early studies, Al Rais was grouped with Renazzo based on its high metallic Fe abundance (e.g., Mason, 1962, 1971).

2.2. Antarctic finds

2.2.1. Provenance and mass of Antarctic finds

The impact that the Antarctic suite has had on our understanding of CR chondrites is difficult to overstate. In terms of mass, variety of features, and low degrees of terrestrial weathering, Antarctic CRs provide unique scientific opportunities. As of February of 2019, a total of 101 stones belonging to the CR group had been recovered from Antarctica. Of these 101 stones, 18 were recovered by Japanese expeditions to the Asuka and Yamato Mountains. In fact, the first Antarctic CR chondrites were collected in 1979 at Yamato. The American Antarctic Search for Meteorites (ANSMET) program collected the remaining Antarctic CR chondrites.

Despite the large number of stones, many Antarctic CR chondrites belong to a large pairing group (i.e., were initially part of a single meteor). This group, EET 87711 pairing group, includes 50 stones. These samples were collected during the 1987 and 1992 field seasons. GRO 17063 and GRO 17064 also form a small pairing group. After accounting for pairing, 50 different CR meteors appear to be represented in the Antarctic

collections. It is possible that other pairing groups exist and will be identified as we learn more about these samples.

The current total mass of Antarctic CR chondrites is 10.77 kg. However, many Antarctic CR chondrites of the highest scientific interest (e.g., QUE 99177, MET 00426) have small masses (Righter et al., 2017). Of the 50 unpaired Antarctic CRs, 19 have masses <10 g. Based on their scarcity, NASA's Antarctic CRs have been assigned to the list of protected samples. The 12 most massive CRs and the EET 87711 pairing group represent >90% of total Antarctic CR mass. One meteorite alone, MIL 090001, represents >58% of the total Antarctic CR mass. As discussed below, whether MIL 090001 is a CR is debated (Alexander and Bowden, 2018). The EET 87711 pairing group has a combined mass of 1.34 kg or 12.4% of the total Antarctic CR mass.

The largest Antarctic CR chondrite that has been recovered to date is MIL 090001, weighing 6.29 kg (Table 1). The classification of this meteorite has been a subject of controversy. It was initially classified as a CV chondrite (Keller, 2011). Soon after, the meteorite was reclassified based on whole-rock oxygen isotope studies (Keller et al., 2012; Alexander et al., 2012). However, Alexander and Bowden (2018) have recently argued that the bulk H content and δD from MIL 090001 plot below the trend established by other CR chondrites. They argued that MIL 090001 might actually be an ungrouped petrologic type 2 carbonaceous chondrite with affinities to ungrouped C2 LEW 85332. Authors have undertaken a detailed petrologic comparison between these meteorites. However, results from this work are beyond the scope of this review.

2.2.2. Effect of weathering on Antarctic finds

Antarctic finds are prone to chemical interaction with the terrestrial environment. To indicate the degree to which meteoritic minerals have been affected by their interaction with the ice, collection curators use weathering grades A, B, C, and e (e.g., Gooding, 1981, 1986; Velbel et al., 1988; Losiak and Velbel, 2011). Grades A-C denote increasing elemental mobilization and mineral replacement. Grade e is independently assigned to samples with evaporite deposits.

Weathering ubiquitously affected Fe-Ni metal and Fe-oxides in CR chondrites (e.g., Abreu 2016a). Abreu (2016a) described that the effect of Antarctic weathering on Fe-Ni metal included thick rust rims, oxide sub-grains, and even complete pseudomorphic replacement in some cases. The effects of these processes are shown in Fig. 2, where the metal from stones of the same pairing group is shown. Most Fe-Ni metal grains are located inside the chondrules or on the margins of chondrules adjacent to fine-grained matrix. Abreu (2016a) observed that there are no systematic differences between the weathering features in Fe-Ni grains in chondrule interiors versus those in direct contact with the matrix.

Abreu (2016a) also reported the presence of Fe-hydroxide veins on the periphery of metal grains. In a grade C CR chondrite, she observed Fe-hydroxide veins that cut across the length of a petrographic thin-section. Ferric Fe phases, such as those found in the veins described in weathered CRs, are generally assumed to be terrestrial in origin. However, Le Guillou et al. (2015a) suggested that some pure ferric Fe phases (e.g., hematite and ferrihydrite) might, in fact, have formed as matrix silicates. As they progressively altered, their $Fe^{3+}/\sum Fe$ ratios decreased. It is not known if or how much hematite and ferrihydrite are present in the most aqueously altered CR fall, Al Rais. If significant amounts of these preterrestrial ferric Fe minerals are present in Al Rais, the origin of ferric Fe minerals in Antarctic chondrites ought to be revisited.

The effect of terrestrial alteration on the silicate mineralogy of CR chondrites remains mostly unexplored. Ascertaining the effect is a challenging question to address because terrestrial alteration products, in particular those formed under Antarctic conditions, may resemble aqueous alteration occurring at the low temperature, low water:rock ratios, thought to also be prevalent in the CR parent body. Abreu (2016a) observed that in weathering grade B/C MIL 07525, matrix regions adjacent to altered Fe-Ni metal are unusually Fe-rich. Amorphous Fe-Mg matrix silicates in MIL 07525 contain ~17 wt.% more FeO than similar materials in regions that did not show textural evidence of terrestrial weathering. In MIL 07525, amorphous Fe-Mg silicates are associated with the ferroan serpentine and hisingerite. More in-depth studies are necessary because the effect of terrestrial weathering of CR silicates is not easily resolved.

2.3. North African finds

2.3.1. Provenance and mass of North African finds

As of February 2019, 72 individual stones from hot deserts have been classified as CR chondrites. The current total mass of Saharan CRs is over twice the total mass of Antarctic CR chondrites (27.05 kg Saharan vs. 10.77 kg Antarctic CRs – based on the Meteoritical Bulletin Database; Table 1). The Saharan CR suite includes eight of the ten most massive CRs (combined mass = 15.1 kg). Like Antarctic finds, some North African finds are also paired. Four pairing groups have been proposed: (1) El Djouf 001, Acfer 059, 087, 097, 114, 139, 186, 187, 209, 270; (2) Acfer 270 and 324; (3) Acfer 394-400; and (4) NWA 801 and NWA 1776 (Bischoff et al., 1993a,b; Ruzicka et al., 2014, 2015). As with the Antarctic finds, it is possible that there are more paired samples. One challenge that is unique to this CR sample suite is that little field information is available for most of these stones, which makes pairing more difficult.

The North African CR suite has significantly grown over the last two decades – 59 of the 72 stones were recovered since 2000, many of which have not been studied. Although several studies have described the general characteristics of some of the Saharan CR chondrites (e.g., Bischoff et al., 1993a,b; Harju et al., 2014), less is known about their sub-micron mineralogy.

In addition to the 72 North African CR chondrites, seven highly equilibrated (i.e., petrologic types 6 and above) samples have been reported to have affinities with the CR group, most remarkably, Tafassasset. Gardner-Vandy et al. (2012) presented a wide array of analyses and reclassified Tafassasset as a primitive achondrite. Bunch et al. (2013) argued that NWA 7531 is a polymict breccia composed of both ordinary chondritic and CR chondritic clasts formed during a collisional event. Only a brief description from the Meteoritical Bulletin Database was available for the newest equilibrated sample, NWA 11561. They described the sample as having affinities with Tafassasset and NWA 7531. Ruzicka et al. (2015) reported that NWA 6921 and 7317 are paired with NWA 2994, NWA 3250, and NWA 6901, which are not currently classified as CR chondrites. Instead, these meteorites were classified as primitive achondrites. Further studies are

needed to determine if and how these highly equilibrated meteorites are related to the CR group.

2.3.2. Terrestrial weathering of North African finds

Meteorites recovered from hot deserts are generally affected by extensive terrestrial weathering (e.g., Jull et al., 1991; Wlotzka, 1993; Wlotzka et al.,1995; Al-Kathiri et al., 2005; Bland et al., 2006 and references therein). The dominant effects that terrestrial weathering have on meteorites – Fe oxidation and mobilization – might affect CR chondrites more extensively than other hydrated meteorites, because the CRs are comparatively rich in Fe–Ni metal. Saharan meteorites are classified according to a different scheme than Antarctic meteorites, ranging from W0-W2 for progressive weathering of Fe-Ni metal, W3-W4 for progressive weathering of troilite, and W5-W6 for weathering of mafic silicates (e.g. Bland et al., 2006 and references therein). Although some Saharan CR chondrites have been studied in detail, there have not been systematic studies of their weathering features. In fact, only 38 of the 66 known Saharan CRs have been assigned to a terrestrial weathering grade – representing 58% of the total number and only 43% of the total mass available for study.

3. Bulk compositional and isotopic characteristics of the CR chondrites

3.1. Bulk chemical compositions

The bulk composition of several CR chondrites is presented in Table 2. Elements more volatile than Cr show increasing depletions with respect to CI chondrites (Weisberg et al., 1993; Bischoff et al., 1993a; Kallemeyn et al., 1994; Huss, 2004; Braukmüller et al., 2018). For elements more refractory than Cr, lithophile and siderophile elements are unfractionated with respect to each other and show ~40% with respect to CI chondrites for most elements (e.g., Huss, 2004). Braukmüller et al. (2018) noted that major elements were slightly below CI values and that REEs were flat.

3.2. Bulk hydrogen, nitrogen, and carbon contents

Although CR chondrites show a broad range of aqueous alteration, several studies have shown that their H, N, and C contents are low relative to other hydrated carbonaceous chondrites. Alexander et al. (2012) measured the bulk composition of these three elements for Renazzo, Al Rais, EET 92042, EET 96286, GRA 95229, GRO 95577, LAP 02342, LAP 04720, MET 00426, PCA 91082, and QUE 99177. It is noteworthy that they found no differences between falls and finds, indicating that terrestrial weathering did not modify the total H content measurably. Bonal et al. (2013) also studied the hydrogen isotopic composition of water in QUE 99177, MET 00426, EET 92042, GRA 95229, Renazzo, and Al Rais. Alexander et al. (2013) analyzed three other Antarctic CRs, anomalous MIL 090001, and heated GRA 06100 and GRO 03116.

Alexander et al. (2012) measured the average bulk H content to be 0.6 wt.%. Hydrogen contents for individual CRs ranged from 0.4 wt.% in CR3 MET 00426, to 0.9 wt.% in anomalous, matrix-rich CR2 Al Rais, to 1.3 wt.% in CR1 GRO 95577. Both CR minerals and organic matter contain H – structural OH and H in minerals are termed "water." To estimate the amount of this structural water, Alexander et al. (2013) subtracted the H measured in organics. The average structural water in CRs is ~4.2 wt.%., with a range from 2.7-10.9 wt.%. They noted that both the hydrogen contents and the structural water contents of bulk CR chondrites are low compared with CM chondrites (H ~1.2 wt.%; 0.9-1.5 wt.% range) and maximum structural "water" (9.4 wt.% and ~7.1-12.2 wt.% range). At values of ~0.1 wt.% H, the structural water content for GRA 06100 and GRO 03116 are disproportionally low compared to the average H content in CRs (Alexander et al., 2013). This is to be expected since GRA 06100 experienced some heating, which is not the case for other CR chondrites.

Alexander et al. (2012) determined that the nitrogen and carbon contents of CR chondrites are also low compared to CM chondrites. The average nitrogen of the CR chondrites is 0.08 wt.% versus 0.10 wt.% in the CMs, and the average C in the CRs is 1.3 wt.% versus 2.0 wt.% in the CMs. As with hydrogen, heated CR chondrites have low carbon contents (Alexander et al., 2013).

3.3. Bulk hydrogen, nitrogen, and carbon isotopic compositions

The bulk H, N, and C isotopic compositions of CRs are distinct from other groups. δD values are high for CRs compared to other carbonaceous chondrites (e.g., Kung and Clayton, 1978; Robert and Epstein, 1982; Grady et al., 1991; Pearson et al., 2006; Alexander et al., 2012, 2013; Bonal et al., 2013). Alexander et al. (2012) measured the isotopic compositions for Renazzo, Al Rais, EET 92042, EET 96286, GRA 95229, GRO 95577, LAP 02342, LAP 04720, MET 00426, PCA 91082, and QUE 99177. They determined that the average δD content for unheated CR chondrites is 639.0‰ (compared with CMs: δD ~ -57.7‰). These high values were also reported by Bonal et al. (2013), which measured δDs as high as 1600‰ and high variability in isotopic composition at the micron scale. Furthermore, Bonal et al. (2013) found no δD trends along the CR aqueous alteration sequence. In contrast, heated CR2s GRA 06100 and GRO 03116 have very low δD contents (δD = - 80.3 ± 0.0 and - 96.6 ± 0.0 respectively; Alexander et al., 2013). The average $\delta^{13}C$ for the CR chondrites is -4.6 ‰, which is comparable with values for the CMs (-2.9 ‰ - Alexander et al., 2013). Finally, CR chondrites have a high average $\delta^{15}N$ = 174.3‰, compared with the $\delta^{15}N$ of the CM chondrites, which is 56.3‰ (e.g., Kung and Clayton, 1978; Robert and Epstein, 1982; Grady et al., 1991; Alexander et al., 2012). The high positive $\delta^{15}N$ value is a characteristic that CR chondrites share with other members of the CR clan (e.g., Krot et al. 2002).

3.4. Bulk oxygen isotopic composition

The bulk oxygen-isotopic composition of CR chondrites lies on a line below the terrestrial fractionation line and has a distinct slope of ~0.7 (Weisberg et al., 1993; Weisberg et al., 1995; Clayton and Mayeda, 1999; Schrader et al., 2011, 2014; Harju et al., 2014). Schrader et al. (2011) refined the value of the CR slope line to be 0.70 ± 0.04 (2 σ) and determined that the $\delta^{17}O$-intercept is -2.23 ± 0.14 (2σ) (Fig. 3). These authors noted some spread around the line. This bulk CR chondrite oxygen line has been explained by mixing between ^{16}O-poor phyllosilicates and a ^{16}O-rich anhydrous silicate component, which are thought to represent at least two distinct reservoirs. Since the CR

line represents mixing between a hydrous and an anhydrous reservoir, the relationship between oxygen isotopic composition of CR chondrites and their degree of aqueous alteration has been the subject of extensive investigations. Schrader et al. (2011) found that the oxygen isotopic composition of QUE 99177 is ^{16}O-rich, and GRA 06100 is ^{16}O-poor. However, the correlation between aqueous alteration and O-isotopic compositions remains an area of active research.

4. Chondrules in CR chondrites

CR chondrules are made up of coarse-grained ferromagnesian silicates, nano-crystalline and glassy mesostasis, and Fe-Ni opaque nodules (Weisberg et al., 1993; Zolensky et al., 1993; Kallemeyn et al., 1994; Wasson, 1996; Kong and Palme, 1999; Krot et al., 2002; Schrader et al., 2008, 2011, 2013, 2015, 2018a; Wasson and Rubin, 2010; Berlin et al., 2011). Most CR chondrules are porphyritic olivine (PO) and porphyritic olivine/pyroxene (POP) (e.g., Weisberg et al., 1993; Zolensky et al., 1993; Kallemeyn et al., 1994; Kong and Palme, 1999; Krot et al., 2002; Schrader et al., 2008, 2011, 2015) **(**Fig. 4). However, other mineralogies and textures are also represented, including barred olivine (BO), compound PO/BO, compound BO/POP, compound porphyritic olivine/radial olivine (PO/RO), and compound porphyritic olivine/granular olivine (PO/GO). Authors inferred that the preponderance of PO and POP chondrules indicates that few of the chondrule precursors were totally melted or that the CR region of chondrule formation was possibly dusty (e.g., Hewins et al., 2005; Schrader et al., 2015).

CR chondrules have a variety of textures, including well-rounded, extensively melted chondrules with large silicate phenocrysts and opaque grains, and irregular, slightly melted, fine-grained objects. Some of these objects have multiple concentric igneous rims, made up of micro-porphyritic and granular silicates, as well as Fe-Ni metal grains (e.g., Weisberg et al. 1992; Huss et al. 1996; Krot et al., 2002; Ebel et al., 2008; Wasson and Rubin, 2010). Figures 4a-b show an example of this texture. Wasson and Rubin (2010) estimated the average thickness of CR igneous rims to be ~270 microns, which is thick compared with rims around CK chondrules (190 microns), ordinary chondrules

(160 microns), and CM, CO, EH, and EL chondrules (30-60 microns). The compositional differences in Fe-Ni metal nodules in igneous rims and the implications of these differences for chondrule formation are discussed in sections below. Using on 3D tomography, Ebel et al. (2008) imaged the olivine-pyroxene layering sequence in chondrules with igneous rims. They argued that because olivine condenses at higher temperatures than pyroxene, the olivine-pyroxene layering sequence is consistent with high-temperature equilibration of chondrule melts with a solar gas. Weisberg et al. (1993) suggested that both the chondrule cores and igneous rims originated from the same reservoirs. CR chondrites also contain compound chondrules (e.g., Wasson and Rubin, 2010). These objects consist of two chondrules, either in contact or nested within each other. Finally, some CR chondrules have agglomeratic, or partially melted grains, ranging in sizes from 1-80 microns (e.g., Schrader et al., 2018a).

Chondrule sizes have been used both as criteria to classify chondrites and as a constraint for chondrule formation conditions. Like CV and CK chondrites, chondrules in CR chondrites are large compared with CM and CO chondrules (e.g., Bischoff et al., 1993a; Kallemeyn et al., 1994; Wasson and Rubin, 2010; Friedrich et al., 2015). For a relatively small sample, Kallemeyn et al. (1994) reported that the average radius of CR chondrules was ~ 700 μm. Based on the textural complexity of CR chondrules, Friedrich et al. (2015) cautioned that it is possible that different authors used different delineation criteria for chondrule edges and introducing additional uncertainty in the measurements. Campbell et al. (2005) hypothesized that the grain size of silicate phenocrysts increases with the degree to which chondrule precursors melted in the nebula. Along with CV and CK chondrites, Wasson and Rubin (2010) attributed the large chondrule diameters of CR chondrules to re-melting in slow-cooling, dust-rich environments, in which chondrules accumulated dust layers on their surfaces.

In addition to mineralogical and textural classifications, CR chondrules are subdivided into three types based on their chemical compositions, which are thought to have been established under different nebular conditions. Type I and type II chondrules are classified based on the iron to magnesium ratio of their olivines and pyroxenes (Fig. 4; Tables 3, 4). Type I chondrules are reduced, MgO-rich, and FeO-poor (Fe/(Fe+Mg) <10%). Type II chondrules are oxidized, MgO-poor, and FeO-rich (Fe/(Fe+Mg) >10%).

In addition to ferromagnesian chondrules, CR chondrites contain objects dominated by high-Ca, low-Ca pyroxenes, and Mg-bearing anorthitic plagioclase termed Anorthite-Rich Chondrules or ARCs, which have affinities somewhat intermediary between types I and II chondrules and CAIs (e.g., Krot and Keil, 2002; Table 5).

In the CR chondrites, there is a sharp gap in iron to magnesium ratios between type I and type II chondrules. This gap is more prominent than in other carbonaceous chondrite groups. Schrader et al. (2017) interpreted this paucity in composition as evidence that chondrules in CR chondrites formed under distinct nebular conditions and that no chondrules from other groups mixed with the CRs.

Of the three compositional types of chondrules, only type I chondrules are abundant in CR chondrites. These MgO-rich chondrules account for ~63.1% (range 30-74%) of the total CR chondrites' areas, as studied by Schrader et al. (2011). Type II chondrules comprise approximately 2.3 area % (range 0.1 to 5.6%), and ARCs are the least common, accounting for ~0.5% (range 0-1.6%) of the total CR areas (Schrader et al. 2011).

4.1. Type I chondrules

Type I chondrules vary in size from ~400-1000 μm and may reach up to 3 mm in apparent diameter (e.g., Fig. 4a,c). They are relatively rich in Fe-Ni metal and are often multilayered, with cores dominated by forsteritic olivine and in some cases low-Ca pyroxene phenocrysts, and silicate-rich layers (e.g., Weisberg et al., 1993; Kallemeyn et al., 1994; Krot et al., 2002; Schrader et al., 2008, 2013, 2015; Tenner et al., 2013, 2015; **Table 3**). Igneous rims have silica-rich outer layers. In addition, these chondrules have mesostasis, containing nanophase crystals, which in some cases are partially to entirely replaced by phyllosilicates, most commonly serpentine and chlorite (e.g., Weisberg et al., 1993; Keller, 2011). An example of mesostasis containing predominantly anhydrous nanocrystalline phases is shown in Fig. 5 a-d. Type I mesostases have higher albite and orthoclase contents than mesostases in type II chondrules (e.g., Krot et al., 2002).

Whereas Fe-sulfides are common in type I chondrules in other chondrite groups, they are scarce in type I CR chondrules (e.g., Wasson and Rubin, 2010). The low abundance of sulfur in type I chondrules has been interpreted as evidence of multiple heating events

(e.g., Schrader et al., 2008; Wasson and Rubin, 2010; Jacquet et al., 2013). However, the mechanism and conditions under which S losses occurred is an active area of research. For example, Schrader et al. (2008) argued that type I chondrules formed by heating gas and dust in a reducing and non-sulfidizing (low fO_2 and fS_2) region. In contrast, Wasson and Rubin (2010) suggested that the low S contents of type I CR chondrules resulted from slow cooling during re-melting events, which allowed migration of S to chondrule surfaces and eventual evaporative losses. Jacquet et al. (2013) also argued for at least two nebular heating events affecting type I CR chondrules, with the first event lasting > 1 day and resulting in equilibration between chondrules and Fe-Ni metal and in evaporative loss of Fe from the chondrule. This first heating event would be followed by accretion of a fine-grained mantle on the chondrule surface. Like Wasson and Rubin (2010), Jacquet et al. (2013) suggested that a second heating event would explain the formation of igneous rims. However, unlike Wasson and Rubin (2010), who suggested for the second heating event to be slow, Jacquet et al. (2013) argued that the second heating event was rapid, at least compared to element diffusion and limited to the outside of the chondrule.

4.1.1. Fe-Ni metal in Type I CR chondrules

Numerous studies have focused on the characteristics and origins of Fe-Ni metal nodules in CR chondrites and used these characteristics to constrain conditions for chondrule formation (e.g., Wood, 1963a,b; Lee et al., 1992; Kong et al., 1999; Connolly et al., 2001; Ebel et al., 2008; Jacquet et al., 2013). These nodules are the reservoir of approximately a third of the total iron in CR chondrites (Campbell et al., 2005). Fe-Ni metal nodules are found in the interiors of chondrule phenocrysts and mesostasis (~45-50%), chondrule margins (~15%), and embedded in fine-grained matrix (e.g., Lee et al., 1992; Connolly et al., 2001; Ebel et al., 2008). Ebel et al. (2008) used X-ray microtomography to determine that Fe-Ni grains make up to 37% of the volume of type I chondrules. The distribution, as well as the composition and textural characteristics of these nodules, appear to vary with petrologic setting and degree of chondrule melting (e.g., Lee et al., 1992; Weisberg et al., 1993; Connolly et al., 2001; Humayun et al., 2002;

Campbell et al., 2005). Fe-Ni metal is concentrated in porphyritic type I chondrules, whereas non-porphyritic types do not generally contain any.

The petrologic setting of Fe-Ni metal nodules places constraints on their chemical compositions. Those in chondrule interiors have higher contents of refractory siderophile elements than Fe-Ni metal on margins (e.g., Co, Ni, Re, Os, W, Ir, Ru, Mo, Pt - Jacquet et al., 2013). Conversely, Fe-Ni metal located on chondrule margins has relatively higher abundances of moderately volatile elements (e.g., Fe, Cu, Au). Campbell et al. (2005) noted that small Fe-Ni metal grains that are poikilitically enclosed in MgO-rich silicates have high, correlated concentrations of Ni and P and low Fe and Cr. Moreover, Wasson and Rubin (2010) observed that Fe-Ni metal composition is uniform within individual concentric shells in chondrules. Fe-Ni metal grain sizes are also smaller in igneous rims around chondrules compared with chondrule interiors and margins (e.g., Fig. 4b). However, as Ebel et al. (2008) found, the two-dimensional arrangement of Fe-Ni metal grains in chondrules – on which these correlations rely – may not be representative of the three-dimensional arrangement of metal.

Based on the shapes and sizes of silicate phenocrysts, Zanda et al. (2002) determined that the texture of Fe-Ni metal grains varies with the degree to which their CR chondrule hosts underwent melting. They reported that Fe-Ni metal is stochastically distributed throughout type I chondrules with small silicate phenocryst sizes. These chondrules with finer-grained phenocrysts would have formed by less extensive melting episodes than chondrules with round outlines and large silicate phenocrysts, which have well-developed shells made of coarse-grained Fe-Ni metal grains. In extensively melted chondrules, olivines have higher forsterite contents and Fe-Ni metal grains have higher Ni and P.

Several studies argued for a common origin for Fe-Ni metal nodules in all chondrules and matrix (e.g., Zanda et al., 1994; Kong et al., 1999). In fact, Kong et al. (1999) suggested that Fe-Ni metal grains outside chondrules probably were also derived from chondrules. How these grains formed, however, has been the subject of debate. To test the validity of Fe-Ni metal formational hypotheses, their petrologic textures, settings, and minor and trace elements were studied. Formational hypotheses for metal grains include: (1) reduction during thermal metamorphism in the CR parent body(s); (2) direct condensation from a nebular gas; (3) evaporation and re-condensation during chondrule

formation; and (4) segregation of immiscible metallic Fe melts from chondrule melts in the nebula.

While current discussions center around a nebular setting, early workers suggested that Fe-Ni metal formed by reduction of Fe^{2+} during thermal metamorphism (e.g., Lee et al., 1992). This hypothesis is inconsistent with newer evidence that thermal metamorphism of the CR parent body was minimal (e.g., Wasson and Rubin, 2010; Schrader et al., 2015; Abreu, 2016a). Also, Wasson and Rubin (2010) noted that the negative correlation between Ni in the metallic shell and olivine Fa contents in the host silicates precludes in-situ, thermally-driven reduction.

A second hypothesis that has fallen out of favor is the direct condensation of Fe-Ni metal from a nebular gas. Early studies appeared to indicate that Fe-Ni metal could have condensed directly from the nebula before silicate formation, based on their abundances of Ni, Cr, and P (e.g., Wood, 1963a,b, 1967; Grossman and Olsen, 1974). However, later work indicated that some CRs show a positive, linear correlation between Co and Ni and an approximately solar ratio of ~ 0.046 (Lee et al. 1992; Weisberg et al. 1993; Connolly et al. 2001; Jacquet et al. 2013). Weisberg et al. (1993) interpreted the correlation between Co and Ni as a result of thermodynamically-controlled condensation under nebular conditions. It is noteworthy that several studies show that the Co/Ni ratios are not constant within individual or across different minimally heated CRs (e.g., Zanda et al., 1994, 2002; Wasson and Rubin, 2010; Schrader et al., 2015). Researchers have argued against the direct nebular condensation hypothesis, based on the presence of a graphite layer on Fe-Ni metal surfaces, thermodynamic equilibrium of metallic Fe melts under nebular conditions, and trace siderophile element abundances (e.g., Kong et al., 1999; Connolly et al., 2001; Humayun et al., 2002; Jacquet et al., 2013). Kong et al. (1999) observed that Fe-Ni metal grains have low-Ni contents and were embedded in graphite layers. They argued that scenarios for nebular condensation could either reproduce the low-Ni composition of Fe-Ni metal or the presence of the graphite layer, but not both features. The Ni contents would require isolation of metal from the nebular gas at high temperature. In contrast, graphite could only be stable at temperatures of 600K (at 10^{-5} bar) in the nebula, requiring long exposure of Fe-Ni metal to the nebular gas at low temperatures. Finally, Humayun et al. (2002) found a linear correlation between Ni/Fe

and Pd/Fe ratios in the CR2 Renazzo, which cannot be explained by the order of condensation from a gas of solar composition.

The two remaining hypotheses suggest that Fe-Ni metal formed in the aftermath or as a part of the chondrule-forming events. Wasson and Rubin (2010) suggested that separation of Ni and Co from Fe-metal occurred during volatilization at low ambient nebular temperatures associated with chondrule formation. Some argued that large Fe-Ni metal grains formed by reduction of FeO and separation from the silicate fraction of chondrule melts (Connolly et al., 1994, 2001; Zanda et al., 1994; Campbell et al. 2002, 2005). This hypothesis was initially based on the depletion of volatile siderophile elements. Connolly et al. (2001) suggested that FeO reduction was assisted by the presence of carbon. Graphite-assisted reduction is supported by the fact that this mineral is spatially associated with Fe-Ni metal (Kong et al., 1999). Some studies explained the Co-Ni trend observed in some CR metal in terms of oxidation/reduction reactions, based on the observation that Fe-Ni metal and silicates appear to be in redox equilibrium with each other within individual chondrules (Lee et al., 1992; Zanda et al., 1994). Because Ni and Co are slightly more refractory than Fe, the initial metal composition would have been enriched in Ni and Co with respect to the last condensates.

The last two hypotheses are not mutually exclusive. In fact, Connolly et al. (2001) suggested that they were both at play, depending on whether Fe-Ni metal grains were located in rims or interiors of chondrules. They suggest that rim metal grains formed by evaporation/re-condensation. Metal grains in chondrule interiors would have formed by the separation of immiscible metal-silicate chondrule melt. Connolly et al. (2001) and others also argued that at least some of the Fe-Ni metal formed by devolatilization, concurrent with the formation of immiscible metal-silicate chondrule melts and subsequent recondensation from the resulting vapor, which would be depleted in refractory siderophiles (Kong et al., 1999; Kong and Palme, 1999). This scenario can explain both the fact that rim Fe-Ni metal grains are depleted in refractory siderophiles as well as the complementarity between the Au, As, Sb, and Ga contents of coarse Fe-Ni metal and non-magnetic Fe-Ni matrix phases. However, Campbell et al. (2005) argued that such a scenario is unlikely because elements such as Au and Cu may not be easily mobilized from the melt under the kind of reducing conditions needed to form Fe-Ni

metal. Jacquet et al. (2013) presented additional evidence against the re-condensation of metal vapor based on their observations of inconsistent depletion of refractory siderophile elements in metal along chondrule margins compared to chondrule interiors.

A variety of different types of Fe-Ni metal precursors have been proposed. Some authors have suggested that decomposition of pre-existing Fe-Ni sulfides resulted in the formation of Fe-Ni metal grains (e.g., Zanda et al., 1997, 2002; Hewins et al., 1997). Zanda et al. (2002) argued that the correlation between the degree of melting and the composition of silicates and Fe-Ni metal supports this hypothesis. In contrast, Jacquet et al. (2013) suggested that Fe-Ni metal precursors resembled the least melted chondrules.

As stated above, Fe-Ni metal nodules are commonly found in concentric layers within and along the periphery of chondrules. Multiple hypotheses have been proposed to explain the arrangement of Fe-Ni metal. Wood and McSween (1977b) explained the shell-like distribution of Fe-Ni metal by addition and/or condensation of successive layers in the nebula. Alternatively, multiple authors have suggested that metallic Fe migrated to the periphery of chondrules via centrifugal force density differential, acting on immiscible metallic Fe versus forsteritic melts (e.g., Grossman and Wasson, 1985; Kong et al., 1999; Kong and Palme, 1999; Humayun et al., 2002; Tsuchiyama et al., 2009). Wasson and Rubin (2010) argued that centrifugal forces could not reproduce the shell-like, concentric structures that Fe-Ni globules formed within many chondrules. Instead, they suggested that surface tension resulted in the mobilization of the metallic Fe melt across channels. The metallic melt then redistributed itself on the surface of the silicate melt via interfacial tension. If the rate of cooling of the mobilized metallic Fe melt was slow compared to Ni diffusion, this would result in the uniform composition of individual concentric shells, but this model is inconsistent with the trace element data obtained by Connolly et al. (2001). Wasson and Rubin (2010) argued that the variations in PGE contents within shell reported by Connolly et al. (2001) were artifacts of ion microprobe analysis. However, similar PGE patterns were independently reproduced using ICP-MS (Humayun et al., 2002; Campbell et al., 2002).

4.1.2. Mesostasis of Type I chondrules

Only a few studies of CR mesostasis are currently available (e.g., Richardson, 1981; Ichikawa and Ikeda, 1995; Burger, 2005; Harju et al., 2014; Tenner et al., 2015). It is noteworthy that some studies did not specify the type of chondrule where mesostases were described. In both type I and type II chondrules, mesostasis generally appears non-isotropic or made up of minute crystals too small for reliable resolution and identification via optical microscope. Isotropic glass in type I chondrules was only identified in a few pristine CRs (Harju et al., 2014; Burger, 2005; Abreu and Brearley, 2010). Not all members of each pairing group contain clear mesostasis, revealing heterogeneities in their asteroidal and/or terrestrial histories.

Mesostasis anisotropies have been generally attributed to the presence of asteroidal phyllosilicates or excessive thin section thickness (cf., Harju et al., 2014). However, conclusive identification of phyllosilicates in CR mesostasis has only been carried out for MIL 090001 and GRO 95577 (Keller, 2011). In a MIL 090001 thin section, emerald-green to slightly reddish materials are found in chondrule interiors, consistent with phyllosilicate replacing the glass. Mesostasis in GRO 95577 underwent both compositional and textural integration with chondrule phenocrysts, which makes it challenging to determine which phyllosilicates replaced which materials. Tenner et al. (2015) described the mineralogy of mesostasis in 48 type I chondrules from MET 00426 and QUE 99177 as heterogeneous in texture, typically consisting of fine-to-coarse grained pyroxene and plagioclase. Tenner et al. (2014) reported silica excesses in chondrule plagioclase.

Harju et al. (2014) measured the composition of the mesostasis in POP two chondrules in LAP 02342 and EET 92062. In LAP 02342, they found that the boundary between mesostasis and fine-grained matrix was enriched in Na and depleted in Ca, Ti, and Cr. They attributed these trends to parent body aqueous alteration. Tenner et al. (2015) used EDS to measure the composition of the mesostasis in one region of recrystallized mesostasis (SiO_2, Al_2O_3, FeO, MgO, CaO, and Na_2O contents of 56, 24, 1, 3, 12, and 2.5 wt.%, respectively) and one region of glassy mesostasis (SiO_2, Al_2O_3, FeO, MgO, CaO, and Na_2O contents 68, 15, 4, 1.5, 6.5, and 3.5 wt.%, respectively).

4.1.3. Oxygen isotopes in type I chondrules

Multiple authors have analyzed the oxygen isotopic compositions of type I chondrules in CRs (e.g., Weisberg et al., 1993; Krot et al., 2006a-b; Schrader et al., 2013, 2014, 2017; Tenner et al., 2015). Krot et al. (2006b) measured the O-isotopic compositions of all major phases in nine chondrules from three CRs and found that they plot near the carbonaceous chondrite anhydrous mineral (CCAM) line. They observed that, except for relict grains, chondrules are isotopically homogeneous, with all minerals and mesostasis from each chondrule plotting in small clusters at $\Delta^{17}O \sim \pm 2$ ‰. Interchondrule variations range from $\Delta^{17}O = 0$ to -5 ‰. Krot et al. (2006b) suggested that the oxygen isotopic composition of CR chondrules was established during melting and isotopic homogenization of precursor materials with a ^{16}O-poor gas. Schrader et al. (2013) studied olivine grains in eight type I chondrules from pristine CRs QUE 99177 and GRA 95229 and heated GRA 06100 using secondary ion mass spectrometry. They concluded that individual chondrules acted as independent igneous systems with their own isotopic composition. They also argued that aqueous alteration of the meteorites studied had not modified the oxygen isotopes of their chondrules.

Schrader et al. (2014) analyzed 7 barred olivine (BO) chondrules and 3 silica-bearing porphyritic type I chondrules from Gao-Guenie (b), GRA 95229, PCA 91082, and Shişr 033. They found that the oxygen-isotope compositions of olivine plotted along a slope-1 line. Oxygen isotopic variations of BO chondrule olivines are small (i.e., $\Delta^{17}O \sim 2.5$ ‰). They noted that olivine grains in type I BO chondrules have similar major and minor elements and O-isotope compositions as those of olivine in porphyritic chondrules. Based on these similarities in isotopic compositions, they argued against the chondrule formation model in which porphyritic chondrules formed in transient planetesimals. Using secondary ion mass spectrometry, Tenner et al. (2015) measured the O-isotopic composition of olivine, pyroxene, and plagioclase in 45 type I chondrules from pristine CRs QUE 99177 and MET 00426. Consistent with prior studies, they observed that $\Delta^{17}O$ values are nearly homogeneous for all minerals analyzed.

The question of whether the O isotopes in chondrule melts equilibrated with the nebular gas is an area of active research. Schrader et al. (2014) concluded that even

barred olivine chondrules, which were at one point completely melted, only record partial equilibration with the nebular gas. In contrast, Tenner et al. (2015) argued that the chondrule melts and the surrounding nebular gas exchanged oxygen isotopes efficiently. They found an inverse correlation between $\Delta^{17}O$ and Mg-numbers, which they suggested had implications for the processes forming type II chondrules. They used the trend between $\Delta^{17}O$ and Mg-numbers to constrain the amount of dust and/or H_2O enhancements needed for type I chondrules to form. They proposed a 100-200x dust enrichment and that these dust precursors had 0-0.8 x CI chondrite water abundance. Schrader et al. (2017), however, noted that their study of seven other CR chondrules did not reproduce the correlation between $\Delta^{17}O$ and Mg-numbers.

4.1.4. Radiogenic isotopes in Type I chondrules

Several systems have been investigated for these chondrules, including the Al-Mg, Hf-W, and Mn-Cr geochronometers. Studies of the Al-Mg systematics of CR chondrules show few ^{26}Mg excesses (e.g., Krot and Keil, 2002; Hutcheon et al., 2009; Nagashima et al., 2014; Olsen et al., 2016). Schrader et al. (2017) and Budde et al. (2018) independently found the same average age for CR chondrite chondrules using different isotopic systems.

Schrader et al. (2017) chose CRs that had not been sufficiently affected by thermal metamorphism to ensure that their isotopic signatures had not been altered and measured the oxygen and Al-Mg systematics for seven type I porphyritic chondrules. They estimated that only approximately 32% of chondrules show resolvable excesses of ^{26}Mg. Furthermore, based on the probability density of the Al-Mg ages, they suggested that CR chondrites contain three different generations of chondrules. Some authors have interpreted the scarcity of chondrules with ^{26}Mg excess as evidence that CR chondrules are younger than their counterparts from other chondritic groups. Other researchers attributed this paucity to spatial variations of the $^{26}Al/^{27}Al$ ratio in the protoplanetary disk. Olsen et al. (2016) interpreted the variability in ^{26}Mg as the result of Mg-isotope heterogeneity of the chondrule precursors.

Budde et al. (2018) applied the short-lived ^{182}Hf-^{182}W chronometer to chondrule Fe-Ni metal and obtained ages that are 3.6 ± 0.6 million years (Ma) after the formation of CAIs, which corresponds to ~1–2 Ma later than chondrules found in most other groups of chondrite. The younger chondrule ages support the hypothesis of late CR chondrule formation. Along with the low variability in ^{54}Cr observed in CR chondrules, Olsen et al. (2016) argued that these chondrules must have formed in a spatially constrained region, possibly located in the outer solar system.

4.2. Type II chondrules

Type II chondrules (e.g., Fig. 4 c,d; Table 4) are much less abundant than type I chondrules, and they often occur as fragments (41%; Schrader et al., 2015). Schrader et al. (2008) suggested that the preferential breakup of type II chondrules resulted either from formation in a more dynamically active or denser nebular region or because these chondrules are more brittle and/or porous than type Is.

Several authors have explored the relationship between type I and type II chondrules. Connolly et al. (2008) argued that type II chondrules formed by flash-heating of both dust and pre-existing type I chondrules under higher than canonical fO_2 and fS_2. Connolly and Huss (2010) tested this hypothesis by measuring the oxygen isotopic compositions of type II CR chondrules (see below in the discussion of isotopes). Schrader et al. (2013) studied the relationship between the FeO contents of olivines and their minor element contents (MnO, Cr_2O_3, Na_2O) to ascertain whether type I chondrules are the precursor materials for type II chondrules. They argued that this relationship is unlikely. Schrader et al. (2015) observed compositional overlaps between FeO and minor elements in type I silicate phenocrysts compared with FeO-poor silicate relicts located in type II chondrules. Overlaps suggest that while the origin of type II chondrules from type I chondrule materials is possible, it is also possible that both types originated from similar precursors. In either case, additional precursors were invoked to account for compositional differences between these two types of chondrules.

To establish if a relationship among type II chondrules from different chondritic groups exists, the Fe-Mg-Mn systematics of silicates in CR type II chondrules were

studied: Berlin et al. (2011) argued that chondrules from different chondritic groups could be differentiated based on the trends defined by their Fe/Mn versus Fe/Mg ratios. However, Schrader et al. (2015) collected a much larger dataset that showed significant overlap among groups. They suggested that a variety of factors might explain the Fe-Mg-Mn systematics, including (1) individual type II chondrules behaving as individual igneous systems formed under distinct oxygen fugacities (Schrader et al., 2013); (2) formation from variable precursors (e.g., Berlin et al., 2011); (3) formation at different cooling rates (e.g., Jones and Lofgren, 1993; Berlin et al., 2011); or (4) experiencing complete/incomplete condensation.

4.2.1. Opaque assemblages in Type II chondrule

Compared with type I chondrules, the mineralogy of opaques is more complex in type II chondrules (Schrader et al., 2008, 2015). Opaques in type II chondrules are Fe-Ni metal, troilite, pentlandite, magnetite, and phosphates (e.g., Schrader et al., 2008, 2015). Although Schrader et al. (2008) had indirectly identified tochilinite in these assemblages, a later study determined that these occurrences were instead sub-micron mixtures of magnetite, pyrrhotite, and pentlandite (Schrader et al., 2015).

Schrader et al. (2008) proposed a two-stage process for the formation of these opaque assemblages. In the first stage, Fe-Ni metal and troilite would form by flash-heating/cooling, condensation and corrosion reactions during chondrule formation in the solar nebula. They envisioned that this was a dynamically violent environment, explaining the fragmentation of chondrules described above (Schrader et al., 2008). In the second stage, magnetite and phosphates formed via replacement of Fe-Ni metal in the CR parent body at temperatures ~ 300ºC, which they supported with subsequent experimental studies (Schrader and Lauretta, 2010). They reproduced the mineralogy of the type II chondrule opaque assemblages by reacting Co, Cr, P-bearing, Fe-Ni alloys with H_2–H_2O–CO–CO_2–H_2S gas mixtures at 1000ºC and cooling them at a 3000ºC/hour rate. Subsequent TEM observations showed that pentlandite in type II chondrules might be nebular (Schrader and Lauretta, 2010; Schrader et al., 2015). Schrader et al. (2018b) further constrained the subsolidus cooling rates for 230-600 ºC to be 10^0-10^1ºC/hour

using type II chondrule pyrrhotite and pentlandite. These authors argued that the rapid cooling rates are consistent with chondrule formation by shocks triggered by the accretion of Jupiter or other planetary embryos.

4.2.2. Mesostasis in Type II chondrules

Few studies have described the mesostasis in type II CR chondrules. Tenner et al. (2015) characterized the mesostasis in 3 type II chondrules in MET 00426 and QUE 99177 as glassy, and they used EDS to measure the composition in one region of glassy mesostasis to be 60 SiO_2, 8-14 Al_2O_3, 13, FeO, 2 MgO, 5 CaO, and 0.5 Na_2O (all in wt.%). Burger (2005) collected EPMA point analyses of mesostases in type II chondrules from paired EET 87770 and EET 92106. He measured lower Al_2O_3 and significantly higher Na_2O contents (53-61 SiO_2, 5-7 Al_2O_3, 12-16, FeO, 2-6 MgO, 2-3 CaO, and 7-10 Na_2O (all in wt.%). Burger (2005) identified small areas of glassy mesostasis. Aqueous alteration appears to have affected mesostasis in type II chondrules, but these effects appear to be spatially limited (e.g., Burger, 2005; Brearley and Burger, 2009).

4.2.3. Oxygen isotopes in Type II chondrules

Although individual type II CR chondrules show larger $\Delta^{17}O$ values than type I chondrules, their oxygen isotopic compositions are generally similar (e.g., Krot et al., 2006b; Connolly and Huss, 2010; Schrader et al., 2013). Krot et al. (2006b) measured the O-isotopic composition of olivine and mesostasis in one type II chondrule from MAC 87320, which generally plotted between the CCAM and the terrestrial fractionation line. Connolly and Huss (2010) analyzed the oxygen isotopic composition of 11 type II porphyritic chondrules from Renazzo, EET 92011, and MAC 87320. Similar to type I CR chondrules, minerals in individual chondrules are nearly isotopically homogenous within each chondrule, and each chondrule is distinct from others. Connolly and Huss (2010) found that type II chondrules tend to be more $\delta^{17}O$- and $\delta^{18}O$ -rich than type I chondrules and have $\Delta^{17}O$ ranging from -2.0±0.7 to 0.5±0.7‰. Schrader et al. (2013) measured

olivines in 8 relict-free, type II chondrules from weakly alternated QUE 99177 and GRA 95229 and heated GRA 06100. These analyses included POP and compound BO/POP and radial olivine/POP chondrules. For individual chondrules, olivines have O-isotope compositions ranging in $\delta^{17}O$ = 1.7-3.9‰, in $\delta^{18}O$ = 5.7-8.0‰, and in $\Delta^{17}O$ = -1.8-0.9‰.

Connolly and Huss (2010) observed that relict grains in type II chondrules have a lighter oxygen isotopic composition than their hosts. They hypothesized that these relict grains originated from type I CR chondrules. They also envisioned that type II chondrule formation was aided by the combination of dust enhancements and the addition of ^{16}O-poor (^{17}O and ^{18}O-rich) ice to precursors. Schrader et al. (2013) found that relict-grain-bearing type II chondrules have much larger ranges in $\delta^{17}O$ and $\delta^{18}O$ (~ 14‰) and in $\Delta^{17}O$ (~ 7‰) compared to relict-free ones. They calculated that relict-grain-free type II chondrules formed under H_2O/H_2 ratios between 230 and 740 times solar, whereas, relict grain-bearing type-II chondrules formed under a narrower range of H_2O/H_2 ratios, 350 and 510 times solar. They suggested that the type II CR chondrule dust precursor had a higher S content than the type I chondrule precursor, accounting for the paucity of sulfides in type I chondrules.

Tenner et al. (2015) studied three type II chondrules from pristine QUE 99177 and MET 00426. As discussed above, they used type I chondrule trends between $\Delta^{17}O$ and Mg-numbers to support the hypothesis of Connolly and Huss (2010), in which type I chondrules were the precursors for type II chondrules.

Schrader et al. (2014) studied four barred olivine and one porphyritic olivine pyroxene chondrule from Gao-Guenie (b), GRA 95229, PCA 91082, and Shişr 033. They found that the oxygen-isotope compositions of olivines in type II BO chondrules span a slightly larger range in $\Delta^{17}O$ ~ 2.1 ‰ compared with olivines in BO type I chondrules. Based on their observations, they suggested that there was isotopic exchange, but not homogenization between chondrules and the surrounding nebular gas.

4.2.4. Radiogenic isotopes in Type II chondrules

Studies of radiogenic isotopes from type II chondrules are scarce. Nagashima et al. (2014) found excesses of ^{26}Mg at the 2-sigma level in one out of two mineralogically

pristine type II chondrules from GRA 95229. Schrader et al. (2017) observed a ^{26}Mg excess in plagioclase while simultaneously measuring the oxygen isotopes and the Al-Mg systematics of one type II porphyritic CR chondrule from heated GRO 03116, suggesting that at least some type II CR chondrules might have formed before the formation of most type I CR chondrules.

4.3. Anorthite-rich chondrules

Anorthite-rich chondrules (ARCs) are the least abundant chondrule type (<1 vol.%) in CR chondrites. Some ARCs have regions that resemble type I chondrules. In particular, ARCs are dominated by pyroxene and olivine phenocrysts, which generally have high Mg-numbers and also contain Fe-Ni metal nodules (Krot and Keil, 2002; Table 5). ARCs have crystalline mesostases made up of silica, anorthite, and high-Ca pyroxene. However, anorthite-rich chondrules are mineralogically distinct from other types (e.g., Krot et al., 2002). Unlike type I chondrules, ARCs have interstitial anorthite and Al-Ti-Cr-rich low-Ca and high-Ca pyroxenes, and in some cases, contain refractory inclusions (Krot and Keil, 2002). The association with refractory inclusions is the basis of the argument that ARCs formed by melting of the spinel–anorthite–pyroxene CAIs mixed with ferromagnesian precursors compositionally similar to type I chondrules (Krot and Keil, 2002; Krot et al., 2006b). The high abundances of moderately-volatile elements in ARCs suggest that these chondrules could not have been formed by the volatilization of type I chondrule precursors or by the melting of refractory materials only (e.g., Cr, Mn, Si; Krot and Keil, 2002).

Krot et al. (2006b) measured the isotopic composition of different minerals in five ARCs. Unlike type I and type II chondrules, which they found to be essentially isotopically homogeneous, they reported that two out of five ARCs were heterogeneous, with large variations in Δ^{17}O (-6 to -15‰ and -2 to -11‰). They attributed these variations to the formation from incomplete melting of CAI-like precursors.

Using SIMS, Nagashima et al. (2014) measured seven ARCs. Not all these chondrules showed evidence of in-situ decay of ^{26}Al. They noted that ^{26}Mg excesses in CR chondrules were small compared with excesses in other pristine chondrites, such as

LLs, COs, or unique carbonaceous chondrite Acfer 094. These small ^{26}Mg excesses were attributed to CR chondrule formation occurring about a million years after chondrules from other pristine chondrites.

5. Refractory inclusions in CR chondrites

Refractory inclusion is an umbrella term for both calcium-aluminum-rich refractory inclusions (CAIs) and amoeboid olivine aggregates (AOAs) (e.g., McPherson et al. 2014). Refractory inclusions are not very common in CRs (CAIs ~0.4-<1 vol.%; Aléon et al., 2002; Schrader et al., 2011).

CAIs in CR chondrites are relatively small (<500 μm), irregularly shaped, some have igneous textures, and most are fragmented (Aléon et al., 2002; Krot et al., 2017; Table 6). Based on their mineralogy and petrography, Aléon et al. (2002) divided the CAIs in CR chondrites into grossite +/- hibonite-rich, melilite-rich, pyroxene-anorthite-rich, and spinel-pyroxene-melilite aggregates. They measured the oxygen isotopic compositions of minerals in 27 CAIs from seven CRs and determined that they are ^{16}O rich. The Δ^{17}O for hibonite, melilite, spinel, pyroxene, and anorthite is < -13 ‰. It is noteworthy that most CAIs appear to have escaped both aqueous alteration and thermal metamorphism (Aléon et al., 2002).

Amoeboid olivine aggregates are assemblages of anhedral forsterite grains and refractory inclusions of spinel, pyroxene, and anorthite, with some with Fe-Ni metal grains (Aléon et al., 2002; Weisberg et al., 2004). The composition of Fe-Ni metal in AOAs is similar to that in type I chondrules. Texturally, these AOAs have irregular shapes, can be fluffy, and lack the mesostasis present in chondrules (Weisberg et al., 2004). Aléon et al. (2002) measured -24 ‰ < Δ^{17}O < -20 ‰ in forsterite, spinel, anorthite, and pyroxene in AOAs. According to Weisberg et al. (2004), AOAs record a complex nebular history, beginning with gas-solid condensation, reactions between minerals and nebular gas, small degrees of melting, and sintering of the assemblage. They

also described a textural association between an AOA and a type A CAI, suggestive of heating during the same nebular event.

6. Fine-grained materials in CR chondrites

As in other chondrites, the bulk of CR matrix was probably interstellar dust that was processed in a variety of ways in the solar nebula and, hence, can be considered to be of local origin (e.g., Nuth et al., 2005). The oxygen isotopic compositions of matrices are reported in Fig. 7. Matrices are a complex mixture of fine-grained materials whose origins have been the subject of considerable debate. Matrices are volumetrically important components of CRs, only second to chondrules in abundance. CR matrices are the repository of organic and presolar materials. Their grain size is generally < 1μm. Fine-grained materials are texturally variable, occurring as fine-grained rims, interchondrule matrix, or within dark inclusions (Fig. 6; Table 7), "feathered" matrix, and smooth rims (e.g., Abreu and Brearley, 2010; Harju et al., 2014; Wasson and Rubin, 2014; Abreu, 2016a).

The mineralogy of CR matrices is highly dependent on the degree to which they were affected by aqueous alteration. The least altered CR matrices are dominated by amorphous Fe-Mg silicates, Fe-nanophase sulfides, and minor olivine and pyroxene (Abreu, 2007; Abreu and Brearley, 2010; Howard et al., 2015a; Le Guillou et al., 2015a-b; Abreu, 2016a; Table 8). Examples of matrices from both unheated and weakly heated CRs are shown in Figs. 8 and 9. Matrices have been extensively hydrated, even in the most pristine CR that were initially classified as type 3 based on the absence of phyllosilicates (Alexander et al., 2013; Bonal et al., 2013; Beck et al., 2014; Garenne et al., 2014; Le Guillou et al., 2015). Hydration only resulted in extensive phyllosilicate formation in the most altered CRs, in which pre-accretionary phases have been replaced to varying degrees by Fe-Mg phyllosilicates, magnetite, partly oxidized Fe-sulfides, and tochilinite (Abreu, 2007; Abreu and Brearley, 2010; Harju et al., 2014; Le Guillou et al., 2015; Abreu, 2016a).

6.1. Mineralogy and petrology of fine-grained materials

One of the key characteristics of matrices in weakly and moderately altered CR chondrites is that they contain variable amounts of Fe- and Mg-rich, Si-bearing amorphous material, referred to hereafter as amorphous Fe-Mg silicates (Figs. 8, 9). According to Abreu (2016a), the composition of these silicates is highly variable, containing 30-53 FeO, 8-20 MgO, 33-58 SiO_2, and minor Al_2O_3 (0.2-3.9) and S (0.1-1.6), all in wt.%. Amorphous Fe-Mg silicates are not separate units with clearly defined boundaries, such as the ones observed in glass with embedded metal and sulfides (GEMS) in interplanetary dust particles (e.g., Bradley and Dai, 2004; Keller and Messenger, 2011). Instead, they are diffuse regions of silicate material with no crystallographic structure (Fig. 8a and, e.g., Abreu and Brearley, 2010; Le Guillou and Brearley, 2014; Le Guillou et al. 2014, 2015a; Abreu, 2016a). Using coordinated scanning transmission X-ray microscopy (STXM) and TEM, Le Guillou et al. (2015a) determined that amorphous Fe–Mg silicates are hydrated and have high $Fe^{3+}/\sum Fe$ ratios (68-78%) in weakly to moderately altered CRs. They reported that the major element composition is intermediate between serpentine and saponite in weakly to moderately altered CRs, whereas altered and extensively altered CRs were richer in Mg and Si. Intriguingly, amorphous Fe–Mg silicates were predicted to be the most reactive phases in these matrices, yet they are also one of the last ones to be fully replaced. The matrix of the most altered CR identified to date, GRO 95577, contains some amorphous Fe–Mg silicates along with a few relict metal, olivine, and pyroxene phenocrysts (Abreu, 2016a; Howard et al., 2015b).

Fe-Mg phyllosilicates are the second most common type of silicate in CR matrices (e.g., Abreu, 2007, 2016a; Abreu and Brearley, 2010; Le Guillou et al., 2015a). By far, the most common phyllosilicates have compositions between serpentine and saponite. Most phyllosilicates are generally only a few unit cells (e.g., Abreu, 2007, 2016a). However, Le Guillou et al. (2014a) identified both fine-grained Fe-Mg phyllosilicates and coarser-grained (~100 nm) Fe-rich cronstedtite in the matrix of Renazzo. Very few areas contain only amorphous Fe-Mg silicates or only phyllosilicates (e.g., Abreu, 2016a). Although there is significant compositional overlap between amorphous Fe-Mg silicates and phyllosilicates, the latter are richer in MgO and SiO_2 and contain FeO (8-

41), MgO (6-31) and SiO_2 (40-58, all in wt.%), and, like the amorphous material, contain small amounts of Al_2O_3 (0.1-4.6 wt.%). The texture and composition (oxides and water contents) of these materials form a continuum between amorphous Fe-Mg silicates and Fe-Mg phyllosilicates, which suggests that phyllosilicates formed by replacement of amorphous silicates (e.g., Abreu, 2007, 2016a; Abreu and Brearley, 2010; Le Guillou et al., 2015a).

There are a variety of opaque phases distributed within the amorphous Fe-Mg silicates and phyllosilicates (Fig. 8), with nanophase pyrrhotite and pentlandite being the most common (Lee et al., 1992; Abreu and Brearley, 2010; Abreu, 2016a). Fe sulfides with a range of Ni contents are generally thought to have formed in the solar nebula (e.g., Schrader et al., 2008). Sub-micron and nanophase sulfides have been partially oxidized in moderately altered CRs (Abreu, 2016a). Authors have identified nanophase tochilinite in some of the most pristine CR matrices (e.g., Le Guillou and Brearley, 2014; Abreu, 2016a). The latter observed spatial relationships among pentlandite, tochilinite, and serpentine, including layers of tochilinite on sulfide surfaces. Based on their occurrence as overgrowths of magnetite and association with siderite grains, Tyra (2013) argued that at least some of the coarse-grained Fe-sulfides in GRO 95577 are asteroidal.

The second most common group of opaques in CR matrices are Fe-oxides. The oxygen isotopic composition of these oxides ranges from $\delta^{17}O$ = -9.7-3.8‰, in $\delta^{18}O$ = -18-5‰ (Jilly-Rehak et al., 2018). In weakly to moderately altered CRs, Fe-oxides are generally fine-grained (<50 μm) and scarce (Abreu and Brearley, 2010). However, in some weakly altered CRs, rounded Fe-oxides are found decorating the periphery of fine-grained rims around chondrules. Some Fe-oxides occur as independent rounded or platelet grains disseminated throughout the matrix, whereas others form framboidal aggregates (e.g., Kallemeyn et al., 1994; Abreu and Brearley, 2010; Tyra 2013; Abreu, 2016a). The abundance of Fe-oxides increases with aqueous alteration, as surmised from their high abundance in altered GRO 95577, where Fe-oxides are comparatively large (100 μm - 1 mm), and texturally and mineralogically complex (e.g., Weisberg and Huber, 2007; Tyra, 2013). Morlok and Libourel (2013) explained the presence of Fe-oxides in GRO 95577 by alteration of Fe-Ni metal nodules instead of primary matrix phases. Kallemeyn et al. (1994) argued that Fe-oxides formed during hydrothermal alteration at

temperatures between 350-540 K. They proposed that, as precursor phases were replaced during aqueous alteration, Fe was released and entered magnetite and phyllosilicates. According to their model, the preferential formation of either phyllosilicates or magnetite depended on the relative thermodynamic stabilities of these phases.

Finally, although most CR matrices some contain carbonates, reports of significant presence of these minerals are limited to the most altered meteorites (e.g., Weisberg et al. 1993; Endress et al., 1994; Abreu and Brearley, 2010; Brunner and Brearley, 2011; Abreu, 2016a). However, Alexander et al. (2015) found no systematic differences in the abundances of C in carbonates, which ranged from 0.04 wt.% in heated GRA 06100 to 0.19 wt.% in matrix-rich, aqueously altered Al Rais (Alexander et al. 2015). Both weakly altered GRA 95229 and extensively altered GRO 95577 contained 0.16 wt.% C in carbonate.

The composition of matrix carbonates is variable. Carbonates in weakly to moderately altered CR chondrites are predominantly Ca-rich, although Mg-bearing siderite was found in both Acfer 059/El Djouf 001 and in pristine MET 00426 (Weisberg et al. 1993; Endress et al., 1994; Brunner and Brearley, 2011). Tyra (2013) also reported the presence of calcite, "siderite," and minor dolomite in GRO 95577.

Carbonates are distributed either throughout the matrix or along the periphery of chondrule pseudomorphs in GRO 95577 (Tyra, 2013). Calcite was also reported in a GRO 95577 chondrule interior as a replacement product for mesostasis (Jilly-Rehak et al., 2018). Matrix carbonates are texturally associated with one another, with phyllosilicates, Fe-oxides, and Fe-sulfides.

Several groups have measured the isotopic compositions of carbonates in CR matrices (Weisberg et al. 1993; Alexander et al., 2015; Jilly-Rehak et al., 2018). Alexander et al. (2015) established two populations in terms of ^{13}C contents: weakly altered CRs had $\delta^{13}C$ ~ 30-40‰ and extensively altered CRs had $\delta^{13}C$ ~ 65-80‰. Jilly-Rehak et al. (2018) found that the $\delta^{18}O$ of calcite ranges from 9 to 35‰, and the $\delta^{17}O$ of calcite ranges from ~11 to 14‰. These compositions plot on a line with a slope of ~ 0.64. They found no clear relationship with the degree of aqueous alteration recorded by each meteorite. Extensively altered GRO 95577 experienced little to no fluid evolution during carbonate precipitation, which Jilly-Rehak et al. (2018) attributed to the high

water-to-rock ratio of the sample. They used the isotopic fractionation in carbonate-magnetite assemblages in Al Rais to estimate that their precipitation temperature was approximately 60ºC and that the global aqueous alteration temperature of the CR parent body was between 55-88ºC. Also, they identified dolomite in dark inclusions, with $\delta^{18}O$ ranging from ~ 23 to 27‰.

Jilly-Rehak et al. (2017) measured the ^{53}Mn–^{53}Cr chronometer of carbonates for three different CR-chondrite lithologies in moderately altered Renazzo and extensively altered GRO 95577. Renazzo carbonates formed approximately 4.3–5.3 Myr after CAIs in CV chondrites, which overlaps with the time for aqueous alteration of Tagish Lake, CI and CM chondrites. On the other hand, calcite grains in GRO 95577 are younger, having formed approximately 12.6 Myr (Jilly-Rehak et al., 2017) and ≥24 Myr (Tyra, 2013) after CAI formation.

6.2. CR interchondrule matrix

Abreu (2007, 2016a) observed that the majority of fine-grained materials in CR chondrites show no clear spatial association with chondrules (i.e., it does not form rims), but simply occupies the space between them. The size of interchondrule matrix regions is very variable; some areas are occupied by relatively large (500-800 μm) units, whereas in other areas, chondrules are barely separated from each other.

Abreu (2007) distinguished texturally distinct types of interchondrule matrix, including exclusively fine-grained (crystals < 5 μm), matrix clasts, and distinct Fe-rich regions. The interchondrule matrix contains a mixture of the sub-micron materials described above (i.e., amorphous Fe-Mg silicates, phyllosilicates, Fe-sulfides, Fe-oxides and in some cases calcite), mineral fragments (generally forsteritic olivine), polymineralic chondrule fragments, Fe-Ni metal, and coarser prismatic to rounded Fe-sulfides (e.g., Zolensky et al., 1993; Abreu and Brearley, 2010; Harju et al., 2014; Wasson and Rubin, 2009, 2014; Abreu, 2016a).

6.3. CR fine-grained rims

Fine-grained rims are significantly less abundant in CRs compared to CM chondrites (e.g., Abreu, 2007, 2016a; Abreu and Brearley, 2010; Tyra, 2013; Wasson and Rubin, 2009, 2014). In pristine and weakly altered CR chondrites, continuous, well-defined rims are < 200 μm in thickness and consist of homogeneous, fine-grained materials as described above, decorated with magnetite and sulfide crystals (Abreu, 2007; Abreu and Brearley, 2010). In addition to fine-grained rims, Harju et al. (2014) identified smooth rims around chondrules in pristine LAP 02342. These rims are featureless in texture in back-scattered electron images. Harju et al. (2014) argued that these smooth rims are dominated by phyllosilicates formed as a consequence of aqueous alteration. However, Abreu (2016a) performed direct mineralogical characterization of one of these LAP 02342 rims using TEM and found that amorphous Fe-Mg silicates dominated it, suggesting that they might have a similar origin as the rest of CR matrix.

6.3. CR dark inclusions

Most CR chondrites contain numerous, matrix-like, extensively aqueously altered dark inclusions (DI). They are distinct, fine-grained clasts that differ from their host meteorites because they have lower abundances of chondrules and finer-grained matrix material that makes them appear dark in plane-polarized light. They are generally <3 mm along their maximum dimensions (e.g., Scott et al., 1988). Dark inclusions are more abundant in the CR group compared to other chondrites, comprising up to ~ 20 vol.% of the fine-grained materials in some weakly and moderately altered CRs (e.g., Bischoff et al., 1993a,b; Endreβ et al., 1994; Krot et al., 2002). Dark inclusions are unusually large in CR1 GRO 95577 (Weisberg and Huber, 2007; Tyra, 2013).

Despite their textural differences and sharp boundaries with their hosts, the mineralogy of DIs is similar to that of chondritic matrix, resembling particularly that in CI chondrites. Dark inclusions are made of fine-grained silicates, Fe-oxides and sulfides, roughly in order of decreasing abundance. These clasts contain variable amounts of μm-sized opaques, which generally occur as framboidal masses (up to 50 μm in length) or

rounded (<20 μm) Fe-oxides, probably magnetite. Other textures are large, elongated, feathery, and filamentous. Opaques in some DIs are oriented.

7. Presolar grains in CR chondrites

A small portion of presolar grains survived secondary processing in nebular and asteroidal environments and still retained the isotopic signatures of their parent stars. As such, they are identified by their highly anomalous isotopic compositions compared to solar system materials. Numerous presolar phases have been identified in chondritic matrices, including nanodiamonds, SiC and other carbides, graphite, Si_3N_4, oxides, and silicates (e.g., Zinner, 2014). These nanometer- to micrometer-sized grains originated from red giant and asymptotic giant branch (AGB) stars, supernovae (SNe), and novae. Aside from nanodiamonds, silicate grains are the most abundant presolar phase (Zinner, 2014). They are also the most mineralogically and chemically diverse (Nguyen et al., 2016; Floss and Haenecour, 2016a).

Presolar silicates, oxides, and SiC grains have been identified in sixteen CR chondrites of all degrees of aqueous alteration. Their abundances are shown in Fig. 10. We note that reported presolar silicate and oxide abundances obtained by raster ion imaging of thin sections or dense grain separates are lower limits due to beam overlap onto adjacent, isotopically normal grains (Nguyen et al., 2003, 2007).

7.1. Abundance of presolar SiC

Although most studies suggest that the abundance of silicon carbides is higher in CR chondrites than in most other chondritic groups, there are some disagreements, depending on the analytical techniques used. Noble gas analyses indicate that Renazzo has a very low abundance of presolar SiC (1.86 ppm). Huss et al. (2003) interpreted this low abundance as having resulted from moderate temperatures during nebular processing of CR precursors, which destroyed SiC grains. Conversely, in situ isotopic studies of Renazzo matrix and extracted insoluble organic matter (IOM) revealed much higher presolar SiC abundances of 35 – 55 ppm (Davidson et al., 2014a; Floss and Stadermann,

2005; Leitner et al., 2012b). In fact, with few exceptions, the presolar SiC abundances in CR chondrites are ~30-50 ppm, substantiating the view that CRs are among the most primitive chondrites (Fig. 10). Pristine MET 00426, and moderately altered NWA 852 and GRV 021710 have unusually high presolar SiC abundances of 90 ppm, 160 ppm, and 182 ppm, respectively (Floss and Stadermann, 2009b; Leitner et al., 2012a; Zhao et al., 2013). These high abundances could be a consequence of presolar grain clustering in the matrix (e.g., Floss and Stadermann, 2009a), or of the heterogeneous distribution of presolar grains in the CR parent body forming region. Davidson et al. (2014a, 2015) determined the presolar SiC abundances in the insoluble organic matter (IOM) extracted from primitive meteorites of various groups and degrees of alteration. They found that the abundances among seven CR chondrites of petrographic types 1-3 range from 24-47 ppm, with an average of 32 ppm. Primitive chondrites of other groups also have abundances ~30 ppm. Davidson et al. (2014a) concluded that the relatively uniform concentration in CRs of different petrographic types indicates any aqueous and thermal processing experienced in the nebula or in the CR parent body was not extensive enough to destroy SiC grains, and that the distribution of presolar grains in the chondritic forming region was homogenous.

7.2. Abundance of presolar silicates and oxides as indicators of asteroidal processing

The abundances of presolar oxide grains vary widely among different chondritic groups. In CR chondrites, they are <10 ppm, except NWA 852, which has an abundance of 38 ppm (Leitner et al., 2012a). It is unclear whether this variation is due to asteroidal processes, the differential degree to which these processes might have affected different chondritic components, or to the heterogeneous distribution of presolar grains in the solar nebula. A recent study of a carbon-rich clast (CRC) in LAP 02342 thought to originate in a comet (Nittler et al., 2019). This CRC contains an abundance of SiCs that is similar to CR values, but more numerous O-bearing presolar grains. A higher abundance of these presolar materials suggests that the distribution of presolar grains indeed heterogeneous.

CR chondrites have a wide range of concentrations of presolar silicates, reflecting the degree of alteration experienced in the solar nebula and on their parent body (Fig. 10).

The primitive QUE 99177 has among the highest abundance of presolar silicates (150 – 220 ppm) observed in meteorites (Floss and Stadermann, 2009a; Nguyen et al., 2010). This abundance is surpassed only by that of the chondrites DOM 08006 (CO3), MET 00526 (L/LL3.05), and RBT 04133 (CV3), primitive interplanetary dust particles (IDPs), and returned samples from comet Wild 2 (Busemann et al., 2009; Davidson et al., 2014b; Floss and Haenecour, 2016b; Floss et al., 2006, 2013; Nittler et al., 2018). Note that the abundance determined for RBT 04133 is based on only 3 grains and is therefore uncertain (Davidson et al., 2014b), and the calculated abundance for Wild 2 is based on an estimated presolar grain loss rate from sample collection (Floss et al., 2013). Some analyzed regions of QUE 99177 display clusters of presolar grains and have abundances that are analogous to primitive IDPs (375 ppm) (Floss and Stadermann, 2009a). These matrix regions either accreted a higher concentration of presolar grains in the solar nebula or were not altered as much as presolar grain-poor areas. The ratios of presolar silicates to presolar oxides, which have been used to infer the degree of parent body processing, are also very high in pristine QUE 99177 and MET 00426, and in CR2 GRV 021710 (Floss and Stadermann, 2009a; Zhao et al., 2013). These ratios are similar to those observed in primitive IDPs and to the theoretical value from AGB stars (Leitner et al., 2012a), clearly attesting to the primitive nature of these CRs. These samples could, therefore, be a measure of the initial abundances of presolar silicate and oxide grains in the region of the solar nebula where CR parent bodies formed. Conversely, the CR2 NWA 852 has a low presolar silicate/oxide ratio and lower presolar silicate abundance, indicating preferential destruction of presolar silicate grains by aqueous and thermal alteration (Leitner et al., 2012a). Renazzo and GRA 06100 have experienced extensive asteroidal processing and consequently have the lowest abundances of presolar silicate grains among CR chondrites (Leitner et al., 2012b, 2015).

Recent studies suggest that the petrologic setting of presolar grains influences their abundances. Leitner et al. (2016b) conducted a survey of presolar grain abundances in the matrix and fine-grained rims of chondrules of moderately altered NWA 801 and Renazzo, weakly altered EET 92161, GRA 95229, MIL 07525, and pristine MET 00426. The presolar SiC abundances are similar for all the CRs studied. Except for EET 92161 and MET 00426, the presolar silicate and oxide abundances in the rims and the matrices

are the same within 2σ error. However, the combined data for CR2 chondrites indicate that the abundances of presolar O-rich phases (i.e., silicates and oxides) are ~3 times greater in the chondrule rims than in the interchondrule matrix. In contrast, a higher concentration of presolar O-rich grains was found in the matrix of MET 00426. Overall, the presolar O-rich grain abundances in the fine-grained chondrule rims are the same for all of the samples analyzed. Abundances in the matrix are similar, except for MET 00426, which has a significantly higher abundance of presolar silicates and oxides than the CR2 chondrites. Leitner et al. (2016b) suggested that the fine-grained rims accreted onto chondrules in the solar nebula before parent body formation and were less affected by aqueous alteration than the interchondrule matrix material. However, it is noteworthy that petrologic observations do not show systematic differences in the degree of aqueous alteration between interchondrule matrix and rims (e.g., Abreu, 2016a). The much lower abundance of presolar O-rich phases in the fine-grained rims compared to the interchondrule matrix in the pristine CR chondrite must also be accounted for. Haenecour et al. (2018) studied three CO3 chondrites and found that the presolar silicates are more abundant in the matrix than in chondrule rims, whereas the abundances of the presolar SiC are the same. These authors concluded that matrix and rim materials originated from the same nebular reservoir, but pre-accretionary aqueous alteration of the fine-grained rim material destroyed a fraction of the presolar silicates. The possibility that this scenario could be extended to CR chondrites is a subject of current debate.

7.3. Chemical compositions of presolar silicate grains

The chemical properties and mineralogy of circumstellar dust grains have classically been inferred by astronomical infrared spectroscopy. Observations of circumstellar O-rich dust indicate an abundance of amorphous silicate grains of olivine-like compositions (Tielens et al., 1998). These grains are Fe-bearing with estimated Fe contents of ~50% (Kemper et al., 2001). In contrast, the crystalline silicates are extremely Mg-rich, with pyroxene being more abundant than olivine (Molster et al., 2002). The mineralogical and chemical analyses of presolar silicate grains in the laboratory can bring

ground truth to these remote observations, as well as trace the effects of alteration in the solar nebula and on the parent body.

Due to the small size of presolar silicate grains (typically < 300 nm), their chemical compositions are best characterized by Auger spectroscopy (Floss and Stadermann, 2009a; Leitner et al., 2016b; Zhao et al., 2013) and energy-dispersive X-ray spectroscopy (EDX) in the TEM. Presolar silicates from several CR chondrites have been analyzed by these techniques: QUE 99177 (Floss and Stadermann, 2009a; Nguyen et al., 2016, 2017a), MET 00426 (Floss and Stadermann, 2009a; Nguyen et al., 2017b; Stroud et al., 2009), GRV 021710 (Zhao et al., 2013), GRA 95229 and EET 92161 (Leitner et al., 2016b). Most of the grains have stoichiometries consistent with olivine or pyroxene, but about a third have non-stoichiometric elemental compositions in between these minerals. In addition, some grains are Si-poor or Si-rich, and two grains are tentatively identified as SiO_2 (Floss and Stadermann, 2009a; Zhao et al., 2013).

The majority of presolar silicate grains in CRs are ferromagnesian with a small portion containing Ca and/or Al, similar to findings in other primitive chondrites. The Fe-contents are high and vary widely, with up to 31 at.%. The pyroxene grains and those with intermediate compositions are more Fe-rich than olivine grains (Floss and Stadermann, 2009a; Zhao et al., 2013). Presolar silicates from the pristine QUE 99177 and MET 00426 and weakly altered GRA 95229, EET 92161, and GRV 021710 share similar ranges of elemental compositions. However, presolar silicates from GRV 021710 have lower Fe-contents than those from QUE 99177 and MET 00426. This, coupled with the high presolar silicate abundance and matrix petrology, led Zhao et al. (2013) to suggest that GRV 021710 is probably as pristine as QUE 99177 and MET 00426.

The high concentration of Fe in presolar silicates was somewhat unexpected, given the primitive nature of the CR chondrites studied. However, isotopically normal matrix silicates in pristine CR chondrites are also Fe-rich compared to silicates in other chondritic groups, including those that have undergone much more significant aqueous alteration such as the CM chondrites (e.g., Abreu, 2007, 2016a; Abreu and Brearley, 2010). Grain condensation models predict Fe-rich silicates formed under non-equilibrium conditions and Mg-rich silicates under equilibrium conditions (Ferrarotti and Gail, 2001). Thus, Fe could have been incorporated into the presolar silicates during condensation

under non-equilibrium conditions. The silicate matrix in thermally altered chondrites is Fe-rich, and this Fe could have been assimilated into presolar silicate grains during parent body thermal annealing (e.g., Brearley, 1991; Floss and Stadermann, 2012). The fact that the matrix grains in the CR chondrites were not extensively annealed suggests thermal metamorphism was not responsible for their Fe-contents. However, presolar silicates from the CR chondrites have a wider range of elemental compositions and higher Fe-contents than presolar silicates from IDPs (Busemann et al., 2009; Keller and Messenger, 2011; Messenger et al., 2005). These IDPs are more primitive than CR chondrites, and their chemical compositions of the presolar silicates better represent the original presolar compositions. It is thus likely that for many of the CR presolar silicates, most of the Fe was acquired during primary condensation, and secondary alteration enhanced the Fe-content. Of all the presolar phases identified, presolar silicates have the most varied elemental compositions, a consequence of both primary condensation and subsequent alteration.

7.4. Mineralogy of presolar silicate and oxide grains

Nine presolar silicates and one large presolar oxide from CR chondrites have been studied. All originated in AGB stars except for one supernova silicate. The mineralogy of presolar SiC grains in CRs have not been characterized.

The mineralogical characterization of presolar silicate grains attests to their highly diverse nature. Nguyen et al. (2016) studied five presolar silicate grains with sizes < 500 nm from QUE 99177, with one being a euhedral olivine crystal with composition Fo_{80}. The Fe in this grain could have been acquired from parent body alteration, but presolar Fe-bearing olivine crystals have also been identified in anhydrous IDPs that have largely escaped parent body processes (Busemann et al., 2009; Messenger et al., 2005).

Nguyen et al. (2017a) studied a 500×350 nm, Fe-rich, non-stoichiometric, amorphous silicate grain with 3 crystalline silicate inclusions, one of which is an ~100 nm triangular Mg-rich pyroxene, and two are Mg-rich olivine grains that are 45 nm and 90 nm across, respectively. Such compound silicates are rare and provide insight into the conditions around the parent AGB star during grain condensation. The crystalline

silicates formed first at ~1200 K under equilibrium conditions, and the amorphous silicate mantle formed around these grains at a greater radial distance and lower temperature of ~900 K. Their Fe was likely incorporated during condensation, as extensive secondary processing would likely have altered the small crystalline inclusions. Two non-stoichiometric, very Fe-rich amorphous silicates, one of which is a supernova grain, were also identified (Nguyen et al., 2017a). The Fe is uniformly distributed throughout the grains and is likely a primary condensation feature, as QUE 99177 did not undergo thermal metamorphism. These two grains formed under similar non-equilibrium conditions at low temperatures or in an Fe-rich gas. Nguyen et al. (2017b) also analyzed by TEM three presolar silicates from MET 00426 – one is a crystalline Mg-rich olivine and is unusually large for a presolar silicate (2000×750 nm). Strain contrast and dislocations suggest parent body compaction and lithification. A grain comprised of amorphous silicate and nanocrystalline olivine has varying elemental composition on a 10 nm scale, and a presolar silicate of similar structure has a more homogeneous elemental composition (Stroud et al., 2009).

Evidence for radiation damage in space is rare. One presolar silicate from QUE 99177 was found to be an amorphous silicate of stoichiometric enstatite composition with a crystalline enstatite core (Nguyen et al., 2016). The fact that the entire grain has the composition of stoichiometric enstatite suggests it originally formed as a single enstatite crystal but later was partially amorphized by high-energy radiation in space. A portion of the grain is rimmed with Fe, which Nguyen et al. (2016) argued was likely acquired from surrounding grains during parent body alteration.

In addition to the silicates, Leitner et al. (2012a) studied a large (1750×300 nm^2) presolar Al-rich hibonite crystal ($CaAl_{12}O_{19}$) from NWA 852. The grain has micro-cracks caused by stress from grain-grain collisions. The hibonite contains a central <100 nm perovskite-like sub-grain with a Ca/Ti ratio ~1, which formed at high temperature in a Ti-enriched gas before being enclosed in the host crystal.

8. Carbonaceous materials in CR chondrites

The carbonaceous material in CR chondrites, with a bulk carbon content between 0.3-2.5 wt.% (Bischoff et al., 1993a; Cody et al., 2008), has been of particular interest, as it may shed light on the chemical activity of organics from their formation in interstellar environments to their incorporation into asteroidal bodies.

8.1. Soluble organic materials in CR chondrites

The molecular diversity of soluble organic compounds in CRs has been studied using high-field nuclear magnetic resonance and ultrahigh-resolution mass spectrometry, resulting in an estimated millions of unique chemical structures of organic compounds that remain free and that are readily extractable using water and other polar and non-polar solvents. Given the impossibility of identifying each individual molecular structure, chondritic soluble organic compounds are traditionally extracted and analyzed as groups of compounds sharing the same chemical functionalities (Glavin et al., 2011, 2018). The total numbers of molecular species that have been extracted from CRs to date are listed in Table 9 (concentrations in ppm or μg/g of meteorite).

8.1.1. Amino acids

Aliphatic primary monoamino, monocarboxylic, nonheteroatom (or "simple") amino acids are some of the building blocks for proteins and enzymes in all terrestrial life. Based on their astrobiological importance, these compounds have been extensively studied in carbonaceous chondrites (Burton et al., 2012a-b; Cobb and Pudritz, 2014; Elsila et al., 2016).

Concentrations of amino acids in some pristine and weakly altered Antarctic CRs are the highest ever recorded from any group of carbonaceous chondrite (Glavin et al., 2011). The total amino acid concentrations in CR chondrites range from a few to over 300 ppm (Table 9). Two other independent laboratories confirmed the high abundance of amino acids in CRs (Pizzarello et al., 2008, 2012; Pizzarello and Holmes, 2009; Glavin et al., 2011). Although the total concentrations of amino acids in CR2 Renazzo are similarly low as those in the CIs Orgueil and Ivuna (Botta et al., 2002), amino acids in weakly

altered CRs EET 92042 and GRA 95229 are at least 10 times higher than those found in CM2 chondrites such as Murchison and Murray (Martins et al., 2007).

Amino acids in CR chondrites appear to be primarily dominated by α-amino isomers, though their complete molecular diversity has not been fully investigated. The high abundance is of the same order of those in moderately aqueously altered CM2 chondrites (Glavin et al., 2011) and differs from what is seen in heavily aqueously altered and thermally metamorphosed carbonaceous chondrites, which are richer in β- and other *n*-ω-amino acid isomers (Ehrenfreund et al. 2001; Burton 2012a-b; Elsila et al. 2016). The high abundance of α-amino acids in CR chondrites suggests the Strecker-cyanohydrin synthesis as one of the most active mechanisms generating amino acids in the CR parent body (Peltzer et al., 1984; Lerner et al., 1993; Matthews and Minard, 2008).

One significant similarity between amino acids in CR and those in CI and CM chondrites is the L-enantiomeric excess of isovaline in CR1 GRO 95577 ($ee_{\text{L-isovaline}}$ = 11.0 ±7.2‰; Glavin et al., 2011). Isovaline is an α-methyl-α-amino acid, and thus it is not susceptible to the loss of enantiomeric enrichment or racemization through aqueous or radiogenic processing on geological timescales (Pollock et al., 1975; Bonner et al., 1979). In addition, isovaline is not very common in the terrestrial biosphere and has shown large heavy isotope enrichments (D/H, $^{13}C/^{12}C$, $^{15}N/^{14}N$) in CR2 and CM2 chondrites (Elsila et al., 2012). Isovaline can be a product of the Strecker-cyanohydrin synthesis through aqueous alteration inside a parent body, using an achiral ketones (2-butanone) as starting material. Although the exact mechanisms for the break in symmetry and amplification of a small enantiomeric excess are subject of ongoing debate (Takano, 2007; De Marcellus et al., 2011; Meinert et al., 2014; Modica et al., 2014), a correlation between the L-enantiomeric excesses and degree of aqueous alteration experienced in their parent bodies has been observed for CR, CM, and CI chondrites (Glavin and Dworkin, 2009; Glavin et al., 2011).

8.1.2. Amines

Acyclic aliphatic monoamines ("amines") are compounds that are structurally related to amino acids and, therefore, their study provides insights about the synthesis of chondritic amino acids. Pizzarello et al. (2008) were the first to report the presence of amines in CRs. They found that, similar to amino acids, amines were more abundant in CRs than in CM chondrites (Pizzarello and Holmes, 2009; Pizzarello et al., 2012).

There are both similarities and differences between amines in CR and CM chondrites. For example, there is a trend in both CM2s and CR2s for amines to have the amino group ($–NH_2$) on a secondary carbon, compared with having the $–NH_2$ in a primary or tertiary carbon. Contrary to amines in CM chondrites, the abundance of some of the homologous series of the CR2 amines does not decline with increasing length of chain. This observation was confirmed by Aponte et al. (2016), who also found that isopropylamine is the most abundant amine species in CR2 chondrites, while methylamine is the most abundant in CM2 and CM1/2 chondrites. The ratios of amino acids to amines concentration are different for CR and CM chondrites. In CRs, the concentration of amino acids is higher than that of amines. In CM chondrites, however, amines are more abundant than amino acids. Aponte et al. (2016, 2018) interpreted these differences as either original signatures of distinct parent bodies, or as evidence that aqueous alteration, which was more active in the CM parent body, was more destructive to amino acids than to amines.

Like amino acids, some amines can be chiral and, thus, might potentially exhibit enantiomeric excesses, such as those reported for isovaline. The structural analog of isovaline is *sec*-butylamine, and a large range of enantiomeric compositions has been reported for this α-methyl-amine. Pizzarello and Yarnes (2016) reported enantiomeric distributions of (*S*)-*sec*-butylamine ranging from 0% to 66% in five Antarctic CRs. In contrast, Aponte et al. (2016) reported only racemic compositions for *sec*-butylamine in three Antarctic CR chondrites, which include GRA 95229 and LAP 02342 previously investigated by Pizzarello and Yarnes (2016). Aponte et al. (2016) explained the differences in enantiomeric compositions reported for *sec*-butylamine extracted from the same meteorites as the result of sample heterogeneities. However, a thorough examination of the methodology used for extraction and derivatization of amines might not rule out the potential for sample contamination and deracemization. It remains likely

that the different enantiomeric compositions might originate from the different methodologies used. Regardless, studies of the anisotropy of aliphatic amines and amino acids suggest that ultra-violet circularly polarized light (UVCPL) might induce enantiomeric excesses in aliphatic amino acids, but not in aliphatic amines (Meinert et al., 2012, 2016; Myrgorodska et al., 2017).

8.1.3. Monocarboxylic acids

Until recently, the abundances of monocarboxylic acids (MCAs) in CR chondrites were believed to be lower than those in Murchison. Antarctic CR2s GRA 95229 (Pizzarello et al., 2008, 2012) and EET 87770 (Aponte et al., 2011) were the first CR2 chondrite analyzed for acyclic aliphatic monocarboxylic acids. Both meteorites have substantially lower contents of MCAs than CM chondrites. However, a new study reevaluated the abundance of MCAs in GRA 95229 and quantified the abundances in LAP 02342, MIL 090657, and MIL 090001 (Aponte et al., 2019). These measurements suggested that the total abundances of MCAs, just like those of amino acids and amines, are higher in CRs than in all other investigated chondrites. The disagreement in measurements was attributed to instrumental causes. MCAs measurements require preparatory and analytical methods (i.e., multi-stepped extraction, purification, and derivatization methods), as well as the use of different analytical instrumentation in different laboratories, which might introduce significant bias and contribute to the difficulty in cross-comparison of meteoritic organics (Glavin et al., 2011). Indeed, MCAs in CRs are the highest among all chondritic soluble organics and approach those for chondritic carbonates and insoluble organic matter (IOM; Aponte et al., 2019).

Like amino acids, but contrary to aliphatic amines, the abundance of MCAs decreases with increasing molecular weight – acetic acid being the most abundant in all CRs. Also, the abundance of MCAs decreases linearly with increasing aqueous alteration and thermal metamorphism of the host meteorite (Aponte et al., 2019).

Similar to aliphatic amino acids and amines, MCAs can be chiral, 2-methylbutanoic acid being the structural analog of isovaline and *sec*-butylamine. The enantiomeric composition of 2-methylbutanoic acid has been determined for CM and CR

chondrites using a variety of methods, and in some cases, they are racemic (Pizzarello et al., 2008, 2012; Aponte et al., 2014, 2019). The racemic composition of chondritic 2-methylbutanoic acid is consistent with that of *sec*-butylamine, as anisotropy studies of both molecules have suggested that UVCPL may not be able to induce enantiomeric excesses in them (Meinert et al., 2016). Thus, no amplification of an original imbalance is expected to occur inside the asteroid parent body. The lack of enantiomeric excess in 2-methylbutanoic acid and *sec*-butylamine suggests that these compounds may have been racemic before their incorporation to the parent body or that the processes that resulted in the L-enantio-enrichments in its structurally analogous amino acid, isovaline, did not have a significant effect on them.

8.1.4. Other soluble organic compounds

Analyses of other aliphatic and aromatic soluble organics reported from CR chondrites include aldehydes and ketones, hydroxy monoaldehydes, polyols, hydroxy monocarboxylic acids, dicarboxylic acids, hydrocarbons, polycyclic aromatic hydrocarbons (PAHs), and purines (Table 9; -Pizzarello et al., 2008, 2012; Cooper and Rios, 2016; Callahan et al., 2011). Compared to amino acids and MCAs concentrations in CRs, these compounds constitute trace species, and in some cases, their presence has been questioned. The detection and quantification of purines in CRs is an important case study. As discussed above, CR chondrites contain the largest amount of amino acids, amines, and MCAs among carbonaceous chondrites, including the C-rich CM group. Additionally, ammonia (NH_3), which is thought to be a key starting material for the abiotic synthesis of purines (Callahan et al., 2011), has been reported as one of the most abundant inorganic species present in CRs. Further, only trace amounts of ammonia were detected in the CM2 Murchison (Pizzarello et al., 2011; Pizzarello and Williams, 2012). Purines, however, unlike other nitrogen-bearing molecules, were found in low concentrations in CR chondrites (Callahan et al., 2011).

8.2. Insoluble organic materials in CR chondrites

Based on their exotic isotopic signatures, extracts of insoluble organic material (IOM) and solid carbonaceous material from CR chondrite matrices may contain a component of interstellar organics (e.g., Ash and Pillinger, 1995; Messenger et al., 2000; Cody and Alexander, 2005; Busemann et al., 2006, 2007; Pizzarello et al., 2006; Alexander et al., 2007).

The complexity of carbonaceous material in carbonaceous chondrites is most likely the result of multistage processing through a variety of mechanisms in several diverse environments. Organic compounds may have formed by a combination of some or all the mechanisms that operated in the interstellar medium, solar nebula, and asteroidal parent bodies (Gilmour, 2003). A component of the organics in meteorites probably formed in diffuse interstellar regions and was later injected into the molecular cloud from which the solar nebula originated (Sanford, 1996; Sanford et al., 2001). This material likely experienced further synthesis and processing in the solar nebula and planetesimals by aqueous alteration and thermal processing (e.g., Kerridge, 1999; Gilmore and Pillinger, 1994).

8.3. Carbonaceous materials and their relationship with CR matrices

A variety of microbeam techniques has been used to characterize organic matter *in situ*. TEM observations showed that carbonaceous materials are distributed at the nanoscale in a variety of textural occurrences (e.g., Abreu, 2007; Floss et al., 2014; Le Guillou and Brearley, 2014; Le Guillou et al., 2014). Le Guillou and Brearley (2014) documented the presence of nanoglobules, elongated veins, and networks of sub-rounded grains connected by cracks. They attributed these textural differences to variations in the degree of aqueous alteration of organics, which had originally accreted into the CR parent body as ice-organics particles. Organic materials show a very low degree of graphitization (e.g., Abreu, 2007; Le Guillou and Brearley, 2014). These organics occur both as isolated masses and in association with nano-sulfides, tochilinite, carbides, magnetites, and phyllosilicates (e.g., Abreu, 2007; Le Guillou and Brearley, 2014). Le Guillou et al. (2014) observed that CR2 Renazzo contains individual grains of molecularly homogeneous organic materials, but in some cases have heterogeneous

morphologies and D/H ratios. They speculated that these grains probably contained insoluble organic compounds. Consistent with TEM observations, Auger microscopy showed that organic grains had both nanoglobule and irregular morphologies. TEM analysis revealed a high degree of crystallographic disorder (Floss et al., 2014). They found no correlations between isotopic composition and morphology, petrographic association, or elemental composition and suggested that the diffuse regions formed by redistribution of organics during aqueous alteration. Based on comparative studies with CI (Orgueil) and CM (Murchison) chondrites, Le Guillou et al. (2014) also argued that organic materials were altered during aqueous alteration.

Abreu (2007) suggested that some of the organic materials in CR chondrites must have formed or been reprocessed after interstellar synthesis, favoring Fischer-Tropsch type synthesis as a mechanism playing a role in the formation of organics in the solar nebula based on the mineral-organic spatial relationships. She suggested that the association between nanophases and carbonaceous materials resulted from Fischer-Tropsch type reactions. Catalysis would have occurred below ~ 300ºC, probably during nebular cooling after the formation of sulfides and amorphous Fe-Mg silicates during high-temperature evaporation and recondensation events. This solar carbonaceous material would later be mixed with an interstellar component, giving rise to the exotic isotopic signatures characteristic of CRs.

Based on coordinated NanoSIMS, Auger, and FIB-TEM, organics in CR chondrites are isotopically anomalous with respect to solar system values (e.g., Floss and Stadermann, 2009a,b; Floss et al., 2014). Floss and Stadermann (2009a) reported the presence of both ^{13}C-enriched and ^{13}C-depleted organic regions in CRs. Additionally, Floss et al. (2014) found that organic matter has solar carbon isotopic compositions, but significant enrichments in ^{15}N compared to solar (average ~ 195‰).

9. Processes affecting the CR parent asteroid(s)

9.1. Aqueous alteration of CR chondrites

The interest in secondary minerals in CRs stems from the fact that this group contains some of the least and the most aqueously altered carbonaceous chondrites in our collections. A summary of the effects of aqueous alteration in different petrologic CR types is given in Fig. 11. Even the earliest studies of CR chondrites recognized that they contained hydrous silicates (e.g., Mason and Wiik, 1962). The presence of these silicates placed most CRs in between petrologic types 2 and 3 but considered them unusual as they preserved metallic Fe (e.g., Mason 1971).

Compared with the other hydrated carbonaceous chondrites, CRs are not as water-rich. However, some CRs have affinities with both the CM and CI chondrites (e.g., Bischoff et al., 1993a,b; Zolensky et al., 1993; Kallemeyn et al., 1994; Abreu 2016a). Alteration of CIs resulted in the formation of phyllosilicates, oxides, carbonates, sulfides, and sulfates (Kerridge et al., 1979; Tomeoka and Buseck, 1985; Tomeoka et al., 1988; Zolensky et al., 1993). CR, CI, and some CM chondrites contain framboidal and platelet magnetite. Alteration of CM matrices resulted in the formation of phyllosilicates, tochilinite, carbonates, Fe-sulfides, sulfates, oxides, and hydroxides (e.g., Browning et al., 1996; Chizmadia and Brearley, 2008; de Leuw et al., 2010; Hanowski and Brearley, 2001; Hewins et al., 2014; McSween Jr, 1979a,b; Rubin et al., 2007; Tomeoka and Buseck, 1985; Zega and Buseck, 2003; Zolensky et al., 1993). Most of these minerals are also present in the CRs, though in lesser abundances.

9.1.1. Effects of aqueous alteration on CR chondrite components

Differences in the degree of alteration originated from the fact that CR chondrites are made up of materials that are not uniformly susceptible to aqueous alteration. Alteration affected chondrule materials to a lesser extent than CR matrices.

Petrologic observations suggest that chondrule phenocrysts and Fe-Ni metal nodules in all but the most altered CR largely escaped aqueous alteration. In extensively altered GRO 95577, most silicate phenocrysts in chondrules were replaced by phyllosilicate pseudomorphs, ranging in sizes from less than 0.05-2 mm (e.g., Weisberg and Huber, 2007; Tyra, 2013; Harju et al. 2014; Abreu, 2016a). Unaltered Fe-Ni metal, occurring as

individual crystals and associated with chondrules, has also been preserved (Krot et al., 2002). However, chondrule mesostasis has been affected by aqueous alteration even in weakly altered CRs (e.g., Ichikawa and Ikeda, 1995; Weisberg et al., 1995; Burger, 2005; Keller, 2011). In these CRs, anhydrous mesostasis silicates have been partially to completely altered to serpentine, saponite, and chlorite (Ichikawa and Ikeda, 1995; Weisberg et al., 1995). Weisberg et al. (1993) reported the mobilization of Ca from a Ca-carbonate rim on the curved surface of a chondrule fragment in Y 790112. Burger (2005) observed extensive replacement, most notably when mesostases were in direct contact with fine-grained matrix in two type II chondrules in paired EET 87770 and EET 92105. He found that whereas unaltered mesostasis regions were albite normative, Na and K were leached from altered mesostasis. In contrast, altered mesostasis and adjacent matrix had high Ca abundance. Burger (2005) added that Ca and P mobilization occurred early in the alteration process. This assertion was supported by later FIB/TEM observations, showing that even in the glassy mesostasis, alteration proceeded by the removal of Ca and P through the formation of Ca-phosphate veins (Brearley and Burger, 2009).

Matrices in CRs have been replaced to different extents by Fe-Mg phyllosilicates (predominantly serpentine), framboidal magnetite, and minor calcite (e.g., Weisberg et al., 1993; Zolensky et al., 1993; Kallemeyn et al., 1994; Abreu and Brearley, 2010; Le Guillou et al., 2015a,b; Abreu, 2016a).

9.1.2. Effects of aqueous alteration on the oxygen isotopes of CR chondrite components

The oxygen isotopic composition of CR chondrule and matrices has been evaluated to place constraints on their aqueous alteration histories. CR chondrules show high $\delta^{17}O$ and $\delta^{18}O$, which have been interpreted as evidence for aqueous alteration (Krot et al., 2002). However, enrichments are not evenly distributed throughout all chondrule components. In contrast, Jilly-Rehak et al. (2018) argued that the variations in oxygen isotopic compositions of matrix minerals in CR chondrites resulted from aqueous alteration processes affecting the CR parent body in a very heterogeneous manner. They

suggested that their observations are inconsistent with carbonates in CR chondrites forming from a single, uniform fluid. They concluded that O-isotopic compositions of the altering fluids evolved from approximately the Al Rais water composition of $\Delta^{17}O \sim 1‰$ and $\delta^{18}O \sim 10‰$, to become increasingly ^{16}O-enriched toward a final fluid composition of $\Delta^{17}O \sim -1.2‰$ and $\delta^{18}O \sim -15‰$. These water compositions may not be consistent with alteration by extremely heavy water compositions such as those recorded from cosmic symplectite found in Acfer 094.

9.1.3. Petrologic sub-types of aqueously altered CR chondrites

A large gap in samples exists between CR chondrites that record intermediate and those that record very extensive aqueous alteration (e.g., Alexander et al., 2013; Harju et al., 2014; Howard et al., 2015a; Abreu, 2016a). With the exception of CR1 GRO 95577, CR chondrites fall between to petrologic types 2 and 3 (e.g., Zolensky et al., 1993; Kallemeyn et al., 1994; Weisberg and Prinz, 2001; Perronnet and Zolensky, 2006; Abreu and Brearley, 2010; Wasson and Rubin, 2014; Le Guillou and Brearley, 2014; Le Guillou et al., 2015a,b; Abreu 2016a).

Three scales have been devised to quantify the degree of aqueous alteration of CRs, with particular emphasis on assigning sub-types to the CR2 chondrites. The first scheme is based on the observation that there is a linear relationship between the bulk H, C, and N elemental and isotopic compositions of CM and, to a lesser extent, CR chondrites (Alexander et al. 2013). The authors used this correlation to assign petrologic subgroups. The second scheme is based on petrologic criteria. Harju et al. (2014) postulated to classify the CRs based on (1) presence/abundance of chondrules containing altered mesostasis, (2) presence/abundance of magnetite, (3) replacement of primary silicate phenocrysts by phyllosilicates, (4) replacement of Fe-Ni metal with oxides, (5) abundance of phyllosilicates in matrix and chondrule rims and (6) S-content of the matrix. Finally, Howard et al. (2015a) used the ratio of phyllosilicates to anhydrous silicates (i.e., olivine and pyroxene) to assign petrologic sub-types. Although the classification schemes proposed by Alexander et al. (2013) and Howard et al. (2015a,b)

are generally consistent with each other, these schemes often disagree with petrologic classifications (Harju et al., 2014) and sub-micron observations (e.g., Abreu 2016a).

Petrology-based classifications require understanding the sequence of mineral replacement and how these replacements relate to aqueous alteration. Abreu (2016a) suggested that differences in classifications might arise from the fact that CRs have very fine-grained matrices dominated by amorphous Fe-Mg silicates, by their abundant Fe-Ni metal, and by extensive brecciation. Identifying evidence of incipient mineral replacement is particularly challenging for CR chondrites because secondary phases are generally very fine-grained. Furthermore, primary and secondary matrix phases are mixed at the sub-micron scale (e.g., Abreu and Brearley, 2010). Abreu (2016) suggested that a multi-technique approach is needed to determine the degree of aqueous alteration of these meteorites. While the bulk elemental and isotopic compositions of CRs provide valuable insights on how prevalent the changes observed at the nanometer scale are, Abreu (2016a) suggested that several characteristics of the CRs limit their applicability as indicators of aqueous alteration. First, these bulk measurements are affected by terrestrial weathering and impact processes. Second, CRs contain variable amounts of clasts from different regions of the CR parent body or from altogether different planetary bodies (i.e., Hiyagon et al., 2016; Abreu, 2013; MacPherson et al., 2009); consequently gram-size samples may contain numerous clasts recording diverse aqueous alteration histories. Third, intra- and inter-sample variations in CR matrix and dark inclusion abundances are too large to allow to resolve CR sub-groups based on bulk compositional and isotopic data alone (Abreu, 2016a). Overcoming these obstacles requires bulk data to be woven together with sub-micron observations.

9.1.4. Constraints on the timeline for CR aqueous alteration

The duration of aqueous alteration, the effect on individual components, and the classification of aqueous alteration features have been studied to improve our understanding of the history of water in the CR parent body. Some have used ^{53}Mn–^{53}Cr systematics of carbonates to constrain the duration of aqueous alteration in the CR parent

body (Tyra, 2013; Jilly-Rehak et al., 2017). Jilly-Rehak et al. (2017) found that whereas alteration of CR2 Renazzo was contemporaneous with unique carbonaceous chondrite Tagish Lake, CI, and CM chondrites, they found that CR1 GRO 95577 preserved much younger carbonates. They argued that the older carbonates found in most CR chondrites (such as calcite and dolomite measured in Renazzo) likely formed via parent body aqueous alteration driven by the presence of liquid water heated by ^{26}Al decay, similar to carbonates in CM, CI, and CO chondrites. However, the ages that both Jilly-Rehak et al. (2017) and Tyra (2013) obtained for GRO 95577 carbonates are too young to be easily explained by decay-driven hydrothermal alteration in a typical chondritic parent body. Jilly-Rehak et al. (2017) proposed two scenarios. First, that the CR parent body was large enough (30-50 km radius) for heat from radiogenic decay to be retained even 8 Myr after accretion. Second, that episodic formation of secondary phases ensued as a consequence of impact-driven metamorphism.

9.1.5. Stages of CR aqueous alteration

Authors argued that aqueous alteration of CR chondrites occurred at low temperatures and involved multiple stages (e.g., Le Guillou et al., 2015a; Jilly-Rehak et al., 2018). Le Guillou et al. (2015a) suggested that aqueous alteration of CR matrices took place on the CR parent body and was a two-step process that began with hydration and oxidation of nebular amorphous Fe^{2+}–Mg silicates to produce metastable, predominantly Fe^{3+} amorphous Fe–Mg silicates, followed by formation of Fe–Mg phyllosilicates with lower $Fe^{3+}/\sum Fe$ ratios (e.g., 55% in extensively altered Al Rais and GRO 95577). Le Guillou et al. (2015b) carried out experimental studies that suggest that these early replacement reactions took place at approximately 90^{o}C. Consistent with these experiments, Jilly-Rehak et al. (2018) measured the oxygen isotopic fractionation between carbonates and magnetites and calculated the precipitation temperatures of these phases to be ~ 60^{o}C. For closed-system alteration of the CR parent body, Jilly-Rehak et al. (2018) estimated that its global temperature during alteration was ~55-88^{o}C, which is generally consistent with the temperatures for phyllosilicate formation.

9.2. Thermal metamorphism of CR chondrites

Mild effects of heating have been consistently reported in CR chondrites. Heating mechanisms include high-temperature reduction, giving rise to low Co and Ni contents at the edges of Fe-Ni metal grains (Lee et al., 1992). Some redistribution of Cr_2O_3 in type II chondrule olivines has been reported (Schrader et al., 2015; Abreu, 2016b).

Most CR chondrites show metamorphism consistent with petrologic types <3.2 (Briani et al., 2013; Schrader et al., 2015). There are two known exceptions, GRA 06100 and GRO 03116, which appear to have been heated to temperatures corresponding to petrologic types as high as 3.6 (Abreu and Singletary, 2011; Abreu and Bullock, 2013; Briani et al., 2013; Schrader et al., 2015). These studies argued that the mechanism driving heating in GRA 06100 and GRO 03116 had a short duration and consistent with an impact event. Briani et al. (2013) studied the effect of thermal metamorphism on the Ni content of Fe-Ni metal nodules, the hydration state of matrix minerals, and the structure and composition of organic matter of fifteen meteorites. Using infrared spectra, Briani et al. (2013) found that, unlike other CR chondrite matrices, the matrices of GRA 06100 and GRO 03116 show significant signs of dehydration. Their organic materials have low carbonyl abundances and high CH_2/CH_3 ratios compared to CRs that were not affected by heating. They concluded that the thermal metamorphism style of the CRs is different from that of other chondrites, in which heating has been attributed to the decay of short-lived radioisotopes. Schrader et al. (2015) measured the effects of thermal metamorphism on the major and minor element abundances of olivine, pyroxene, metal, and sulfides from 15 unpaired CR chondrites. They found that the least thermally altered CR chondrite is EET 96259, followed by QUE 99177, and the most heated is Y-793495, followed by NWA 801, GRA 06100, and EET 87770. However, they cautioned that because type II chondrules are scarce in CR chondrites, some variations in the ordering of these meteorites might be possible.

Abreu and Bullock (2013) studied the effects of thermal metamorphism on opaque minerals in one of the two heated CRs, GRA 06100. They concluded that opaques in GRA 06100 formed through shock metamorphism, followed by shock-driven

hydrothermal alteration of chondrule Fe-Ni metal and chondrule and matrix Fe-(Ni) sulfides. Opaque assemblages in GRA 06100 are aggregates of exotic, high-temperature minerals found in type I and type II chondrules. Therefore, they differ from type II chondrule Fe-Ni metal-sulfide assemblages (e.g., Schrader et al., 2015). Iron-nickel metal in GRA 06100 is rare and dominated by Ni-poor and Ni-rich intergrowths, in which Co appears to have preferentially partitioned into kamacite. Kimura et al. (2008, 2011) observed similar compositional trends in other carbonaceous chondrites and attributed them to thermal metamorphism. Abreu and Bullock (2013) found kamacite-taenite assemblages in GRA 06100, surrounded by fine-grained (<50 microns) phases, including suessite and a diaplectic glass that observed in shocked ureilites (e.g., Rubin, 1988). Other accessory phases include Ti-Cr-Fe-Ni alloys, as well as the high-temperature hydrothermal phosphate-sulfate scorzalite-lazulite and the carbonate ankerite (Abreu and Bullock 2013). Furthermore, these authors noted that opaque assemblages in GRA 06100 are similar in texture and mineralogy to those formerly known as Fremdlinge located in CAIs in CV chondrites (e.g., Blum et al., 1988, 1989). In fact, major, minor, and trace element siderophile element patterns spanning a broad range of volatilities show very similar trends. It is generally accepted that Fremdlinge formed through a complex sequence of high-temperature asteroidal processes. Such processes are consistent with other evidence observed in GRA 06100 opaques, further supporting the hypothesis that this meteorite was processed at temperatures hundreds of degrees higher than other CR chondrites.

Based on observations from GRA 06100, Abreu and Bullock (2013) argued that the CR parent body records at least one impact event in which the initial shock heating resulted in the formation of Ni-poor and Ni-rich subgrains, mobilization of Fe from precursor Fe-Ni metal that created ephemeral shock veins, formation of suessite, and overall comminution and deformation. Subsequent aqueous alteration gave rise to the Fe sulfides and Fe oxides that dominate the mineralogy of opaque assemblages and cracks throughout the meteorite. Exchange of shock metamorphic gases and fluids probably occurred on a centimeter-scale, based on the characteristics of partly filled cracks and low abundances of sulfur in the adjacent matrix.

9.3. Regolith processes affecting CR chondrites

Physical mixing by asteroidal impacts, which has operated throughout the history of asteroids, modified their composition and mineralogy at scales ranging from individual grains to whole bodies (e.g., Bischoff et al., 2006). Impacts resulted in brecciation, regolith gardening, and derivative deformation and mechanical mixing of chondritic fragments sampling a broad range of degrees of thermal and/or aqueous alteration. CR chondrites record evidence of mixing of materials formed in different locations of an asteroid or in altogether different parent bodies. CR chondrites contain two types of foreign lithic fragments: water-rich dark inclusions, and high-pressure xenoliths.

Dark inclusions are juxtaposed against hosts with often widely different degrees of aqueous alteration. The relationship between the host CR chondrites and dark inclusions has not been clearly established. In early studies, Endreß et al. (1994) suggested that CR matrix and DIs bear no genetic relation, based on isotopic evidence, and may have been altered in completely different environments. However, Zolensky et al. (1993) argued that despite the differences in texture and grain size, CR matrices and dark inclusions are genetically related. They suggested that the matrix originated from secondary processing of dark inclusion-material. Subsequent petrologic studies of DIs and matrix show that the abundance of secondary minerals is larger in DIs, indicating that these materials cannot be the precursor of CR matrices but placing no constrains on whether these occurrences are otherwise related (e.g., Abreu, 2007). Jilly-Rehak et al. (2018) observed that carbonates in interchondrule matrix and dark inclusions plot along a single line with slope ~ 0.7, which they interpreted as both lithologies recording alteration by a single evolving fluid on the CR parent body. In addition, the dolomite from dark inclusions in Renazzo yields the same Mn-Cr ages as the calcite in the Renazzo's matrix (Jilly-Rehak et al., 2017), supporting contemporaneous alteration. Finally, it is also possible that some DIs might have formed in the CR parent body, while others had a different origin.

9.4. High-pressure xenoliths from planetary-sized bodies

Two CR chondrites - QUE 99177 and NWA 801 - contain xenolith clasts formed under high pressures, possibly inside large planetary bodies (Abreu, 2007, 2013; Kimura et al., 2013; Hiyagon et al., 2016). These clasts share unusual mineralogical characteristics, most prominently the presence of omphacite, a high-pressure pyroxene that has not been identified in any other meteorite group. Images from the omphacite-bearing clast in QUE 99177 are shown in Fig. 12.

Omphacite clasts have distinct petrographic fabrics. Abreu (2007, 2013) found a clast in pristine QUE 99177 that consists of matrix (~48 vol.%) that is partially integrated with chondrule-like objects that have poorly defined boundaries. The matrix in this clast contains coarse (micron-sized), interlocking, compositionally equilibrated crystals, including graphite laths. The chondrules are extensively recrystallized. They contain no mesostasis, metal, or graphite. Kimura et al. (2013) found clasts that contained omphacite in NWA 801. Unlike the clast in QUE 99177, Kimura et al. (2013) reported that the clasts in NWA 801 did not have a chondrite-like lithology. They described the clasts as assemblages of a finer-grained "graphite-bearing lithology" and coarse-grained "graphite-free lithology." The graphite-bearing lithology represented ~10 vol.% and was dominated by micron-sized silicates. They did not identify chondrule relicts in these clasts.

Clasts in QUE 99177 and NWA 801 shared some mineralogical features. The dominant minerals in clasts in both QUE 99177 and NWA 801 are olivines and pyroxenes. Olivines in the three clasts in NWA 801 are more equilibrated and have slightly higher MgO contents compared to those in the clast in QUE 99177. For the clast in QUE 99177, the olivine compositions range from Fo_{59-64} and $Fo_{62.6}$ average (Abreu, 2013) versus Fo_{66-68} and $Fo_{67.2}$ average for NWA 801 clasts (Kimura et al., 2013). Pyroxenes in the clasts in both meteorites have very similar compositions ($En_{74.0}Fs_{24.4}Wo_{1.5}$ average for QUE 99177 clast; and $En_{73.2}Fs_{26.1}Wo_{0.7}$ average for NWA 801 clasts; Kimura et al., 2013). In both meteorites, graphite crystals in all clasts are interspersed within the fine-grained silicates. However, the graphite crystals in the clast in QUE 99177 are coarser-grained (up to 70 μm) and more abundant than in the clasts in NWA 801 (Abreu, 2007, 2013).

The accessory mineralogy is also similar in all these clasts. In both meteorites, the clasts contain sulfides (pentlandite and troilite) and hydrous phases. The clast in QUE

99177 contains amphiboles (pargasite and pargasitic hornblende), whereas the ones in NWA 801 have small amounts of the phyllosilicate phlogopite. Those in NWA 801 contain chloroapatite and metallic Fe, which have not been identified in the clast in QUE 99177 (Abreu, 2007, 2013; Kimura et al., 2013; Hiyagon et al., 2016). Unlike the clast in QUE 99177, those in NWA 801 contain garnets with large pyrope and almandine components (Kimura et al., 2013). Coexisting omphacite and garnets indicate that these clasts formed in an eclogite-like environment (Kimura et al., 2013).

The characteristics of omphacite indicate that these clasts had different formational histories (Abreu, 2007, 2013; Kimura et al., 2013). The crystal structure of omphacites has been used as a proxy for pressure in terrestrial rocks. The P2/n polymorph indicates high cation ordering, whereas the C2/c corresponds to a higher temperature, higher disordered structure (Fleet et al., 1978; McNamara, 2012; Moghadam et al., 2010; Oberti and Caporuscio, 1991). In slow exhumation in terrestrial tectonic settings, disordered C2/c transitions to the P2/n polymorph (Fleet et al., 1978). An omphacite crystal in the QUE 9177 clast was indexed as P2/n, which corresponds to high cation order. In contrast, omphacites in the clasts in NWA 801 have C2/c structure. These differences might indicate that: (1) omphacite in the QUE 99177 clast formed at a slower rate than in the NWA 801 clasts; (2) these xenoliths were excavated at different rates (highly unlikely), or (3) the clast in QUE 99177 underwent a later metamorphic event that is not recorded by the clasts in NWA 801.

The chemical composition of omphacite suggests that the clasts in NWA 801 formed under higher pressures than the one in QUE 99177, as suggested by its higher Al_2O_3 contents. Hiyagon et al. (2016) reported that omphacites in the NWA 801 clasts are more equilibrated than in the clast in QUE 99177, Na-rich, Ca-poor and more ferroan compared with omphacites in the QUE 99177 clast (i.e., 5.8-7.3 wt.% FeO; Kimura et al., 2013 vs. 5.2 wt.% FeO; Abreu, 2013) and higher in Al_2O_3 (7-9.4 wt.% vs. 6.6 wt.%).

Calculations of minimal overburden pressures for these clasts were performed by very different methods and with very different results. Kimura et al. (2013) used terrestrial geothermobarometers because clasts in NWA 801 have coexisting olivine, pyroxenes, and garnet (garnet is not present in the clast in QUE 99177). They estimated that 2.8–4.2 GPa and 940–1080 °C were required to form the clasts in NWA 801. In

contrast, the compositional and crystallographic features of the QUE 99177 clast indicate that omphacite formed at pressures in excess of 6 GPa (Abreu, 2007, 2013). This pressure corresponds to an overburden depth of ~760 km if typical B-type asteroid densities are assumed.

There is general agreement that these clasts must have formed over long periods of time (i.e., not during impact events), by overburden in planetary-sized, largely undifferentiated bodies that were later catastrophically disrupted (Abreu, 2007, 2013; Kimura et al., 2013; Hiyagon et al., 2016). Based on the diffusion rates for Mg–Fe in olivine and orthopyroxene at a temperature of 1000ºC, Hiyagon et al. (2016) estimated that clasts in NWA 801 formed over timescales of the order of 10^2–10^3 years. However, two very different geological settings have been proposed for the formation of these clasts. Abreu (2007, 2013) proposed that all mineral phases in the QUE 99177 clast formed and experienced transitions in the solid-state during multiple heating events in the interior of a large asteroid. In contrast, Hiyagon et al. (2016) argued that localized igneous processes generated clasts in NWA 801.

Abreu (2013) favored a metamorphic origin in a large chondritic asteroid that was catastrophically disrupted at least once and whose materials re-accreted in the CR-forming region. She argued that omphacite and graphite were the first minerals to form and that a high abundance of carbon clasts resulted from the graphitization of a carbon-rich asteroidal precursor, such as a C-rich carbonaceous chondrite. Amphibole formation postdated graphite formation and occurred by the reaction of olivine, clinopyroxene, and omphacite in the presence of an oxidizing, Na-rich fluid at high temperatures (> 700ºC). Even if omphacites in the clast in QUE 99177 originally formed at high-temperature, a later high-temperature amphibole-forming event could have been sufficient for an order-disorder transition into the P2/n polymorph to occur. The absence of Fe-Ni metal in the QUE 99177 clast was interpreted as evidence that the altering fluid was also rich in sulfur. Abreu (2007, 2013) suggested that amphibole formation may have occurred at initially high temperature (~760°C) and that sulfide (<650°C) and graphite (>550°C) formation occurred as temperature decreased. In this scenario, fluid evolution played a central role in the final mineralogy. Although the conditions under which the clast formed were reducing, interaction with strongly oxidizing fluids could have produced Fe^{3+}-

bearing amphiboles. Further evolution into an H_2S-rich fluid could have sulfidized chondritic Fe-Ni alloys. Formation of omphacite and retention of carbon and sulfur during high-temperature metamorphism is indicative of formation at high depth, instead of during collisional, near-surface conditions.

Hiyagon et al. (2016) suggested a very different sequence of events for clasts in NWA 801. They argued that the presence/absence of graphite in the otherwise similar lithologies was due to the formation of these lithologies at different depths. In this model, the two lithologies were mixed, buried, and sintered over multiple collisional events. A subsequent large collision would have given rise to a Moon-sized planetary object, and the clasts in NWA 801 would be emplaced near the center of this ephemeral planet. In these locations, the following processes would have taken place over 10^2-10^3 years: formation of the eclogitic phases (i.e., omphacite and garnet), homogenization of Fe-Mg olivine and pyroxenes, and redistribution of P and REEs between two lithologies. Finally, a collision would have catastrophically disrupted the Moon-sized body, quenching the clasts and transporting them to the region where they accreted to form the CR parent body. The origin of the single hydrous phase, phlogopite, was not discussed in detail in this model.

It is unclear if clasts in QUE 99177 and NWA 801 came from precursors with widely different histories. Their different mineralogical assemblages, in particular the high abundance of graphite and absence of garnet in the clast in QUE 99177, suggest that the precursors' composition was indeed different (e.g., Hiyagon et al., 2016). More detailed comparative studies are needed to determine if these clasts had indeed the different histories as current investigations suggest. It is important to note that the graphite-free lithology in the NWA 801 clasts (Kimura et al., 2013) closely resembles the objects that Abreu (2013) identified as relict chondrules in the QUE 99177 clast. The graphite-bearing lithology in the NWA 801 clasts also resembles the matrix materials in the QUE 99177 clast. The absence of graphite in relict chondrules in the QUE 99177 clast is easily explained by the fact that chondrule precursors would have been essentially carbon-free (Abreu, 2007, 2013). In contrast, the formation of the graphite-bearing and the graphite-free lithologies at different depths would require a very complex sequence of excavation events and mixing, as suggested by Hiyagon et al. (2016).

10. Physical properties of CR chondrites

Measurements of the physical properties of CR chondrites are scarce. Little is known, for example, about electrical and thermal properties of either bulk samples or their components. Studies of physical properties generally involve destructive analyses, which are hampered by the small masses of many CRs, the largest of which are extensively weathered finds from hot deserts (e.g., Lee and Bland, 2004; Bland et al., 2006).

Terrestrial weathering might affect physical properties, which might, in turn, limit the value of their analyses. However, it is difficult to determine what the effects of weathering might be specifically for CR chondrites because there are only two observed falls that can be used for comparison (Macke et al., 2011). Some researchers have argued that weathering of carbonaceous chondrite finds does not produce discernible changes in their physical properties (Flynn et al., 2017). Perhaps because all changes occur very early during the terrestrial weathering process, it is challenging to find samples that were not affected by them. If most changes in physical properties of CRs occur after mild terrestrial weathering, as it is the case for ordinary chondrites (e.g., Flynn et al. 2017), patterns are not likely to be observable in extensively weathered CR chondrites from hot deserts.

Macke et al. (2011) measured several physical properties of falls Al Rais and Renazzo and finds Acfer 097, Acfer 270, Dhofar 1432, El Djouf 001, and Tafassasset. They found the average bulk porosity to be 9.5% ± 2.7. In comparison, Corrigan et al. (1997) obtained lower porosities for Al Rais and Renazzo matrices (2-8%). Macke et al. (2011) also determined the average bulk and grain densities of 3.11 ± 0.14 g/cm^3 and 3.42 ± 0.08 g/cm^3, respectively. Zolensky et al. (2018) proposed that these values should be adjusted because Gardner-Vandy et al. (2012) reclassified Tafassasset as a primitive achondrite. The adjusted values then are for average porosity 11.23% ± 7.4, for average bulk and grain densities of 2.99 ± 0.35 g/cm^3 and 3.36 ± 0.16 g/cm^3.

The largest variability in the averages for the physical properties was observed for Al Rais and Tafassasset. Macke et al. (2011) explained intra-sample heterogeneities as because most CR chondrites are breccias. Brecciation would result in different sets of physical properties for different lithic fragments. Furthermore, variability in the properties of Al Rais was attributed to the fact that this was the only fall analyzed by Macke et al. (2011). Zolensky et al. (2018) also noted that, aside from being a fall, Al Rais is also an anomalous CR2, having low chondrules:matrix abundance ratios with respect to other CR chondrites. Schrader et al. (2011) found that chondrule:matrix ratios are highly variable in CR chondrites and, for Al Rais is 0.46, compared to 1.87 for average CR chondrites. If fine-grained chondritic materials are more porous than chondrules, Zolensky et al. (2018) hypothesized that the high average porosity of Al Rais might have resulted from the fact that it has a low chondrule:matrix ratio. In light of the re-classification of Tafassasset, it is not surprising that the physical properties of this meteorite are so different from other CR chondrites.

Rochette et al. (2008) analyzed 16 CR chondrites including falls and cold and hot desert finds, and obtained average magnetization of $\log \chi = 5.04 \pm 0.12$ (in 10^{-9} m^3/kg; range 4.51-5.17). These values include Tafassasset and Kaidun, both of which have since been reclassified. If the values from these two chondrites are removed from the CR chondrite average, the result is $\log \chi = 4.93 \pm 0.23$ (in 10^{-9} m^3/kg; range 4.48-5.17). Removing Tafassasset, the average magnetic susceptibility obtained by Macke et al. (2011) is $\log \chi = 4.94 \pm 0.18$. Finally, Ibrahim (2012) determined the mean compressional wave velocity for CR chondrites to be 2770 ± 993 m/s and the average shear wave velocity to be 1751 ± 611 m/s and noted that porosity and velocities are anticorrelated. However, it is not known if differences in the mechanisms that lower the porosities (e.g., aqueous alteration versus impact metamorphism) might influence the compressional wave and shear wave velocities.

Compared with CM chondrites, average CR chondrite densities are slightly higher, and porosities are approximately half (Macke et al., 2011). Higher Fe-Ni metal abundances in CR chondrites probably resulted in their higher density. Differences in porosity could be the results of lower chondrule:matrix ratios in CMs compared to CRs. The magnetic susceptibility of CR chondrites is the highest for all the hydrated

carbonaceous chondrites and only lower than that of enstatite chondrites and the very metal-rich CH and CB chondrites. The average magnetic susceptibility values for CRs are comparable/intermediate between CO and CV chondrites (Rochette et al., 2008; Macke et al., 2011; Flynn et al., 2017). However, Rochette et al. (2008) cautioned that the magnetic susceptibilities of CRs should be interpreted as a lower limit because metallic minerals in CR chondrites have been subjected to significant terrestrial weathering and replacement.

11. Spectral studies of CR chondrites:

For a number of reasons, the spectroscopic properties of CR chondrites are diverse. The petrologic characteristics that affect spectroscopic observations are: (a) presence of both pre- and post-terrestrial Fe oxyhydroxides; (b) the fact that they record the full range of aqueous alteration processes; and (c) some CRs might have been thermally metamorphosed after being aqueously altered. For example, spectral differences between falls and finds were found for CM chondrites, which are mineralogically most similar to type 2 CR chondrites (Cloutis et al., 2011).

11.1. VNIR reflectance spectra of CR chondrites

The most comprehensive study to date of the spectral reflectance properties of CR chondrites was presented by Cloutis et al. (2012). Since then, the spectral reflectance properties of other CR chondrites have been studied (e.g., Abreu et al., 2018; Kiddell et al., 2018). Cloutis et al. (2012) found that a combination of low reflectance (4-16% near 0.75 μm), red spectral slope, and weak silicate absorption bands (<5% deep) seem to characterize CR chondrites. It also appears that CR spectra range from neutral to slightly red-sloped, which may distinguish them from some other carbonaceous chondrite groups. Diagnostic absorption features associated with silicates are weak because of their low FeO contents. However, this weakness may, in fact, be somewhat diagnostic. Overall, the reflectance is also generally low, but not uniquely so.

In terms of uniqueness, CR reflectance spectra do not exhibit particularly diagnostic features (Cloutis et al., 2018b). Some of this stems from the fact that CRs are petrologically diverse, ranging from mafic silicate- to phyllosilicate-dominated. Beyond this, the overprinting effects of terrestrial oxyhydroxides can obscure any diagnostic absorption features below ~1 μm. The consequences of these effects are discussed below.

11.1.1. Effects of terrestrial alteration on spectral features

One factor that affects VNIR reflectance spectra of CR chondrites is the presence of Fe oxyhydroxides. There are only two CR fresh falls, Al Rais and Renazzo, and only Renazzo has been spectrally characterized (one spectrum of one subsample) (Cloutis et al., 2012). Compared to the CR finds, Renazzo has extremely weak absorption features in the 1 μm region (Cloutis et al., 2012). The weakness of absorption features in Renazzo is attributed to the fact that most anhydrous CR silicates have very low Fe-content (e.g., Kallemeyn et al., 1994; Weisberg et al., 1993).

Features consistent with the presence of Fe-oxyhydroxides dominate reflectance spectra of CR finds (Cloutis et al., 2012). The spectra of Fe-oxyhydroxides have very low reflectance below ~0.5 μm, and an Fe^{3+}-associated absorption band in the 0.9 μm region (e.g., Sherman et al., 1982; Morris et al., 1985). As discussed above, both terrestrial and preterrestrial origins have been proposed for Fe-oxyhydroxides (e.g., Le Guillou et al., 2015a; Abreu, 2016a). Fe-oxyhydroxides could have also formed via incipient aqueous alteration in the CR parent body. The reason for the suggestion that Fe-oxyhydroxides formed early in asteroidal history is the same as for their formation in cold terrestrial deserts: CR matrices and Fe-Ni are highly reactive and likely to be affected by even small amounts of water, reacting at low temperatures. This is the reason why Abreu (2016a) noted that terrestrial weathering effects are likely to affect the CR chondrites more strongly than for other groups of carbonaceous chondrites. It also means that these two origins are not mutually exclusive. The preponderance of Fe-oxyhydroxides in CR reflectance spectra is consistent with the alteration of phases prone to reactions with water.

Kiddell et al. (2018) studied the effects of Fe-oxyhydroxides on the spectra of various carbonaceous chondrites, including CR2 NWA 801. As is the case with many hot desert finds, this meteorite is brown/orange in color, with pervasive veins of rust throughout (Connolly et al., 2007). Kiddell et al. (2018) found that "derusting" NWA 801 samples by exposing the samples to a thiol-bearing compound reacts preferentially with hydrated ferric iron resulted in complete or partial removal of the Fe oxyhydroxides, restoring some, but not all, carbonaceous chondrite spectra to their unaltered state. Whereas derusting may mitigate the spectrum-altering effects of Fe oxyhydroxides, some of these phases may be of preterrestrial origin, and hence "derusted" CR spectra may not accurately reflect their preterrestrial condition. In addition, CR chondrites have high ferric to total iron ratios, suggesting abundant preterrestrial Fe-oxyhydroxides. Despite these caveats, "derusting" can mitigate the spectrum-altering effects of Fe-oxyhydroxides. Removing Fe-oxyhydroxides allows diagnostic absorption features from hydrated and anhydrous mafic silicates to be more clearly discerned.

11.1.2. Effects of asteroidal processes on spectral features

CR chondrites show the full range of aqueous alterations, and there are CRs that appear to have undergone thermal metamorphism subsequent to aqueous alteration (e.g., GRA 06100 and GRO 03116). Cloutis et al. (2012) studied CR chondrites of all petrologic types, including a CR1 chondrite (GRO 95577), a number of CR2 chondrites, and a CR3 chondrite (MET 00426). Fig. 13a shows the reflectance spectra of powders of three different petrologic grade CR chondrites. Absolute differences in reflectance spectra are probably attributable, at least in part, to grain size variations, although for such fine-grained powders, the effects are expected to be small (Cloutis et al., 2018a). The steepness of the spectra shortward of ~0.5 μm for MET 00426 and GRO 95577 compared to Renazzo is probably due in part to the Fe oxyhydroxides resulting from terrestrial weathering of these two finds (both GRO 95577 and MET 00462 are weathering grade B or B/C). However, some mineralogical information can be derived even from the CR spectra of weathered samples.

Differences in the degree of aqueous alteration result in changes in CR spectral reflectance properties because this process eventually mobilizes a large fraction of the Fe from Fe-Ni metal nodules into silicates and oxides. CR3s have abundant, nearly intact type I chondrules (MgO-rich and FeO-poor), Fe-Ni metal nodules, and matrices that are rich in amorphous Fe-Mg silicates, resulting in higher fractions of FeO-poor silicates than other petrologic types, if chondrule to matrix ratios are held constant. If the first stage of CR aqueous alteration resulted in the formation of Fe-oxyhydroxides, then this ought to be the largest spectral change observed in type CR2. Along with this process, amorphous Fe-Mg silicates give rise to crystalline Fe-Mg silicates, and amorphous Fe-Mg silicates give rise to Fe-Mg phyllosilicates (dominantly serpentine and saponite). Abreu (2016a) found that the FeO and MgO contents of these phases did not systematically change in most CRs. Furthermore, they observed no changes in the FeO contents of chondrule phenocrysts or mesostases (Abreu, 2016a). These observations suggest that, at least in the early stages of aqueous alteration, there were no changes in the FeO contents of CR silicates. In contrast, FeO mobilization is particularly marked in CR1 GRO 95577, where type I chondrules have been extensively replaced by Fe-Mg phyllosilicates (e.g., Morlok and Libourel, 2013). Increasing aqueous alteration also leads to alteration of metal to magnetite and formation of carbonates (e.g., Tyra, 2013). Consequently, GRO 95577 has the largest abundance of FeO in silicates among the CRs.

Cloutis et al. (2012) found that reflectance declines with increasing aqueous alteration, consistent with higher opaque abundances in lower petrologic grades (Perronnet et al., 2007). Overall, CR spectral reflectance properties in the 0.3-2.5 μm region show evidence of pyroxene ± olivine and/or glassy Fe-Mg silicates (CR3) to phyllosilicate ± olivine/pyroxene (CR2), to fully dominated by Fe-bearing phyllosilicates (CR1). Because FeO contents of the silicates are uniformly low (with the exception of matrix silicates), any associated absorption bands are expected to be weak. Also, it is likely that spectral slopes become less red (bluer). The overall red spectral slope of CRs is likely due to contributions of Fe-Ni metal, poorly graphitized carbon, and sulfides (all of which are red-sloped), but not magnetite (which imparts a blue slope). However, as noted, only one CR chondrite fall has been spectrally characterized (Renazzo), and it is

possible that fresh CRs may have a range of spectral slopes. Continuum removal applied to the 1μm region can allow observing some silicate absorption bands.

Cloutis et al. (2012) determined the characteristics of CRs from different petrologic types as follows. For MET 00426 and other CR3 chondrites, identifying absorption bands associated with chondrule silicates is difficult largely because absorption bands of silicates with low Fe-contents are weak (e.g., King and Ridley, 1987; Clark et al., 1990; Cloutis and Gaffey, 1991). CR3s contain abundant pyroxene (McBride et al., 2001a,b; McSween, 1977b; Perronnet et al., 2007), in large enough amounts that they could affect the reflectance spectra (Cloutis et al., 1986). The spectrum of MET 00426 shows an absorption feature in the 0.9 μm region, consistent with pyroxene, but also highly overlapped by Fe oxyhydroxide absorption bands (Sherman et al., 1982; Morris et al., 1985). Its strength would also be reduced, because pyroxenes, predominantly from type I chondrules, have low FeO contents (McSween, 1977a; McBride et al., 2001a,b; Perronnet et al., 2007; Schrader et al. 2015). The 1.8 μm region shows stronger evidence for pyroxene: a broad, but shallow absorption feature centered near 1.81 μm, consistent with low-Fe pyroxene (Cloutis and Gaffey, 1991); but again, this spectral region can also be affected by Fe oxyhydroxides, and this is suggested by a broad absorption feature near 1950 nm. Thus, spectral evidence for low-FeO mafic silicates is ambiguous, but largely because of terrestrial weathering effects.

The reflectance spectrum for Renazzo shows a weak (≤2% deep) absorption feature in the 1 μm region, consistent with both Fe-bearing serpentine (band near 1.1 μm) and magnetite (broad feature in this region), both of which are abundant in this meteorite (Mason and Wiik, 1962; Zolensky et al., 1993). However, the weakness of this absorption feature makes phase identification problematic. The overall slightly red spectral slope may be due to the small amounts of metal and/or sulfides.

CR1 GRO 95577 contains various phyllosilicates and little or no anhydrous silicates, consistent with pervasive aqueous alteration. Spectrally, the broad 1 μm region shows strong evidence of Fe-bearing phyllosilicates: an absorption band near 1.1 μm, which is not overlapped by Fe oxyhydroxide bands. A small absorption feature just longwards of 2.3 μm is also most consistent with Fe-Mg phyllosilicates (Cloutis et al., 2012), again in agreement with its dominant mineralogy.

11.1.3. Thermal metamorphism effects

The major effects of heating are to (slightly – a few percent) increase the FeO content in the silicates, and dehydrated pre-existing phyllosilicates (Briani et al., 2013; Schrader et al., 2015; Abreu, 2016a). Spectrally, the thermally metamorphosed CRs for which we have spectral reflectance data (Fig. 13a), show intermediate reflectance (~8% at 0.75 μm versus 4-16% for all CRs; Cloutis et al., 2012), suggesting that thermal metamorphism may not affect overall reflectance. However, the 1 μm region shows clear evidence of this metamorphism: specifically, olivine-associated absorption features: an absorption band near 1.05 μm and a shoulder near 1.2 μm; and a possible pyroxene absorption band in the 1.8 μm region.

11.2. Infrared spectra of CR chondrites:

A number of CR chondrites have been spectrally characterized by various infrared spectroscopies and have focused on silicates and organics. For example, Miyamoto and Zolensky (1994) measured the 2.5-25 μm reflectance spectra of a number of carbonaceous chondrites, including Renazzo. They reported that the OH/H_2O-associated absorption feature in the 2.7-3.5 μm region is most similar to CM chondrites in shape, but of lower intensity, consistent with a lower content of hydrated minerals. CRs and other carbonaceous chondrites exhibit a general trend of increasing band intensity with increasing H content. Renazzo also shows a carbonate absorption band in the 7 μm region that is most similar in intensity to those of CM2 carbonaceous chondrites. Osawa et al. (2001) measured diamond cell infrared transmission spectra of two CRs over the range 2.5-16 μm. They found that the transmission spectra are most similar to that of the Murchison CM2 chondrite in terms of shape and position of O-H stretching bands in the 3 μm region, and Si-O stretching bands in the 10 μm region. Osawa et al. (2005) measured 2.5-13 μm infrared transmission spectra of carbonaceous chondrites using KBr and diamond press methods. Their sample suite included 3 Antarctic CR2s. They measured two OH/H_2O-stretching absorptions in the 3 μm region which are less intense

than the same bands in CM spectra. The CR spectra also exhibited a series of absorption bands in the 6-7.5 μm region and a stronger double band in the 9.5-11 μm region, sharing some similarities with CI and CM chondrites.

Briani et al. (2013) presented infrared transmission spectra of insoluble organic matter (IOM) extracted from four CR chondrites, as well as spectra of matrix material from six CR chondrites. The spectra of the IOM from two CR chondrites that experienced thermal metamorphism (as determined by multiple criteria; GRO 03116 and GRA 06100) differ from those of unmetamorphosed CR chondrites. They showed that both metamorphosed CRs display Si-O stretching bands dominated by crystalline olivine. No spectral evidence of hydroxyl was found (in contrast to CI and CM chondrites), but variable evidence of molecular water was noted. Orthous-Daunay et al. (2013) measured 2.5-25 μm infrared absorption spectra of IOM from a suite of carbonaceous chondrites, including three CR chondrites. They found that the absorption bands are similar to petrologic grade 2 carbonaceous chondrites, and variations between meteorites are associated with a high-temperature short-duration heating event.

Beck et al. (2014) measured KBr disk 2-25 μm infrared transmission spectra of a suite of 40 carbonaceous chondrites, including six CR chondrites. They noted that the CR group (petrologic grade 1-2.5) shows the most spectral variability of any of the groups. Spectral types range from CM-like to CV-like. The CV-like spectrum is for GRA 06100, which, as noted, appears to have been thermally metamorphosed. They noted that the 10 μm region of the CR spectra is more complex than for other carbonaceous chondrites, likely because of contributions from both olivine and pyroxene. They also noted that the CR1 chondrite, GRO 95577, shows infrared spectral features similar to those of heavily altered CI and CM chondrites, and to saponite.

Infrared reflectance spectra of powders of four CR chondrites are presented in Figure 13c-d (the CR2s MAC 87320 and PCA 91082; and pristine MET 00426 and QUE 99177). At shorter wavelengths, all four spectra show a somewhat featureless absorption feature in the 3 μm region that suggests contributions from hydroxyl (absorption near 2.8 μm) and water (absorption near 3.1 μm). The shape of this feature differs somewhat between the various spectra, but all show contributions from hydroxyl and molecular water. They all also show minor spectral contributions from aliphatic organics: weak

absorption bands in the 3.4-3.5 μm region. At longer wavelengths, reflectance progressively decreases, and the spectra all show further evidence of molecular water (absorption band near 6.1 μm), and various Si-O stretching bands in the 8-12 μm region. Differences, if any, between these spectra are minor.

12. CR chondrites and exploration of their parent asteroids

Because of their limited availability and scientific importance, NASA's Antarctic CRs have been assigned to the list of protected samples. It is unlikely that these CRs will be widely available for experiments that require masses larger than a few grams or for exploration-driven activities, such as simulant production or comparative studies. Sample mass limitations will likely place demands on the North African CR sample suite.

12.1. Implications of matrix studies for the distribution of water and organics in the solar system, in carbonaceous asteroids, and for ISRU of asteroidal materials

Exploration of CR parent bodies holds great promise for both science and *in-situ* resource utilization (ISRU). Petrologic studies can address the ISRU-relevant questions, including (a) How are Fe-Ni metal nodules affected by aqueous and hydrothermal alteration in asteroids?; (b) What is the distribution of water-bearing minerals in heated and unheated CR-like materials?; and (c) What is the effect of thermal metamorphism on the distribution of organics? Several studies proposed the future use of H_2 and O_2 from water-bearing minerals for in-situ production of fuel and propellants (e.g., Anand et al. 2012). In CRs, the mineralogical hosts of OH and H_2O are amorphous Fe-Mg silicates and phyllosilicates. We are only beginning to characterize these materials. Understanding the effect of asteroidal processes on Fe-Ni metal will constrain the availability, distribution, and mineral host of precious metals for ISRU demonstrations. Extraction of volatiles and metals will involve material processing: removing and mechanically processing the regolith (e.g., drilling, scooping, crushing, sorting, etc.) and chemically processing the regolith (e.g., heat of volatilization, reaction mechanisms). Designing tools

to accomplish ISRU goals should be informed by the distribution, chemical composition, and mineralogical characteristics of analog materials.

12.2. Key spectral characteristics for identification of CR parent bodies

Spectral matches between CRs and potential parent bodies are hindered by the effect of terrestrial weathering on the mineralogy of these meteorites. We face multiple challenges to address this uncertainty. Spectrally, CR chondrites differ from other carbonaceous chondrites in ways that relate to their mineralogies. CR chondrites include different petrologic grades, ranging from ~3 (relatively unaltered) to ~1 (pervasively aqueously altered), as well as two CRs that show evidence of subsequent thermal metamorphism (suggestive of petrologic grade up to ~3.6). These petrologic differences translate into mineralogical properties that vary from abundant amorphous Fe-Mg silicates (petrologic grade 3) to increasing amounts of Fe-Mg phyllosilicates (toward petrologic grade 1), and abundant mafic silicates (above petrologic grade 3). The anhydrous silicates are characterized by, on average, very low FeO contents, and those above petrologic grade 3 include abundant pyroxene.

Collectively we expect the parent asteroids of all CR chondrites to have the following characteristics: (1) weak silicate-associated absorption bands in the 0.3-2.5 μm region (<5% deep); (2) pyroxene-associated absorption bands in the 0.9 and 1.8 μm regions (for petrologic grade ≥3); (4) red-sloped spectra; and (4) low overall reflectance (between 4 and 15% in the visible region).

At longer wavelengths, we expect (1) an absorption feature in the 3 μm region with contributions from both hydroxyl and molecular water; (2) possible weak aliphatic organic absorption bands in the 3.4-3.5 μm region, a molecular water absorption band in the 6 μm region, and (3) Si-O stretching bands in the 9-12 μm region that are consistent with olivine (petrologic grade above ~2) and pyroxene (petrologic grade above ~3).

No one spectral property will uniquely identify CR chondrite parent bodies, but multiple lines of spectral evidence can strengthen the case for linking specific asteroids to CR chondrites. Further spectral analysis of CR chondrites with minimal terrestrial

alteration products, or "derusted" in the laboratory, should yield additional insights into potentially diagnostic spectral parameters.

13. Conclusions

CR-like parent bodies are scientifically important and resource-rich targets for exploration. These meteorites contain some of the most pristine solar nebular materials. In many CRs, post-assembly heating and aqueous alteration were too minor and/or localized to homogenize the material. These highly pristine samples have matrices that are dominated by amorphous, water-rich, Fe-Mg-rich silicates. In other groups of carbonaceous chondrites that record more extensive asteroidal processes, these materials have been progressively converted to hydrous and anhydrous crystalline silicates. The primitive nature of CRs is supported by the presence and high relative abundance of pre-solar grains from a wide variety of stellar and interstellar sources, as well as from the presence of exotic organics.

Parent bodies vary widely in terms of size, gravity, physical state, composition, and volatile abundance (Hutchison, 2004). Imposed on these distinctions is an equally variable history of impacts, alteration, differentiation, and igneous fractionation. Consequently, understanding how these asteroidal processes impact the spectral characteristics of these parent bodies is a fundamental first step in exploration.
The record of aqueous alteration in CRs is one of the most complete among the carbonaceous chondrites. Our collections include very pristine samples and those that have been entirely converted into water-bearing minerals and oxides (i.e., GRO 95577). In addition to these materials that reveal important information about nebular and presolar processes, the CR Suite includes both monomict and polymict breccias. CR polymict breccias potentially come from bodies larger than any present-day asteroids. Finally, spectral analyses of CR chondrites are our baseline for asteroidal observations and exploration of their asteroidal parent bodies.

Acknowledgements

Funded by NNX11AH10G grant to NMA. Analytical work was conducted at the MRI–Penn State. Thanks for technical assistance to Dr. T. Clark, Dr. J. Gray, and Dr. H. Wang at Penn State. Thanks to three anonymous reviewers who generously contributed their time and expertise to improving this manuscript. To Penn State DuBois research students Benjamin George and Abraham George for great conversations about the need for review papers about chondrites. Samples generously provided by the U.S. Antarctic Meteorite Collection. US Antarctic meteorite samples are recovered by the Antarctic Search for Meteorites (ANSMET) program which has been funded by NSF and NASA and characterized and curated by the Department of Mineral Sciences of the Smithsonian Institution and Astromaterials Curation Office at NASA Johnson Space Center.

References

Abreu, N. M., 2007. Fine-scale mineralogical study of the matrices of CR carbonaceous chondrites: Insights on early solar system processes Proquest Dissertations And Theses 2007. Section 0142, Part 0372 225 pages; [Ph.D. dissertation]. The University of New Mexico, United States, New Mexico, Publication Number: AAT 3273431. Source: DAI-B 68/07.

Abreu, N. M., 2011. Petrographic evidence of shock metamorphism in CR2 chondrite GRO 03116 (abstract). Meteorit. Planet. Sci. Suppl., id.5211.

Abreu, N. M., 2013. A unique omphacite, amphibole, and graphite-bearing clast in Queen Alexandra Range (QUE) 99177: A metamorphosed xenolith in a pristine CR3 chondrite. Geochim. Cosmochim. Acta 105, 56-72.

Abreu, N. M., 2016a. Why is it so difficult to classify Renazzo-type (CR) carbonaceous chondrites? - Implications from TEM observations of matrices for the sequences of aqueous alteration. Geochim. Cosmochim. Acta 194, 91-122.

Abreu, N. M., 2016b. Are phyllosilicates in CR chondrite matrices generated by hydrothermal alteration? (abstract). 47th Lunar Planet. Sci. Conf. LPI Contribution No. 1903, p.1926.

Abreu, N. M., Brearley, A. J., 2005. Carbonates in Vigarano: Terrestrial, preterrestrial, or both? Meteorit. Planet. Sci. 40, 609-625.

Abreu, N. M., Brearley, A. J., 2010. Early solar system processes recorded in the matrices of two highly pristine CR3 carbonaceous chondrites, MET 00426 and QUE 99177. Geochim. Cosmochim. Acta 74, 1146–1171.

Abreu, N. M., Bullock, E. S., 2013. Opaque assemblages in CR2 Graves Nunataks (GRA) 06100 as indicators of shock-driven hydrothermal alteration in the CR chondrite parent body. Meteorit. Planet. Sci. 48, 2406-2429.

Abreu, N. M., Singletary, S., 2011. Alteration history of CR2 chondrite GRA 06100: FE-EPMA and TEM analysis (abstract). LPI Contribution No. 1608, p.2659.

*Abreu, N. M., Cloutis, E. A., Hamilton, V. E. 2018. Understanding the effects of Antarctic weathering on the petrologic and spectral characteristics of pristine CR carbonaceous chondrites (abstract). 49th Lunar Planet. Sci. Conf. LPI Contribution No. 2083, id.1297.

Aléon, J., Krot A. N., McKeegan, K. D., 2002. Calcium-aluminum-rich inclusions and amoeboid olivine aggregates from the CR carbonaceous chondrites. Meteorit. Planet. Sci. 37, 1729-1755.

Alexander, C. M. O.'D., Bowden, R., 2018. Lewis Cliff (LEW) 85332 and Miller Range (MIL) 090001, a new Grouplet that is distinct from the CR chondrites? (abstract) 81st Ann. Meet. Meteoritical Society. LPI Contrib. No. 2067, 2018, id.6063.

Alexander, C. M. O.'D., Bowden, R., Fogel, M. L., Howard, K. T., 2015. Carbonate abundances and isotopic compositions in chondrites. Meteorit. Planet. Sci. 50, 810-833.

Alexander, C. M. O. D., Howard, K. T., Bowden, R., Fogel, M. L., 2013. The classification of CM and CR chondrites using bulk H, C and N abundances and isotopic compositions. Geochim. Cosmochim. Acta 123, 244-260.

Alexander, C. M. O.'D., R. Bowden, Fogel M. L., Howard K. T., Herd, C. D. K., Nittler, L. R., 2012. The provenances of asteroids, and their contributions to the volatile inventories of the terrestrial planets. Science 337, 721-723.

Alexander, C. M. O'D., Fogel, M., Yabuta, H., Cody, G. D., 2007. The origin and evolution of chondrites recorded in the elemental and isotopic compositions of their macromolecular organic matter. Geochim. Cosmochim. Acta 71, 4380–4403.

Al-Kathiri, A., Hofmann, B. A., Jull, A. J. T., and Gnos, E., 2005. Weathering of meteorites from Oman: Correlation of chemical/mineralogical weathering proxies with ^{14}C terrestrial ages and the influence of soil chemistry. Meteorit. Planet. Sci. 40, 1215–1239.

Anand, M., Crawford, I. A., Balat-Pichelin, M., Abanades, S., van Westrenen W., Pe´raudeau, G., Jaumann ,R., Seboldt, W., 2012. A brief review of chemical and mineralogical resources on the Moon and likely initial in situ resource utilization (ISRU) applications. Planet. Space Sci. 74, 42–48.

Aponte, J. C., Woodward, H. K., Abreu, N. M., Elsila, J. E., Dworkin, J. P., 2019. Molecular distribution, ^{13}C-isotope, and enantiomeric compositions of carbonaceous chondrite monocarboxylic acids. Meteorit. Planet. Sci. 54, 415-430.

*Aponte, J. C., Abreu, N. M., Keller, L. P., Elsila, J. E., Dworkin, J. P., 2018. Soluble amines in anomalous CR chondrite Miller Range (MIL) 090001 (abstract). 49th Lunar Planet. Sci. Conf., LPI Contrib. No. 2083, id.1543.

Aponte, J. C., McLain, H. L., Dworkin, J. P., Elsila, J. E., 2016. Aliphatic amines in Antarctic CR2, CM2 and CM1/2 carbonaceous chondrites. Geochim. Cosmochim. Acta 189, 296-311.

Aponte, J. C., Tarozo, R., Alexandre, M. R., Alexander, C. M. O'D., Charnley, S. B., Hallmann, C., Summons, R., Huang, Y., 2014. Chirality of meteoritic free and IOM-derived monocarboxylic acids and implications for prebiotic organic synthesis. Geochim. Cosmochim. Acta 131, 1-12.

Aponte, J. C., Alexandre, M. R., Wang, Y., Brearley, A. J., Alexander, C. O'D., Huang Y., 2011. Effects of secondary alteration on the composition of free and IOM-derived monocarboxylic acids in carbonaceous chondrites. Geochim. Cosmochim. Acta 75, 2309-2323.

Ash, R. D., Pillinger, C. T., 1995. Carbon, nitrogen and hydrogen in Saharan chondrites: The importance of weathering. Meteoritics 30, 85-92.

Beck, P., Garenne, A., Quirico, E., Bonal, L., Montes-Hernandez, G., Moynier, F., Schmitt, B., 2014. Transmission infrared spectra (2-25 μm) of carbonaceous chondrites (CI, CM, CV-CK, CR, C2 ungrouped): Mineralogy, water, and asteroidal processes. Icarus 229, 263-277.

Berlin, J., Jones, R. H., Brearley, A. J., 2011. Fe–Mn systematics of type IIA chondrules in unequilibrated CO, CR, and ordinary chondrites. Meteorit. Planet. Sci. 46, 513–533.

Bischoff, A., Palme, H., Ash, R. D., Clayton, R. N., Schultz, L., Herpers, U., Stoffler, D., Grady, M. M., Pillinger, C. T., Spettel, B., Weber, H., Grund, T., Endreß, M., Weber, D., 1993a. Paired Renazzo-type (CR) carbonaceous chondrites form the Sahara. Geochim. Cosmochim. Acta 57, 1587–1603.

Bischoff, A., Palme, H., Schultz, L., Weber, D., Weber, H. W., Spettel, B., 1993b. ACFER 182 and paired samples, an iron-rich carbonaceous chondrite -

Similarities with ALH85085 and relationship to CR chondrites. Geochim. Cosmochim. Acta 57, 2631-2648.

Bischoff, A., Scott, E. R. D., Metzler, K., Goodrich, C. A., 2006. Nature and Origins of Meteoritic Breccias. *In* Meteorites and the Early Solar System II (eds. D.S. Lauretta and H.Y. McSween, Jr.). University of Arizona Press. pp. 679-712.

Bland, P. A., Zolensky, M. E., Benedix, G. K., Sephton, M. A., 2006. Weathering of chondritic meteorites. *In* Meteorites and the Early Solar System II (eds. D.S. Lauretta and H.Y. McSween, Jr.). University of Arizona Press. pp. 853- 867.

Blum, J. D., Wasserburg, G. J., Hutcheon, I. D., Beckett, J. R., Stolper, E. M., 1988. "Domestic" origin of opaque assemblages in refractory inclusions in meteorites. Nature 331, 405–409.

Blum, J. D., Wasserburg, G. J., Hutcheon, I. D., Beckett, J. R., Stolper, E. M., 1989. Origin of opaque assemblages in C3V meteorites—Implications for nebular and planetary processes. Geochim. Cosmochim. Acta 53, 543–556.

Bonal L., Alexander C. M. O.'D., Huss G. R., Nagashima K., Quirico, E., Beck, P., 2013. Hydrogen isotopic composition of the water in CR chondrites. Geochim. Cosmochim. Acta 106, 111-133.

Bonner, W. A., Blair, N. E., Lemon, R. M., 1979. The radioracemization of amino acids by ionizing radiation: geochemical and cosmochemical implications. Origin of Life 9, 279-290.

Botta, O., Glavin, D. P., Kminek, G., Bada, J. L., 2002. Relative amino acid concentrations as a signature for parent body processes of carbonaceous chondrites. Origins of Life Evolution of Biosphere 32, 143-163.

Bradley, J. P., Dai, Z. R., 2004. Mechanism of formation of glass with embedded metal and sulfides. Astrophys. J. 617, 650-655.

Braukmüller, N., Wombacher, F., Hezel, D. C.; Escoube, R., Münker, C., 2018. The chemical composition of carbonaceous chondrites: Implications for volatile element depletion, complementarity and alteration. Geochim. Cosmochim. Acta 239, 17-48.

Brearley, A. J., 1991. Mineralogical and chemical studies of matrix in the Adelaide meteorite, a unique carbonaceous chondrite with affinities to ALH A77307 (CO3) (abstract). 22nd Lunar Planet. Sci. Conf., # 133.

Brearley, A. J., Burger, P. V., 2009. Mechanisms of aqueous alteration of type IIA chondrule glass in the CR chondrite EET 92105: Insights from FIB/TEM analysis (abstract). Meteorit. Planet. Sci., Suppl., 5148.

Briani, G., Quirico, E., Gounelle, M., Paulhiac-Pison, M., Montagnac, G., Beck, P., Orthous-Daunay, F.-R., Bonal, L., Jacquet, E., Kearsley, A., Russell, S. S., 2013. Short duration thermal metamorphism in CR chondrites. Geochim. Cosmochim. Acta 122, 267-279.

Bringa, E. M., Kucheyev, S. O., Loeffler, M. J., Baragiola, R. A., Tielens, A. G. G. M., Dai, Z. R., Graham, G., Bajt, S., Bradley, J. P., Dukes, C. A., Felter, T. E., Torres, D. F., Breugel, W. V., 2007. Energetic processing of interstellar silicate grains by cosmic rays. Astrophys. J. 662, 372.

Browning, L. B., McSween, H. Y., Jr., Zolensky, M. E., 1996. Correlated alteration effects in CM carbonaceous chondrites. Geochim. Cosmochim. Acta 60, 2621-2633.

Brunner, C. E., Brearley, A. J., 2011. Microstructural investigation of the crystalline component of matrix in the pristine CR chondrite MET 00426: Implications for diversity in nebular dust (abstract). 42nd Lunar Planet. Sci. Conf. LPI Contribution No. 1608, p.1815.

Budde G., Kruijer T. S., Kleine T., 2018. Hf-W chronology of CR chondrites: Implications for the timescales of chondrule formation and the distribution of ^{26}Al in the solar nebula. Geochim. Cosmochim. Acta, 222, 284-304.

Bunch, T. E., Wittke, J. H., Irving, A. J., Rumble, D., 2013. Unique polymict breccia Northwest Africa 7531 composed of recrystallized LL clasts associated with CR metachondrite material: Evidence for highly equilibrated ordinary chondritic impactors onto the CR chondrite parent body (abstract). 44th Lunar Planet. Sci. Conf., LPI Contribution No. 1719, p.2214

Burger, P. V., 2005. Incipient aqueous alteration of meteorite parent bodies: Hydration, mobilization, precipitation and equilibration. M.S. thesis, University of New Mexico, Albuquerque, NM, USA.

Burton, A. S., Elsila, J. E., Callahan, M. P., Martin, M. G., Glavin, D. P., Johnson, N. M., Dworkin, J. P., 2012a. A propensity for n-ω-amino acids in thermally altered Antarctic meteorites. Meteorit. Planet. Sci. 47, 374-386.

Burton, A. S., Stern, J. C., Elsila, J. E., Glavin, D. P., Dworkin, J. P., 2012b. Understanding prebiotic chemistry through the analysis of extraterrestrial amino acids and nucleobases in meteorites. Chem. Society Rev. 41, 5459-5472.

Busemann, H., Nguyen, A. N., Cody, G. D., Hoppe, P., Kilcoyne, A. L. D., Stroud, R. M., Zega, T. J., Nittler, L. R., 2009. Ultra-primitive interplanetary dust particles from the comet 26P/Grigg-Skjellerup dust stream collection. Earth Planet. Sci. Lett. 288, 44-57.

Busemann, H., Alexander, C. M. O'D., Nittler, L. R., 2007. Characterization of insoluble organic matter in primitive meteorites by microRaman spectroscopy. Meteorit. Planet. Sci. 42, 1387–1416.

Busemann, H., Young A. F., Alexander, C. M. O'D., Hoppe P., Mukhopadhyay S., Nittler L. R. 2006. Interstellar chemistry recorded in organic matter from primitive meteorites. Science 312, 727-730.

Callahan, M. P., Smith, K. E., Cleaves, II H. J., Ruzicka, J., Stern, J. C., Glavin, D. P., House, C. H., Dworkin, J. P., 2011. Carbonaceous meteorites contain a wide range of extraterrestrial nucleobases. Proc. Natl. Academy Sci. USA 108, 13995-13998.

Campbell, A. J., Zanda, B., Perron, C., Meibom, A., Petaev, M. I., 2005. Origin and thermal history of Fe-Ni metal in primitive chondrites. *In* Chondrites and the protoplanetary disk, edited by Krot A. N., Scott E. R. D., and Reipurth B. Astronomical Society of the Pacific Conference Series, vol. 341. pp. 407–431.

Campbell, A. J., Humayun, M., Zanda, B., 2002. Partial condensation of volatile elements in Renazzo chondrules. Geochim. Cosmochim. Acta 66, A117.

Chizmadia, L. J., Brearley, A. J., 2008. Mineralogy, aqueous alteration, and primitive textural characteristics of fine-grained rims in the Y-791198 CM2 carbonaceous chondrite: TEM observations and comparison to ALHA81002. Geochim. Cosmochim. Acta 72(2), 602–625.

Clark, R. N., King, T. V. V., Klewja, M., Swayze, G. A., 1990. High spectral resolution reflectance spectroscopy of minerals. J. Geophys. Res. 95, 12653-12680.

Clayton, R. N., Mayeda, T. K., 1999. Oxygen isotope studies of carbonaceous chondrites. Geochim. Cosmochim. Acta 63, 2089-2104.

Cloutis, E. A., Pietrasz, V. B., Kiddell, C., Izawa, M. R. M., Vernazza, P., Burbine, T. H., DeMeo, F., Tait, K. T., Bell III, J. F., Mann, P., Applin, D. M., Reddy, V., 2018a. Spectral reflectance "deconstruction" of the Murchison CM2 carbonaceous chondrite and implications for spectroscopic investigations of dark asteroids. Icarus, 305, 203-224.

Cloutis, E. A., Izawa, M. R. M., Beck, P., 2018b. *In* Primitive Meteorites and Asteroids, Chapter 4 – Reflectance Spectroscopy of Chondrites. Physical, Chemical and Spectroscopic Observations Paving the Way to Exploration (N. Abreu, editor); Elsevier, Amsterdam; https://doi.org/10.1016/B978-0-12-813325-5.00004-5 pp. 273-343.

Cloutis, E. A., Hudon, P., Hiroi, T., Gaffey, M. J., 2012. Spectral reflectance properties of carbonaceous chondrites: 3. CR chondrites. Icarus 217, 389-407.

Cloutis, E. A., Hudon, P., Hiroi, T., Gaffey, M. J., Mann P., 2011. Spectral reflectance properties of carbonaceous chondrites: 2. CM chondrites. Icarus 216, 309-346.

Cloutis, E. A., Gaffey M. J., 1991. Pyroxene spectroscopy revisited: Spectral-compositional correlations and relationship to geothermometry. J. Geophys. Res. 96, 22, 809-22,826.

Cloutis, E. A., Gaffey, M. J., Jackowski, T. L., Reed, K. L., 1986. Calibrations of phase abundance, composition, and particle size distribution for olivine-orthopyroxene mixtures from reflectance spectra. J. Geophys. Res. 91, 11,641-11,653.

Cobb, A. K., Pudritz, R. E., 2014. Nature's starships. I. Observed abundances and relative frequencies of amino acids in meteorites. Astrophys. J. 783, 140 (12pp).

Cody G. D., Alexander C. M. O'D., 2005. NMR studies of chemical structural variation of insoluble organic matter from different carbonaceous chondrites groups. Geochim. Cosmochim. Acta 69, 1085–1097.

Cody G. D., Alexander C. M. O'D., Yabuta H., Kilcoyne A. L. D., Araki T., Ade H., Dera P., Fogel M., Militzer B., Mysen B. O., 2008. Organic thermometry for chondritic parent bodies. Earth Planet. Sci. Letters 272, 446-455.

Connolly, Jr., H. C., Huss, G. R., 2010. Compositional evolution of the protoplanetary disk: Oxygen isotopes of type-II chondrules from CR2 chondrites. Geochim. Cosmochim. Acta 74, 2473–2483.

Connolly, H. C., Huss, G. R., Nagashima, K., Weisberg, M. K., Ash, R. D., Ebel, D. S., Schrader, D. L., Lauretta, D. S., 2008. Oxygen isotopes and the nature and origins of type-II chondrules in CR2 chondrites (abstract). 39th Lunar Planet. Sci. Conf., LPI Contribution No. 1391, p.1675.

Connolly Jr., H. C., Smith, C., Benedix, G., Folco, L., Righter, K., Zipfel, J., Yanaguchi, A., Chennaoui Aoudjehane, H., 2007. The Meteoritical Bull. No. 92, Meteorit. Planet. Sci. 42, 1647-1694.

Connolly, Jr., H. C., Huss, G. R., Wassenburg, G. J., 2001. On the formation of Fe–Ni metal in Renazzo-like carbonaceous chondrites. Geochim. Cosmochim. Acta 65, 4567–4588.

Connolly, Jr., H. C., Hewins, R. H., Ash, R. D., Zanda, B., Lofgren, G. E., Bourot-Denise, J., 1994. Carbon and the formation of reduced chondrules. Nature 371, 136–139.

Cooper, G., Rios, A. C., 2016. Enantiomer excesses of rare and common sugar derivatives in carbonaceous meteorites. Proc. Natl. Academy Sci. USA 113, E3322-E3331.

Cordier, L. 1827. Rapport fait 'a I'Academie des Sciences, sur une pierre meteorique tombee pres de Ferrare en 1824. Annales de Chimie et de Physique, 34, 132-139.

Corrigan, C. C., Zolensky, M. E., Dahl, J., Long, M., Weir, J., Sapp, C., 1997. The porosity and permeability of chondritic meteorites and interplanetary dust particles. Meteorit. Planet. Sci. 32, 509-515.

*Das, J. P., Meshik, A. P., Pravdivtseva, O. V., Hohenberg, C. M., 2011. A first test of a new analyte. 193 laser ablation system: in-situ helium, neon and argon compositions of chondrule zones and surrounding matrix in NWA 801 CR2 chondrite (abstract). 42nd Lunar Planet. Sci. Conf., LPI Contribution No. 1608, p. 2238.

Daulton, T. L., Bernatowicz, T. J., Lewis, R. S., Messenger, S., Stadermann, F. J., Amari, S., 2003. Polytype distribution of circumstellar silicon carbide: Microstructural characterization by transmission electron microscopy. Geochim. Cosmochim. Acta 67, 4743-4767.

*Davidson, J., Alexander, C. M. O. D., Schrader, D. L., Nittler, L. R., Bowen, R., 2015. Miller Range 090657: A very pristine Renazzo-like (CR) carbonaceous chondrite (abstract). 46th Lunar Planet. Sci. Conf., #1603.

Davidson, J., Busemann, H., Nittler, L. R., Alexander, C. M. O.'D., Orthous-Daunay, F.-R., Franchi, I. A., Hoppe, P., 2014a. Abundances of presolar silicon carbide grains in primitive meteorites determined by NanoSIMS. Geochim. Cosmochim. Acta 139, 248-266.

Davidson, J., Schrader, D.L., Alexander, C.M.O.D., Lauretta, D.S., Busemann, H., Franchi, I.A., Greenwood, R.C., Connolly Jr., H.C., Domanik, K.J., Verchovsky, A., 2014b. Petrography, stable isotope compositions, microRaman spectroscopy, and presolar components of Roberts Massif 04133: A reduced CV3 carbonaceous chondrite. Meteorit. Planet. Sci. 49, 2133-2151.

de Leuw, S., Rubin, A., Wasson J., 2010. Carbonates in CM chondrites: Complex formational histories and comparison to carbonates in CI chondrites. Meteorit. Planet. Sci. 45, 513–530.

De Marcellus, P., Meinert, C., Nuevo, M., Filippi, J.-J., Danger, G., Deboffle, D., Nahon, L., d'Hendecourt, L. Le S., Meierhenrich, U. J., 2011. Non-racemic amino acid production by ultraviolet irradiation of achiral interstellar ice analogs with circularly polarized light. Astrophys. J. Lett. 727, L27-L32.

Ebel, D. S., Weisberg, M. K., Hertz, J., Campbell, A. J., 2008. Shape, metal abundance, chemistry, and origin of chondrules in the Renazzo (CR) chondrite. Meteorit. Planet. Sci. 43, 1725–1740.

Ehrenfreund, P., Glavin, D. P., Botta, O., Cooper, G., Bada, J. L., 2001. Extraterrestrial amino acids in Orgueil and Ivuna: Tracing the parent body of CI type carbonaceous chondrites. Proc. Natl. Academy Sci. USA 98, 2138-2141.

Elsila, J. E., Charnley, S. B., Burton, A. S., Glavin, D. P., Dworkin, J. P., 2012. Compound-specific carbon, nitrogen, and hydrogen isotopic ratios for amino acids in CM and CR chondrites and their use in evaluating potential formation pathways. Meteorit. Planet. Sci. 47, 1517-1536.

Elsila, J. E., Aponte, J. C., Blackmond, D. G., Burton, A. S., Dworkin, J. P., Glavin, D. P., 2016. Meteoritic amino acids: Diversity in compositions reflects parent body histories. ACS Cent. Sci. 2, 370-379.

Endreß, M., Keil, K., Bischoff, A., Spettel, B., Clayton, R. N., Mayeda, T. K., 1994. Origin of dark clasts in the ACFER 059/El Djouf 001 CR2 chondrite. Meteoritics 29, 26-40.

Ferrarotti, A.S., Gail, H.-P., 2001. Mineral formation in stellar winds II: Effects of Mg/Si abundance variations on dust composition in AGB stars. Astron. Astrophys. 371, 133-151.

Fleet, M. E., Herzberg, C. T., Bancroft, G. M., Aldridge, L. P., 1978. Omphacite studies; I, The P2/n– > C2/c transformation. Amer. Mineral. 63, 1100–1106.

Floss, C., Haenecour, P., 2016a. Presolar silicate grains: Abundances, isotopic and elemental compositions, and the effects of secondary processing. Geochem. J. 50, 3-25.

Floss, C., Haenecour, P., 2016b. Meteorite Hills (MET) 00526: An unequilibrated ordinary chondrite with high presolar grain abundances (abstract). 47th Lunar Planet. Sci. Conf., #1030.

Floss, C., Le Guillou, C., Brearley, A., 2014. Coordinated NanoSIMS and FIB-TEM analyses of organic matter and associated matrix materials in CR3 chondrites. Geochim. Cosmochim. Acta 139, 1-25.

Floss, C., Stadermann, F. J., Kearsley, A. T., Burchell, M. J., Ong, W. J., 2013. The abundance of presolar grains in comet 81P/Wild 2. Astrophys. J. 763, 140-150.

Floss, C., Stadermann, F. J., 2012. Presolar silicate and oxide abundances and compositions in the ungrouped carbonaceous chondrite Adelaide and the K

chondrite Kakangari: The effects of secondary processing. Meteorit. Planet. Sci. 47, 992-1009.

Floss, C., Stadermann, F. J., 2009b. High abundances of circumstellar and interstellar C-anomalous phases in the primitive CR3 chondrites QUE 9917 and MET 00426. Astrophys. J. 697, 1242-1255.

Floss, C., Stadermann, F. J., 2009a. Auger nanoprobe analysis of presolar ferromagnesian silicate grains from primitive CR chondrites QUE 99177 and MET 00426. Geochim. Cosmochim. Acta 73, 2415-2440.

Floss, C., Stadermann, F. J., Bradley, J. P., Dai, Z. R., Bajt, S., Graham, G., Lea, A. S., 2006. Identification of isotopically primitive interplanetary dust particles: A NanoSIMS isotopic imaging study. Geochim. Cosmochim. Acta 70, 2371-2399.

Floss, C., Stadermann, F. J., 2005. Presolar (circumstellar and interstellar) phases in Renazzo: The effects of parent body processing (abstract). 36th Lunar Planet. Sci. Conf., #1390.

Flynn, G. J., Consolmagno, G. J., Brown, P., Macke, R. J., 2017. Physical properties of the stone meteorites: Implications for the properties of their parent bodies. Chem. Erde 78, 269-298.

Friedrich, J. M., Weisberg, M. K., Ebel, D. S., Biltz, A. E., Corbett, B. M., Iotzov, I. V., Khan, W. S., Wolman, M. D., 2015. Chondrule size and related physical properties: A compilation and evaluation of current data across all meteorite groups. Chem. Erde 75, 419-443.

Gardner-Vandy, K. G., Lauretta, D. S., Greenwood, R. C., McCoy, T. J., Killgore, M., Franchi, I. A., 2012. The Tafassasset primitive achondrite: Insights into initial stages of planetary differentiation. Geochim. Cosmochim. Acta 85, 142-159.

Garenne, A., Beck, P., Montes-Hernandez, G., Chiriac, R., Toche, F., Quirico, E., Bonal, L., Schmitt, B., 2014. The abundance and stability of "water" in type 1 and 2 carbonaceous chondrites (CI, CM and CR). Geochim. Cosmochim. Acta 137, 93-112.

Gilmour, I., 2005. Structural and isotopic analysis of organic matter in carbonaceous chondrites. *In* Treatise on Geochemistry; Meteorites, Comets and Planets (ed. Davis, A. M.), pp. 269-290. Elsevier, Amsterdam.

Gilmour, I., Pillinger, C. T., 1994. Isotopic compositions of individual polycyclic aromatic hydrocarbons from the Murchison meteorite. Mon. Not. R. Astron. Soc. 269, 235-240.

Glavin, D. P., Alexander, C. M. O'D., Aponte, J. C., Dworkin, J. P., Elsila, J. E., Yabuta, H., 2018. The origin and evolution of organic matter in carbonaceous chondrites and links to their parent bodies. *In* Primitive Meteorites and Asteroids, 1st Edition, N. Abreu (Ed.), pp 205-271, Elsevier, Amsterdam, Netherlands.

Glavin, D. P., Callahan, M. P., Dworkin, J. P., Elsila, J. E., 2011. The effects of parent body processes on amino acids in carbonaceous chondrites. Meteorit. Planet. Sci. 45, 1948-1972.

Glavin, D. P., Dworkin, J. P., 2009. Enrichment of the amino acid L-isovaline by aqueous alteration on CI and CM meteorite parent bodies. Proc. Natl. Academy Sci. USA 106, 5487-5492.

Gooding, J. L., 1986. Clay-mineraloid weathering products in Antarctic meteorites. Geochim. Cosmochim. Acta 50, 2215-2223.

Gooding, J. L., 1981. Mineralogical aspects of terrestrial weathering effects in chondrites from Allan Hills, Antarctica. Proc. 12th Lunar Planet. Sci. Conf., 1105–1122.

*Grady, M. M., Ash, R. D., Pillinger, C. T. EET 87770: A light element stable isotope study of a new Renazzo-like carbonaceous chondrite. (abstract). 22nd Lunar Planet. Sci. Conf., # 471.

Greshake, A., 1997. The primitive matrix components of the unique carbonaceous chondrite ACFER 094: A TEM study. Geochim. Cosmochim. Acta 61, 437-452.

Grossman, J. N., Wasson, J. T., 1985. The origin and history of the metal and sulfide components of chondrules. Geochim. Cosmochim. Acta 49, 925–939.

Grossman, L., Olsen, E., 1974. Origin of the high-temperature fraction of C2 chondrites. Geochim. Cosmochim. Acta 38, 175-187.

*Haenecour, P., Floss, C., Zega, T. J., Croat, T. K., Wang, A., Jolliff, B. L., Carpenter, P., 2018. Presolar silicates in the matrix and fine-grained rims around chondrules in primitive CO3.0 chondrites: Evidence for pre-accretionary aqueous alteration of the rims in the solar nebula. Geochim. Cosmochim. Acta 221, 379-405.

Hanowski, N. P., Brearley, A. J., 2001. Aqueous alteration of chondrules in the CM carbonaceous chondrite Allan Hills 81002: Implications for parent body alteration. Geochim. Cosmochim. Acta 65, 495-518.

Haramura, H., Kushiro I., Yanai, K., 1983. Chemical compositions of Antarctic meteorites: I. Proc. Eighth Symp. Antarct. Meteor. NIPR. 109-121.

Hashiguchi, M., Yurimoto, H., 2016. Hydrogen isotopic compositions and chemical structures of organic materials in Northwest Africa 801 CR2 chondrite:

Implications for metamorphism histories of extraterrestrial organic materials (abstract). 47th Lunar Planet. Sci. Conf. No. 1903, p. 1216.

Hashiguchi, M., Kobayashi, S., Yurimoto, H. 2013. In situ observation of D-rich carbonaceous globules embedded in NWA 801 CR2 chondrite. Geochim. Cosmochim. Acta 122, 306-323.

Harju, E. R., Rubin, A. E., Ahn, I., Choi, B.-G., Ziegler, K., Wasson, J. T., 2014. Progressive aqueous alteration of CR carbonaceous chondrites. Geochim. Cosmochim. Acta 139, 267-292.

Hertkorn, K., Harir, M., Schmitt-Kopplin, Ph., 2015. Nontarget analysis of Murchison soluble organic matter by high-field NMR spectroscopy and FTICR mass spectrometry. Magnetic Resonance Chem. 53, 754-768.

Hewins, R. H., Bourot-Denise, M., Zanda, B., Leroux, H., Barrat, J.-A., Humayan, M., Göpel, G., Greenwood, R.C., Franchi, I.A., Pont, S., Lorand, J.-P., Cournède, Gatacceca, J., Rochette, P., Kuga, M., Marrocchi, Y., Marty, B., 2014. The Paris meteorite, the least altered CM chondrite so far. Geochim. Cosmochim. Acta 124, 190–222.

Hewins, R. H., Connolly, Jr., H. C., Lofgren, G. E., Libourel, G., 2005. Experimental constraints on chondrule formation. *In* Chondrites and the Protoplanetary Disk (eds. A. N. Krot, E. R. D. Scott and B. Reipurth), pp. 286–316. ASP Conference Series 341. Astronomical Society of the Pacific, San Francisco.

Hewins R. H., Yu Y., Zanda B., Bourot-Denise M., 1997. Do nebular fractionations, evaporative losses, or both, influence chondrule compositions? 21st Symp. Antarctic Meteorites, NIPR, 275-298.

Hiyagon, H., Sugiura, N., Kita, N. T., Kimura, M., Morishita, Y., Takehana, Y., 2016. Origin of the eclogitic clasts with graphite-bearing and graphite-free lithologies in the Northwest Africa 801 (CR2) chondrite: Possible origin from a Moon-sized planetary body inferred from chemistry, oxygen isotopes and REE abundances. Geochim. Cosmochim. Acta 186, 32–48.

Howard, K. T., Alexander, C. M. O'D., Schrader, D. L., Dyl, K. A., 2015a. Classification of hydrous meteorites (CR, CM and C2 ungrouped) by phyllosilicate fraction: PSD-XRD modal mineralogy and planetesimal environments. Geochim. Cosmochim. Acta 149, 206-222.

Howard, K. T., Davidson, J., Alexander, C. M. O'D., Abreu, N. M., 2015b. The glue that holds worlds together: Abundance, origin and significance of amorphous Fe, Mg silicate in carbonaceous chondrites (abstract). 46th Lunar Planet. Sci. Conf. No. 1832, p .2244.

Humayun, M., Campbell, A. J., Zanda, B., Bourot-Denise, M., 2002. Formation of Renazzo chondrule metal inferred from siderophile elements (abstract). 33rd Lunar Planet. Sci. Conf., No. 1965.

Huss, G. R., Meshik, A. P., Smith, J. B., Hohenberg, C. M., 2003. Presolar diamond, silicon carbide, and graphite in carbonaceous chondrites: Implications for thermal processing in the solar nebula. Geochim. Cosmochim. Acta 67, 4823-4848.

*Huss, G. R., Weisberg, M. K., Wasserburg, G. J. 1996. Magnesium and silicon isotopes in layered chondrules from EL Djouf (CR2). (abstract). In Abstracts of the Lunar Planet. Sci. Conf. 27, 575-576.

Hutcheon, I. D., Marhas, K. K., Krot, A. N., Goswami, J. N., Jones, R. H., 2009. ^{26}Al in plagioclase-rich chondrules in carbonaceous chondrites: Evidence for an extended duration of chondrule formation. Geochim. Cosmochim. Acta 73, 5080-5099.

Hutchison, R., 2004. Meteorites. pp. 520. Cambridge University Press, Cambridge, UK.

Ibrahim, E.-M.I., 2012. The elastic properties of carbonaceous chondrites M.Sc. Thesis. University of Calgary, Alberta, Canada.

Ichikawa, O., Ikeda, Y., 1995. Petrology of the Yamato-8449 CR chondrite. Proc. NIPR Symp. Antarctic Meteorites, National Institute of Polar Research 8, 63-78.

Jacquet, E., Paulhiac-Pison, M., Alard, O., Kearsley, A. T., Gounelle, M., 2013. Trace element geochemistry of CR chondrite metal. Meteorit. Planet. Sci. 48, 1981-1999.

Jilly-Rehak, C. E., Huss, G. R., Nagashima, K., Schrader, D. L., 2018. Low-temperature aqueous alteration on the CR chondrite parent body: Implications from in situ oxygen-isotope analyses. Geochim. Cosmochim. Acta 222, 230-252.

Jilly-Rehak, C. E., Huss, G. R., Nagashima, K., 2017. ^{53}Mn-^{53}Cr radiometric dating of secondary carbonates in CR chondrites: Timescales for parent body aqueous alteration. Geochim. Cosmochim. Acta 201, 224-244.

Jones, A. P., Nuth, J. A., III, 2011. Dust destruction in the ISM: a re-evaluation of dust lifetimes. Astron. Astrophys. 530, A44-A55.

Jones, A. P., Tielens, A. G. G. M., Hollenbach, D. J., McKee, C. F., 1994. Grain destruction in shocks in the interstellar medium. Astrophys. J. 433, 797-810.

Jones, R. H., Lofgren, G. E., 1993. A comparison of FeO-rich, porphyritic olivine chondrules in unequilibrated chondrites and experimental analogues. Meteoritics 28, 213-221.

*Jull et al., 1991. Jull A. J. T., Wlotzka F., and Donahue D. J. (1991) Terrestrial ages and petrologic description of Roosevelt County meteorites (abstract). *In* Abstracts of the Lunar Planet. Sci. Conf. 22, 667–668.

Kallemeyn, G. W., Rubin, A. E., Wasson, J. T., 1994. The compositional classification of chondrites: VI. The CR carbonaceous chondrite group. Geochim. Cosmochim. Acta 58, 2873-2888.

Kallemeyn, G. W., Wasson, J. T., 1982. The compositional classification of chondrites-III. Ungrouped carbonaceous chondrules. Geochim. Cosmochim. Acta 46, 2217-2228.

Keller, L. P., McKeegan, K. D., Sharp, Z. D., 2012. The oxygen isotopic composition of MIL 090001: A CR2 chondrite with abundant refractory inclusions (abstract). 43rd Lunar Planet. Sci. Conf. LPI Contribution No. 1659, id.2065.

Keller, L. P., 2011. Mineralogy and petrography of MIL 090001, a highly altered CV chondrite from the reduced sub-group (abstract). 42nd Lunar Planet. Sci. Conf., LPI Contrib. No. 1608, p. 2409.

Keller, L. P., Messenger, S., 2011. On the origins of GEMS grains. Geochim. Cosmochim. Acta 75, 5336-5365.

Kemper, F., Waters, L. B. F. M., de Koter, A. Tielens, A. G. G. M., 2001. Crystallinity versus mass-loss rate in Asymptotic Giant Branch stars. Astron. Astrophys. 369, 132-141.

Kerridge J. F., Mackay A. L., Boynton W. V., 1979. Magnetite in C1 carbonaceous meteorites: Origin by aqueous activity on a planetesimal surface. Science 205, 395-397.

Kerridge, J. F., 1985. Carbon, hydrogen and nitrogen in carbonaceous chondrites: Abundances and isotopic compositions in bulk samples. Geochimica et Cosmochimica Acta 49, 1707-1714.

Kerridge, J. F., 1999. Formation and processing of organics in the early solar system. Space Science Reviews 90, 275-288.

Kiddell, C. B., Cloutis E. A., Dagdick B. R., Stromberg J. M., Applin D. M., Mann J. P., 2018. Spectral reflectance of powder coatings on carbonaceous chondrite slabs: Implications for asteroid regolith observations. J.Geophys. Research – Planets 123, 2803-2840; doi: https://doi.org/10.1029/2018JE005600.

King, T. V. V., Ridley, I. W., 1987. Relation of the spectroscopic reflectance of olivine to mineral chemistry and some remote sensing implications. J. Geophys. Res. 92, 11,457-11,469.

Kimura, M., Sugiura, N., Mikouchi, T., Hirajima, T., Hiyagon, H., Takehana, Y., 2013. Eclogitic clasts with omphacite and pyrope-rich garnet in the NWA 801 CR2 chondrite. Amer. Mineral. 98, 387-393.

Kimura, M., Grossman, J. N., Weisberg M. K., 2011. Fe-Ni metal and sulfide minerals in CM chondrites: An indicator for thermal history. Meteorit. Planet. Sci. 46, 431–442.

Kimura, M., Grossman, J. N., Weisberg M. K., 2008. Fe-Ni metal in primitive chondrites: Indicators of classification and metamorphic conditions for ordinary and CO chondrites. Meteorit. Planet. Sci. 43,1161–1177.

Koch, I., Floss, C., 2017. Abundances and compositions of presolar grains in CR2 chondrite EET 92042 (abstract). 48th Lunar Planet. Sci. Conf., #2984.

Kong, P., Palme, H., 1999. Compositional and genetic relationship between chondrules, chondrule rims, metal and matrix in the Renazzo chondrite. Geochim. Cosmochim. Acta 63, 3673–3682.

Kong, P., Ebihara, M., Palme, H., 1999. Distribution of siderophile elements in CR chondrites: Evidence for evaporation and recondensation during chondrule formation. Geochim. Cosmochim. Acta 63, 2637–2652.

Krot, A. N., Nagashima, K., van Kooten, E. M. M., Bizzarro, M., 2017. High-temperature rims around calcium-aluminum-rich inclusions from the CR, CB and CH carbonaceous chondrites. Geochim. Cosmochim. Acta 201, 155-184.

Krot, A. N., Libourel, G., Goodrich, C. A., Petaev, M. I., 2004. Silica-rich igneous rims around magnesian chondrules in CR carbonaceous chondrites: evidence for fractional condensation during chondrule formation. Meteorit. Planet. Sci. 39, 1931–1955.

Krot, A. N., Keil, K., 2002. Anorthite-rich chondrules in CR and CH carbonaceous chondrites: genetic link between calcium–aluminum-rich inclusions and ferromagnesian chondrules. Meteorit. Planet. Sci, 37, 91–111.

Krot, A. N., Yurimoto, H., McKeegan, K. D., Leshin, L., Chaussidon, M., Libourel, G., Yoshitake, M., Huss, G. R., Guan, Y., Zanda, B., 2006a. Oxygen isotopic compositions of chondrules: implications for evolution of oxygen isotopic reservoirs in the inner solar nebula. Chemie der Erde - Geochemistry 66, 249–276.

Krot, A. N., Libourel, G., Chaussidon, M., 2006b. Oxygen isotope compositions of chondrules in CR chondrites. Geochim. Cosmochim. Acta 70, 767–779.

Krot, A. N., McKeegan, K. D., Leshin, L. A., MacPherson, G. J., Scott, E. R. D., 2002. Existence of an ^{16}O-rich gaseous reservoir in the solar nebula. Science 295, 1051–1054.

Kung, C. -C., Clayton, R. N., 1978. Nitrogen abundances and isotopic compositions in stony meteorites. Earth Planet. Sci. Lett. 38, 421-435.

Lee, M. R., Bland, P. A., 2004. Mechanisms of weathering of meteorites recovered from hot and cold deserts and the formation of phyllosilicates. Geochim. Cosmochim. Acta 68, 893–916.

Lee, M. S., Rubin, A. E., Wasson, J. T., 1992. Origin of metallic Fe-Ni in Renazzo and related chondrites. Geochim. Cosmochim. Acta 56, 2521-2533.

Le Guillou, C., Changela, H. G., Brearley, A. J., 2015a. Widespread oxidized and hydrated amorphous silicates in CR chondrite matrices: Implications for alteration conditions and H2 degassing of asteroids. Earth Planet. Sci. Lett. 420, 162-173.

Le Guillou, C., Dohmen, R., Rogalla, D., Müller, T., Vollmer, C., Becker, H.-W. 2015b. New experimental approach to study aqueous alteration of amorphous silicates at low reaction rates. Chemical Geology 412, 179-192.

Le Guillou, C., Brearley, A. J., 2014. Relationships between organics, water and early stages of aqueous alteration in the pristine CR3.0 chondrite MET 00426. Geochim. Cosmochim. Acta 131, 344-367.

Le Guillou, C., Bernard, S., Brearley, A. J., Remusat, L., 2014. Evolution of organic matter in Orgueil, Murchison and Renazzo during parent body aqueous alteration: In situ investigations. Geochim. Cosmochim. Acta 131, 368-392.

Leitner, J., Hoppe, P., Zipfel, J., 2016a. The presolar grain inventory of the CR chondrite Elephant Moraine 92161 (abstract). 47th Lunar Planet. Sci. Conf., #1873.

Leitner, J., Vollmer, C., Floss, C., Zipfel, J., Hoppe, P., 2016b. Ancient stardust in fine-grained chondrule dust rims from carbonaceous chondrites. Earth Planet. Sci. Lett. 434, 117-128.

Leitner, J., Hoppe, P., and Zipfel, J., 2015. Distribution and abundance of presolar silicate and oxide stardust in CR chondrites (abstract). 46th Lunar Planet. Sci. Conf., #1874.

Leitner, J., Vollmer, C., Hoppe, P., Zipfel, J., 2012a. Characterization of presolar material in the CR chondrite Northwest Africa 852. Astrophys. J. 745, 38.

Leitner, J., Hoppe, P., Zipfel, J., 2012b. The stardust inventories of Graves Nunataks 95229 and Renazzo: Implications for the distribution of presolar grains in CR chondrites (abstract). 43rd Lunar Planet. Sci. Conf., #1835.

Leitner, J., Hoppe, P., Zipfel, J., 2011. The stardust inventory of the CR chondrites GRA 95229 and GRA 06100 assessed by NanoSIMS (abstract). 42nd Lunar Planet. Sci. Conf., #1713.

Lerner, N. R., Peterson, E., Chang, S., 1993. The Strecker synthesis as a source of amino acids in carbonaceous chondrites–Deuterium retention during synthesis. Geochim. Cosmochim. Acta 57, 4713-4723.

Losiak, A., Velbel, M. A., 2011. Evaporite formation during weathering of Antarctic meteorites-A weathering census analysis based on the ANSMET database. Meteorit. Planet. Sci. 46, 443-458.

Macke, R., Consolmagno, G., Britt, D., 2011. Density, porosity, and magnetic susceptibility of carbonaceous chondrites. Meteorit. Planet. Sci. 46, 1842-1862.

MacPherson, G. J., 2014. Calcium-aluminum-rich inclusions in chondritic meteorites. *In* Volume 1 of Treatise on Geochemistry (Second Edition), Meteorites and Cosmochemical Processes, Elsevier (Eds: Andrew M. Davis), p.139-179.

MacPherson, G. J., Mittlefehldt, D. W., Lipschutz, M. E., Clayton, R. N., Bullock, E. S., Ivanov, A. V., Mayeda, T. K., Wang, M.-S., 2009. The Kaidun chondrite breccias: Petrology, oxygen isotopes, and trace element abundances. Geochim. Cosmochim. Acta 73, 5493-5511.

Martins, Z., Alexander, C. M. O. D., Orzechowska, G. E., Fogel, M. L., Ehrenfreund, P., 2007. Indigenous amino acids in primitive CR meteorites. Meteorit. Planet. Sci. 42, 2125-2136.

Mason, B., 1971. The carbonaceous chondrites--a selective review. Meteoritics 6, 59-70.

Mason, B., 1962. The classification of chondritic meteorites. Amer. Museum Novitates 2085, 1-20.

Mason, B., 1960a. The origin of meteorites. J. Geophys. Res. 65, 2965-2970.

Mason, B., 1960b. Origin of chondrules and chondritic meteorites. Nature 186, 230-231.

Mason, B., Wiik, H. B., 1962. The Renazzo meteorite. Amer. Museum Novitates 2106, 1-11.

*Matsuda, S., Nakashima, D., Iio, H., Bajo, K., Nagao, K., 2009. Laser Microprobe Noble Gas Analysis of Chondrules in the NWA 801 CR2 Chondrite (abstract). 40th Lunar Planet. Sci. Conf. LPI Contribution id.1628.

Matthews C. N., Minard, R. D., 2008. Hydrogen cyanide polymers connect cosmochemistry and biochemistry. Proc. IAU Symp. Series 4, 453-457.

McBride, K., McCoy, T., Welzenbach, L., 2001a. MET 00426. Antarctic Meteorite Newslett. 24, 18.

McBride, K., McCoy, T., Welzenbach, L., 2001b. QUE 99177. Antarctic Meteorite Newslett. 24, 14.

McNamara, D. D., 2012. Omphacite—a mineral under pressure! Geology Today 28, 71–75.

McSween, H. Y., Jr., 1979a. Are carbonaceous chondrites primitive or processed? A review. Rev. Geophys. Space Phys. 17, 1059-1078.

McSween, H. Y., Jr., 1979b. Alteration in CM carbonaceous chondrites inferred from modal and chemical variations in matrix. Geochim. Cosmochim. Acta 43, 1761-1770.

McSween, H. Y., Jr., 1977a. Petrographic variations among carbonaceous chondrites of the Vigarano type. Geochim. Cosmochim. Acta 141, 1777-1790.

McSween, H. Y., Jr., 1977b. On the nature and origin of isolated olivine grains in carbonaceous chondrites. Geochim. Cosmochim. Acta, 41, 411-418.

Meinert, C., Jones, N. C., Hoffmann, S. V., Meierhenrich, U. J., 2016. Anisotropy spectroscopy of chiral alcohols, amines, and monocarboxylic acids: Implications for the analyses of extraterrestrial samples. J. Photochem. Photobiol. A 331, 130-137.

Meinert, C., Hoffmann, S. V., Cassam-Chenai, P., Evans, A. C., Giri, C., Nahon, L., Meierhenrich, U. J., 2014. Photonenergy-controlled symmetry breaking with circularly polarized light. Angew. Chem. Int. Ed. 53, 210-214.

Meinert, C., Bredehöft, J. H., Filippi, J. J., Baraud, Y., Nahon, L., Wien, F., Jones, N. C., Hoffmann, S. V., Meierhenrich, U. J., 2012. Anisotropy spectra of amino acids. Angew. Chem., Int. Ed. 51, 4484-4487.

Messenger, S., Keller, L. P., Lauretta, D. S., 2005. Supernova olivine from cometary dust. Science 309, 737-741.

Messenger, S., 2000. Identification of molecular-cloud material in interplanetary dust particles. Nature 404, 968-971.

Miyamoto, M., Zolensky, M. E., 1994. Infrared diffuse reflectance spectra of carbonaceous chondrites: Amount of hydrous minerals. Meteoritics 29, 849-853.

Modica, P., Meinert, C., De Marcellus, P., Nahon, L., Meierhenrich, U. J., d'Hendecourt, L. Le S., 2014. Enantiomeric excesses induced in amino acids by ultraviolet circularly polarized light irradiation of extraterrestrial ice analogs: A possible source of asymmetry for prebiotic chemistry. Astrophys. J. Lett. 788, 79-89.

Moghadam, R. H., Trepmann, C. A., Stockhert, B., Renner, J., 2010. Rheology of synthetic omphacite aggregates at high pressure and high temperature. J. Petrology 51, 921–945.

Molster, F. J., Waters, L. B. F. M., Tielens, A. G. G. M., Koike, C., Chihara, H., 2002. Crystalline silicate dust around evolved stars. III. A correlations study of crystalline silicate features. Astron. Astrophys. 382, 241-255.

Morlok, A., Libourel, G., 2013. Aqueous alteration in CR chondrites: Meteorite parent body processes as analogue for long-term corrosion processes relevant for nuclear waste disposal. Geochim. Cosmochim. Acta 103, 76–103.

Morris, R. V., Lauer Jr., H. V., Lawson, C. A., Gibson Jr., E. K., Nace, G. A., Stewart, C., 1985. Spectral and other physicochemical properties of submicron powders of hematite (α-Fe_2O_3), maghemite (γ-Fe_2O_3), magnetite (Fe_3O_4), goethite (α-FeOOH), and lepidocrocite (γ-FeOOH). J. Geophys. Res. 90, 3126-3144.

Myrgorodska, I., Meinert, C., Hoffmann, S. V., Jones, N. C., Nahon, L., Meierhenrich, U. J., 2017. Light on chirality: Absolute asymmetric formation of chiral molecules relevant in prebiotic evolution. ChemPlusChem 82, 74-87.

Nagashima, K., Krot, A. N., Huss, G. R., 2014. ^{26}Al in chondrules from CR2 chondrites. Geochemic. J. 48, 561-570.

Nagashima, K., Krot, A. N., Yurimoto, H., 2004. Stardust silicates from primitive meteorites. Nature 428, 921-924.

Nakashima, D., Matsuda, S., Iio, H., Bajo, K., Ebisawa, N., Nagao, K., 2009. Noble gases in the NWA 852/801 CR2 chondrites (abstract). 40th Lunar Planet. Sci. Conf., LPI Contribution, id. 1661.

Nguyen, A. N., Keller, L. P., Messenger, S., Rahman, Z., 2017a. Mineralogical characterization of Fe-bearing AGB and Supernova silicate grains from the Queen Alexandra Range 99177 meteorite (abstract). 48th Lunar Planet. Sci., #2371.

Nguyen, A. N., Keller, L. P., Rahman, Z., Messenger, S., 2017b. Microstructural study of an ^{18}O-poor presolar silicate grain from the Meteorite Hills 00426 CR3 chondrite (abstract). Meteorit. Planet. Sci. 80, A6332.

Nguyen, A. N., Keller, L. P., Messenger, S., 2016. Mineralogy of presolar silicate and oxide grains of diverse stellar origins. Astrophys. J. 818, 51-67.

Nguyen, A. N., Nittler, L. R., Stadermann, F. J., Stroud, R. M., Alexander, C. M. O. D., 2010. Coordinated analysis of presolar grains in the Allan Hills 77307 and Queen Elizabeth Range 99177 meteorites. Astrophys. J. 719, 166-189.

Nguyen, A. N., Stadermann, F. J., Zinner, E., Stroud, R. M., Alexander, C. M. O. D., Nittler, L. R., 2007. Characterization of presolar silicate and oxide grains in primitive carbonaceous chondrites. Astrophys. J. 656, 1223-1240.

Nguyen, A. N., Zinner, E., 2004. Discovery of ancient silicate stardust in a meteorite. Science 303, 1496-1499.

Nguyen, A., Zinner, E., Lewis, R. S., 2003. Identification of small presolar spinel and corundum grains by isotopic raster imaging. Astronom. Society of Australia 20, 382-388.

L. R. Nittler, Stroud, R. M., Trigo-Rodríguez, J. M., De Gregorio, B. T., Alexander, C. M. O'D., Davidson J., Moyano-Cambero, C. E., Tanbakouei, S., 2019. A cometary building block in a primitive asteroidal meteorite. Nature Astronomy 3, 659-666.

Nuth, J. A., III, Brearley, A. J., AND Scott, E. R. D., 2005. Microcrystals and amorphous material in comets and primitive meteorites: Keys to understanding processes in the early solar system. *In* Chondrites and the Protoplanetary Disk (eds. A. N. Krot, E. R. D. Scott and B. Reipurth), pp. 675-700. ASP Conference Series 341. Astronomical Society of the Pacific, San Francisco.

Nittler, L. R., Alexander, C. M. O. D., Davidson, J., Riebe, M. E. I., Stroud, R. M., Wang, J., 2018. High abundances of presolar grains and 15N-rich organic matter in CO3.0 chondrite Dominion Range 08006. Geochim. Cosmochim. Acta 226, 107-131.

Oberti, R., Caporuscio, F. A., 1991. Crystal-chemistry of clinopyroxenes from mantle eclogites—a study of the key role of the M2 site population by means of crystal-structure refinement. Amer. Mineral. 76, 1141–1152.

Olsen, M. B., Wielandt, D., Schiller, M., Van Kooten, E. M. M. E., Bizzarro, M., 2016. Magnesium and ^{54}Cr isotope compositions of carbonaceous chondrite chondrules – Insights into early disk processes. Geochim. Cosmochim. Acta 191, 118-138.

Orthous-Daunay, F.-R., Quirico, E., Beck, P., Brissaud, O., Dartois, E., Pino, T., Schmitt, B., 2013. Mid-infrared study of the molecular structure variability of insoluble organic matter from primitive chondrites. Icarus 223, 534-543.

Osawa, T., Kagi, H., Nagao, K., 2001. Mid-infrared transmission spectra of individual Antarctic micrometeorites and carbonaceous chondrites. Antarctic Meteorite Research 14, 71-88.

*Osawa, T., Kagi, H., Nakamura, T., Noguchi, T., 2005. Infrared spectroscopic taxonomy for carbonaceous chondrites from speciation of hydrous components. Meteorit. Planet. Sci. 40, 71-86.

Pearson, V. K., Sephton, M. A., Franchi, I. A., Gibson, J. M., Gilmour, I., 2006. Carbon and nitrogen in carbonaceous chondrites: Elemental abundances and stable isotopic compositions. Meteorit. Planet. Sci. 41, 1899-1918.

Peltzer, E. T., Bada, J. L., Schlesinger, G., Miller, S. L., 1984. The chemical conditions on the parent body of the Murchison meteorite: some conclusions based on amino, hydroxy and dicarboxylic acids. Adv. Space Research 4, 69-74.

Perronnet, M., Berger, G., Zolensky, M. E., Toplis, M. J., Bajagic, M., 2007. The aqueous alteration of CR chondrites: Experimental and geochemical modeling (abstract). 38thLunar Planet. Sci. Conf., #1110.

Perronnet, M., Zolensky, M. E., 2006. Characterization and quantification of metallic and mineral phases in the highly hydrated Grosvenor Mountains 95577 CR1 chondrite (abstract). 37th Lunar Planet. Sci. Conf., no.2402.

Pizzarello, S., Yarnes, T., 2016. Enantiomeric excesses of chiral amines in ammonia-rich carbonaceous meteorites. Earth Planet. Sci. Lett. 443, 176-184.

Pizzarello, S., Schrader, D. L., Monroe, A. A., Lauretta, D. S., 2012. The chiral composition of primitive CR meteorites and the diverse effects of water in cosmochemical evolution. Proc. Natl. Academy Sci. USA 109, 11949–11954.

Pizzarello, S., Williams, L. B., 2012. Ammonia in the early solar system: An account from carbonaceous meteorites. Astrophys. J. 749, 161 (6pp).

Pizzarello, S., Williams, L. B., Lehman, J., Holland, G. P., Yarger, J. L., 2011. Abundant ammonia in primitive asteroids and the case for a possible exobiology. Proc. Natl. Academy Sci. USA 108, 4303-4306.

Pizzarello, S., Holmes, W., 2009. Nitrogen-containing compounds in two CR2 meteorites: ^{15}N composition, molecular distribution and precursor molecules. Geochim. Cosmochim. Acta 73, 2150-2162.

Pizzarello, S., Huang, Y., Alexandre, M. R., 2008. Molecular asymmetry in extraterrestrial chemistry: Insights from a pristine meteorite. Proc. Natl. Academy Sci. USA 105, 3700-3704.

Pizzarello, S., Cooper, G., Flynn, G., 2006. The nature and distribution of the organic material in carbonaceous chondrites and interplanetary dust particles. *In* Meteorites and the Early Solar System II. Univ. Arizona Press (Eds: D. Lauretta and H. McSween), p.p. 625-651.

Pollock, G. E., Cheng, C.-N., Cronin, S. E., Kvenvolden, K. A., 1975. Stereoisomers of isovaline in the Murchison meteorite. Geochim. Cosmochim. Acta 39, 1571-1573.

Richardson, S. M., 1981. Alteration of mesostasis in chondrules and aggregates from three C2 carbonaceous chondrites. Earth Planet. Sci. Lett. 52, 67-75.

Righter, K., Satterwhite, C., Funk, R., Harrington, R. 2017. Historical trends in US Antarctic meteorite allocations, with a close look at CR chondrites (abstract). 80th Ann. Meet. Meteoritical Soc., LPI Contribution No., 1987, id. 6303.

Robert, F., Epstein, S., 1982. The concentration and isotopic composition of hydrogen, carbon and nitrogen in carbonaceous meteorites. Geochim. Cosmochim. Acta 46, 81-95.

Rochette, P., Gattacceca, J., Bonal, L., Bourot-Denise, M., Chevrier, M., Clerc, J.-P., Consolmagno, G., Folco, L., Gounelle, M., Kohout, T., Pesonen, L., Quirico, E., Sagnotti, L., Skripnik, A., 2008. Magnetic classification of stony meteorites: 2. Non-ordinary chondrites. Meteorit. Planet. Sci. 43, 959–980.

Rubin, A. E., 1988. Formation of ureilites by impact-melting of carbonaceous chondritic material. Meteoritics 23, 333-337.

Rubin, A. E., Trigo-Rodríguez, J. M., Huber, H., Wasson, J. T., 2007. Progressive aqueous alteration of CM carbonaceous chondrites. Geochim. Cosmochim. Acta 71, 2361-2382.

Russell, S. S., Zipfel, J., Grossman, J. N., Grady, M. M. (2002). The Meteoritical Bulletin, No. 86, 2002 July. Meteorit. Planet. Sci. 37, A157-A184.

Ruzicka, A., Grossman, J. N., Bouvier, A., Herd, C. D. K., Agee, C. B., 2015. The Meteoritical Bull. No. 102. Meteorit. Planet. Sci. 50, 1662-1662.

Ruzicka, A., Grossman, J. N., Garvie, L., 2014. The Meteoritical Bulletin, No. 100. Meteorit. Planet. Sci. 49, E1-E101.

Sandford, S. A., 1996. The inventory of interstellar materials available for the formation of the solar system. Meteorit. Planet. Sci. 31, 449-476.

Sandford, S. A., Bernstein, M. P., Dworkin, J. P. 2001. Assessment of the interstellar processes leading to deuterium enrichment in meteoritic organics. Meteorit. Planet. Sci. 36, 1117-1133.

Schmitt-Kopplin, P., Gabelica, Z., Gougeon, R. D., Fekete, A., Kanawati, B., Harir, M., Gebefuegi, I., Eckel, G., Hertkorn, N., 2010. High molecular diversity of extraterrestrial organic matter in Murchison meteorite revealed 40 years after its fall. Proc. Natl. Academy Science USA 107, 2763-2768.

Schrader, D. L., Lauretta, D. S., 2010. High-temperature experimental analogs of primitive meteoritic metal-sulfide-oxide assemblages. Geochim. Cosmochim. Acta 74, 1719-1733.

Schrader, D. L., Nagashima, K., Waitukaitis, S. R., Davidson, J., McCoy, T. J., Connolly, H. C., Lauretta, D. S., 2018a. The retention of dust in protoplanetary disks: Evidence from agglomeratic olivine chondrules from the outer Solar System. Geochim. Cosmochim. Acta 223, 405-421.

Schrader, D. L., Fu, R. R., Desch, S. J., Davidson, J. 2018b. The background temperature of the protoplanetary disk within the first four million years of the Solar System. Earth Planet. Sci. Lett. 504, 30-37.

Schrader, D. L., Nagashima, K., Krot, A. N., Ogliore, R. C., Yin, Q.- Z., Amelin, Y. A., Stirling, C. H., Kaltenbach, A., 2017. Distribution of ^{26}Al in the CR chondrite chondrule-forming region of the protoplanetary disk. Geochim. Cosmochim. Acta 201, 275–302.

Schrader, D. L., Connolly, Jr. H. C., Lauretta, D. S., Zega, T. J., Davidson, J., Domanik, K. J., 2015. The formation and alteration of the Renazzo-like carbonaceous chondrites III: Toward understanding the genesis of ferromagnesian chondrules. Meteorit. Planet. Sci. Suppl. 50, 15-50.

Schrader, D. L., Nagashima, K., Krot, A. N., Ogliore, R. C., Hellebrand, E., 2014. Variations in the O-isotope composition of gas during the formation of chondrules from the CR chondrites. Geochim. Cosmochim. Acta 132, 50–74.

Schrader, D. L., Connolly, H. C. Jr., Lauretta, D. S., Nagashima, K., Huss, G. R., Davidson, J., Domanik, K. J., 2013. The formation and alteration of the Renazzo-like carbonaceous chondrites II: Linking O-isotope composition and oxidation state of chondrule olivine. Geochim. Cosmochim. Acta 101, 302–327.

Schrader, D. L., Franchi, I. A., Connolly, Jr. H. C., Greenwood, R. C., Lauretta, D. S., Gibson, J. M., 2011. The formation and alteration of the Renazzo-like carbonaceous chondrites I: Implications of bulk-oxygen isotopic composition. Geochim. Cosmochim. Acta 75, 308-325.

Schrader, D. L., Connolly, Jr. H. C., Lauretta, D. S., 2008. Opaque phases in type-II chondrules from CR2 chondrites: Implications for CR parent body formation. Geochim. Cosmochim. Acta 72, 6124-6140.

Sherman, D. M., Burns, R. G., Burns, V. M., 1982. Spectral characteristics of the iron oxides with application to the Martian bright region mineralogy. J. Geophys. Research 87, 10169-10180.

Scott, E. R. D., Barber D. J., Alexander, C. M., Hutchinson, R., Peck, J. A., 1988. Primitive material surviving in chondrites – Matrix. *In* Meteorites and the early solar system, (eds Kerridge J. F. and Matthews M. S.). University of Arizona Press, 718-745.

Stroud, R. M., Floss, C., Stadermann, F. J., 2009. Structure, elemental composition and isotopic composition of presolar silicates in MET 00426 (abstract). 40th Lunar Planet. Sci. Conf., #1063.

Takano Y., Takahashi J., Kaneko T., Marumo K., Kobayashi K., 2007. Asymmetric synthesis of amino acid precursors in interstellar complex organics by circularly polarized light. Earth Planet. Sci. Lett. 254, 106-114.

Tenner, T. J., Nakashima, D., Ushikubo, T., Kita, N. T., Weisberg, M. K., 2015. Oxygen isotope ratios of FeO-poor chondrules in CR3 chondrites: Influence of dust enrichment and H_2O during chondrule formation. Geochim. Cosmochim. Acta 148, 228–250.

Tenner, T. J., Ushikubo, T., Nakashima, D., Kita, N. T., Weisberg, M. K., 2013. ^{26}Al in chondrules from the CR3.0 chondrite Queen Alexandra Range 99177: A link with O isotopes (abstract). 44th Lunar Planet. Sci. Conf., LPI Contrib. No. 1719, 2010.

Tielens, A. G. G. M., McKee, C. F., Seab, C. G., Hollenbach, D. J., 1994. The physics of grain-grain collisions and gas-grain sputtering in interstellar shocks. Astrophys. J. 431, 321-340.

Tielens, A. G. G. M., Waters, L. B. F. M., Molster, F. J., Justtanont, K., 1998. Circumstellar silicate mineralogy. Astrophys. Space Sci. 255, 415-426.

Tomeoka, K., Buseck, P., 1988. Matrix mineralogy of the Orgueil CI carbonaceous chondrite. Geochim. Cosmochim. Acta 52, 1627-1640.

Tomeoka, K., McSween, Y. H., Jr., Buseck, R. P., 1988. Aqueous alteration of CI and CM carbonaceous chondrites: A review. 13th Symp. Antarctic Meteorites, NIPR, 160.

Tomeoka, K., Buseck, P. R., 1985. Indicators of aqueous alteration in CM carbonaceous chondrites: Microtextures of a layered mineral containing Fe, S, O and Ni. Geochim. Cosmochim. Acta, 49, 2149-2163.

*Treiman, A. H., Gross, J. 2015. The CR2 chondrite NWA 801: Petrography and petrology (abstract). 78th Ann. Meet. Meteoritical Soc., LPI Contribution No. 1856, p. 5077.

Tsuchiyama, A., Mashio, E., Imai, Y., Noguchi, T., Miura, Y., Yano, H., Nakamura, T., 2009. Strength measurement of carbonaceous chondrites and micrometeorites using micro compression testing machine (abstract). Meteorit. Planet. Sci. Suppl., 5189.

Tyra, M. A., 2013. Using oxygen and carbon stable isotopes, ^{53}Mn-^{53}Cr isotope systematics, and petrology to constrain the history of carbonates and water in the CR and CM chondrite parent bodies. ProQuest Dissertations And Theses; Thesis (Ph.D.) -- The University of New Mexico, 2013; Publication Number: AAT 3588093; ISBN: 9781303260063; Source: Dissertation Abstracts International, Volume: 74-11(E), Section: B.; 235 p.p.

Urey, H. C., Craig H., 1953. The composition of the stone meteorites and the origin of the meteorites. Geochim. Cosmochim. Acta 4, 36-82.

van Dishoeck, E. F., 2004. ISO spectroscopy of gas and dust: from molecular clouds to protoplanetary disks. Ann. Rev. Astron. Astrophys. 42, 119-167.

van Schmus, W. R., Wood, J. A., 1967. A chemical-petrologic classification for the chondritic meteorites. Geochim. Cosmochim. Acta 31, 755-765.

Velbel, M. A., Long, D. T., Gooding, J. L., 1991. Terrestrial weathering of Antarctic stone meteorites - Formation of Mg-carbonates on ordinary chondrites. Geochim. Cosmochim. Acta 55, 67-76.

Wasson J. T., 1996. Chondrule formation: Energetics and length scales. *In* Chondrules and the Protoplanetary Disk. Cambridge Univ. Press (ed. R. H. Hewins, R. H. Jones and E. R. D. Scott), pp. 45–54.

Wasson, J. T., Rubin, A. E., 2014. Absence of matrix-like chondrule rims in CR2 LAP 02342. Meteorit. Planet. Sci. 49, 245-260.

Wasson, J. T., Rubin, A. E., 2010. Metal in CR chondrites. Geochim. Cosmochim. Acta 74, 2212-2230.

Wasson, J. T., Rubin, A. E., 2009. Composition of matrix in the CR chondrite LAP 02342. Geochim. Cosmochim. Acta 73, 1436-1460.

Weisberg, M. K., Huber, H., 2007. The GRO 95577 CR1 chondrite and hydration of the CR parent body. Meteorit. Planet. Sci. 42, 1495-1503.

Weisberg, M. K., McCoy, T. J., Krot, A. N., 2006. Systematics and evaluation of meteorite classification. *In* Meteorites and the Early Solar System II (eds. D.S. Lauretta and H.Y. McSween, Jr.). University of Arizona Press. pp. 19-52.

Weisberg, M. K., Connolly, H. C., Jr., Ebel, D. S., 2004. Petrology and origin of amoeboid olivine aggregates in CR chondrites. Meteorit. Planet. Sci. 39, 1741-1753.

Weisberg, M. K., Prinz, M., Clayton, R. N., Mayeda, T. K., Grady, M. M., Pillinger, C. T., 1995. The CR chondrite clan. Antarctic Meteorite Res. 8, 11.

Weisberg, M. K., Prinz, M., Clayton, R. N., Mayeda, T. K., 1993. The CR (Renazzo-type) carbonaceous chondrite group and its implications. Geochim. Cosmochim. Acta 57, 1567-1586.

*Weisberg, M. K., Prinz, M., Clayton, R. N., Mayeda, T. K., 1992. Formation of layered chondrules in CR2 chondrites: A petrologic and oxygen isotopic study. Meteorit. 27, 306.

*Weisberg, M. K., Prinz, M., 2001. The Grosvenor Mountains 95577 CR1 chondrite and hydration of the CR chondrites (abstract). Meteorit. Planet. Sci. 35, A168.

Wiik, H. B., 1956. The chemical composition of some stony meteorites. Geochim. Cosmochim. Acta 9, 279-289.

*Wlotzka F. 1993. A weathering scale for the ordinary chondrites (abstract). Meteorit. 28, 460.

*Wlotzka, F., Jull, A. J. T., Donahue D. J. 1995. Carbon-14 terrestrial ages of meteorites from Acfer, Algeria. *In* Meteorites from Cold and Hot Deserts. LPI Tech. Rpt. 95-02, 72–73.

Wood, J. A., 1962. Metamorphism in chondrites. Geochim. Cosmochim. Acta 26, 739-742.

Wood, J. A., 1963a. Chondrites and chondrules. Scientif. Amer. 4, 64-82.

Wood, J. A., 1963b. On the origin of chondrules and chondrites. Icarus 2, 152-180.

Wood, J. A., 1967. Chondrites: Their metallic minerals, thermal histories, and parent planets. Icarus 6, 1-49.

Wood, J. A., McSween, H. Y. Jr., 1977. Chondrules as condensation products. *In* Comets, asteroids, meteorites: Interrelations, evolution and origins; Proced. Thirty-ninth Internat. Colloquium, 365-373.

*Zanda, B., Bourot-Denise, M., Hewins, R. H., Cohen, B. A., Delaney, J. S., Humayun, M., Campbell, A. J., 2002. Accretion textures, iron evaporation and re-condensation in Renazzo chondrules (abstract). 33rd Lunar Planet. Sci. Conf. 1852.

Zanda, B, Yu, Y., Bourot-Denise, M., Hewins, R., 1997. The history of metal and sulfides in chondrites (abstract). Workshop on Parent-Body and Nebular Modification of Chondritic Materials, Lunar Planet. Institute, p.68.

Zanda, B., Bourot-Denise, M., Perron, C., Hewins, R. H., 1994. Origin and metamorphic redistribution of silicon, chromium, and phosphorus in the metal of chondrites. Science 265, Issue 5180, 1846-1849.

Zega, T. J., Buseck, P. R., 2003. Fine-grained-rim mineralogy of the Cold Bokkeveld CM chondrite. Geochim. Cosmochim. Acta 67, 1711–1721.

Zhao, X., Floss, C., Lin, Y., Bose, M., 2013. Stardust investigation into the CR chondrite Grove Mountain 021710. Astrophys. J. 769, article id. 49, 16 pp.

Zinner, E., 2014. Presolar Grains, *In* Meteorites and Cosmochemical Processes, Volume 1 (Ed. Andrew Davis), Treatise on Geochemistry (Second Edition). Elsevier, Oxford, pp. 181-213.

Zolensky, M. E., Abreu, N. M., Velbel, M. A., Rubin, A., Chaumard, N., Michikami T., 2018. Physical, chemical, and petrological characteristics of chondritic materials and their relationships to small Solar System bodies *In* Chapter 2 of Primitive Meteorites and Asteroids. Physical, Chemical and Spectroscopic Observations Paving the Way to Exploration (N. Abreu, editor); Elsevier, Amsterdam; https://doi.org/10.1016/B978-0-12-813325-5.00004-5 pp.

Zolensky, M. E., Barrett, R., Browning, L., 1993. Mineralogy and composition of matrix and chondrule rims in carbonaceous chondrites. Geochim. Cosmochim. Acta 57, 3123-3148.

FIGURE CAPTIONS

Fig. 1.
Back-scattered electron images of petrographic thin sections of Antarctic CR chondrites showing the range of different asteroidal features recorded by this group of meteorites. (a) Weakly altered CR EET 92105. Chondrules and metal show no signs of aqueous alteration. (b) Moderately aqueously altered LAP 04720. At the mm-µm scale, few appreciable mineralogical changes are noted. Chondrules and metal show no signs of aqueous alteration. (c) Extensive aqueously altered GRO 95577. Chondrules and metal have been extensively replaced by phyllosilicates and oxides. (d) Heated and recrystallized CR GRA 06100. CHO = chondrule; DI = dark inclusion; Fe-Ni = FeNi metal nodule; Mtx = matrix.

Fig. 2.
Back-scattered electron images showing the characteristics of Fe-Ni metal in type I chondrules from different members of the EET 87111 pairing group that have been affected by terrestrial weathering to different degrees. Although weathering processes progressively replace Fe-Ni metal nodules, there is significant heterogeneity in alteration features within individual stones. Abundant Fe-Ni metal grains are preserved in stones from weathering grade C. Fe-Ni = Fe-Ni metal nodule.

Fig. 3.
Three-oxygen isotope plot for bulk isotopic analyses from CR chondrites. Data from: Weisberg et al. (1993); Clayton and Mayeda (1999); Schrader et al. (2011, 2014); Harju et al. (2014). CCAM = Carbonaceous chondrite anhydrous minerals line. Y&R = Young and Russell line. TFL = Terrestrial fractionation line. Samples measured by multiple studies are denoted with an asterisk.

Fig. 4.
Back-scattered electron micrographs of the most common types of chondrules in CR chondrites. (a) Layered MgO-rich, type I chondrule (CHO) in MIL 090657, where the boundaries between the core and outer layers are outlined by Fe-Ni metal nodules. (b) Close up from (a), showing details on the outer chondrule shell, igneous rim with smaller Fe-Ni metal grains compared with interior nodules, and fine-grained rim containing tochilinite. (c) FeO-rich, type II chondrule in EET 92105. (d) Close up from (c), showing

opaque assemblages (Fe-Ni metal and Fe-Ni sulfides) in a type II chondrule in EET 92105. CHO = chondrule; Fe-Ni = FeNi metal nodule.

Fig. 5.

Electron micrographs of CR mesostasis in type I and type II chondrules. (a) BSE image of region within a type I chondrule in EET 96259. A box shows the area where a FIB section was retrieved. Notice that the metal grains show signs of weathering. (b) Bright-field TEM image from a FIB section from mesostasis in a type I chondrule in EET 96259. The mesostasis is made up of crystalline andesine and Mn-bearing augite. The band that was partially replaced was identified as predominantly SiO_2, with <5 wt.% combined total for other oxides (e.g., Al_2O_3, Cr_2O_3, MgO, FeO, and S). (c) Z-contrast, high-angle annular dark-field (HAADF) micrograph of the area of mesostasis boxed in (b). (d) X-ray elemental map overlay. Al= blue; Ni=white; Ca= orange; Na=green; Fe=yellow; K=magenta; Mg=red; Mn=pink. (e) BSE image of FeO-rich chondrule fragment with a rim of coarse-grained Fe and Fe-Ni sulfides from GRA 95229. Sulfides are also distributed interstitially to pyroxene bars. A box shows the area where a FIB section was retrieved. (f) Z-contrast, high-angle annular dark-field (HAADF) micrograph of a region in the FIB section of fayalitic olivine (Ol), pyrrhotite (Po), and quartz-pyroxene normative glass (Glass).

Fig. 6.

BSE images showing the different textural occurrences of fine-grained materials in CR chondrites.

(a) Micrograph of fine-grained matrix in MIL 090657, dominated by fine-grained silicates, with micron and sub-micron Fe-sulfides and Fe-oxides. (b) BSE image of a fine-grained rim around a type I chondrule in GRA 95229. Unlike interchondrule matrix, CR rims do not contain clastic materials (e.g., chondrule fragments). (c) BSE of a region in a dark inclusion in MET 00426, which is nearly featureless, but does contain some chondrule fragments. Dark inclusions in CRs are variable in textures. (d) BSE of a clast in MIL 090657, containing angular chondrule fragments set in fine-grained materials that are more FeO-rich (brighter in BSE) than the matrix in the host meteorite.

Fig. 7.

Three-oxygen isotope plot for matrix isotopic analyses from CR chondrites. Data from: Weisberg et al. (1993); Clayton and Mayeda (1999); Schrader et al. (2014). CCAM =

Carbonaceous chondrite anhydrous minerals line. Y&R = Young and Russell line. TFL = Terrestrial fractionation line. Samples measured by multiple studies are denoted with an asterisk.

Fig. 8.
TEM of images of the matrix of LAP 02342. (a) Z-contrast, high-angle annular dark-field (HAADF) micrograph of a matrix region from a FIB section. An assemblage of Fe-Mg amorphous silicates, Ca-bearing pyroxene (pyx), Mg-rich olivine, tochilinite, pentlandite, and organics is shown. (b) X-ray elemental map overlay. Ca= yellow; S=green; Fe=turquoise; Si=indigo; and C=red.

Fig. 9.
Electron micrographs of a matrix region located in mildly heated GRO 03116. (a) BSE image of the region of clastic matrix from which a FIB section was extracted (FIB-Mtx1). (b) Bright-field TEM image of a FIB section, showing an angular type I chondrule (CHO) fragment and fine-grained matrix materials. (c) Bright-field TEM image of Fe-Mg-rich phyllosilicates from the fine-grained matrix in (b). (d) High-resolution TEM image of Fe-Ni-metal (FeNi) embedded in Fe-Mg-rich amorphous silicates in matrix, inlaid diffraction pattern. (e) High-resolution TEM image of a rounded olivine (ol) crystal in matrix.

Fig. 10.
Presolar grain abundances in CR chondrites. The petrographic grades are 2 unless otherwise noted. Average abundances are shown for meteorites in which multiple surveys were conducted. All presolar grain surveys in CRs were conducted by raster ion imaging using a Cameca NanoSIMS ion probe, except for the study of NWA 530 (Nagashima et al., 2004), which used a SCAPS-equipped Cameca IMS 1270 of poorer spatial resolution. The reported abundance for this meteorite is a lower limit and cannot be directly compared to abundances determined through NanoSIMS analyses. (Data from Davidson et al., 2015, 2014a; Floss and Stadermann, 2005, 2009a,b; Koch and Floss, 2017; Leitner et al., 2011, 2012a,b, 2015, 2016a,b; Nagashima et al., 2004; Nguyen et al., 2010; Zhao et al., 2013).

Fig. 11.
Summary of the effects of aqueous alteration recorded by the components of CR chondrites from different petrologic types.

Fig. 12.

Electron micrographs of an omphacite and graphite-bearing clast in pristine QUE 99177, modified from Abreu (2013). (a) BSE image of clast and contacts with host meteorite. (b) Map of the distribution of different components and minerals based on X-ray compositional maps collected using EPMA. Note that the areas labeled as chondrules have significantly larger grains sizes and no graphite. (c) BSE image of a chondrule-like area, showing triple-junctions between olivine (Ol) crystals, interstitial hornblende, and omphacite (Hbl-Omp) crystals and Fe-sulfides. (d) BSE image of a matrix-like area, containing olivine (Ol), pargasite (Prg), troilite (Tro), and large graphite laths.

Fig. 13.

Infrared spectra of CR chondrites from different petrologic types. (a) Reflectance spectra (0.3-2.5 μm) of powdered samples of a CR1, CR2, and CR3 carbonaceous chondrite (from Cloutis et al., 2012). (b) Reflectance spectrum (0.35-2.5 μm) of a powdered sample of the thermally metamorphosed GRA 06100 CR3.6 chondrite. (c) Infrared reflectance spectra (2-5 μm) of powdered samples of some CR chondrites. (d) Infrared reflectance spectra (5-15 μm) of powdered samples of some CR chondrites.

Figure 1

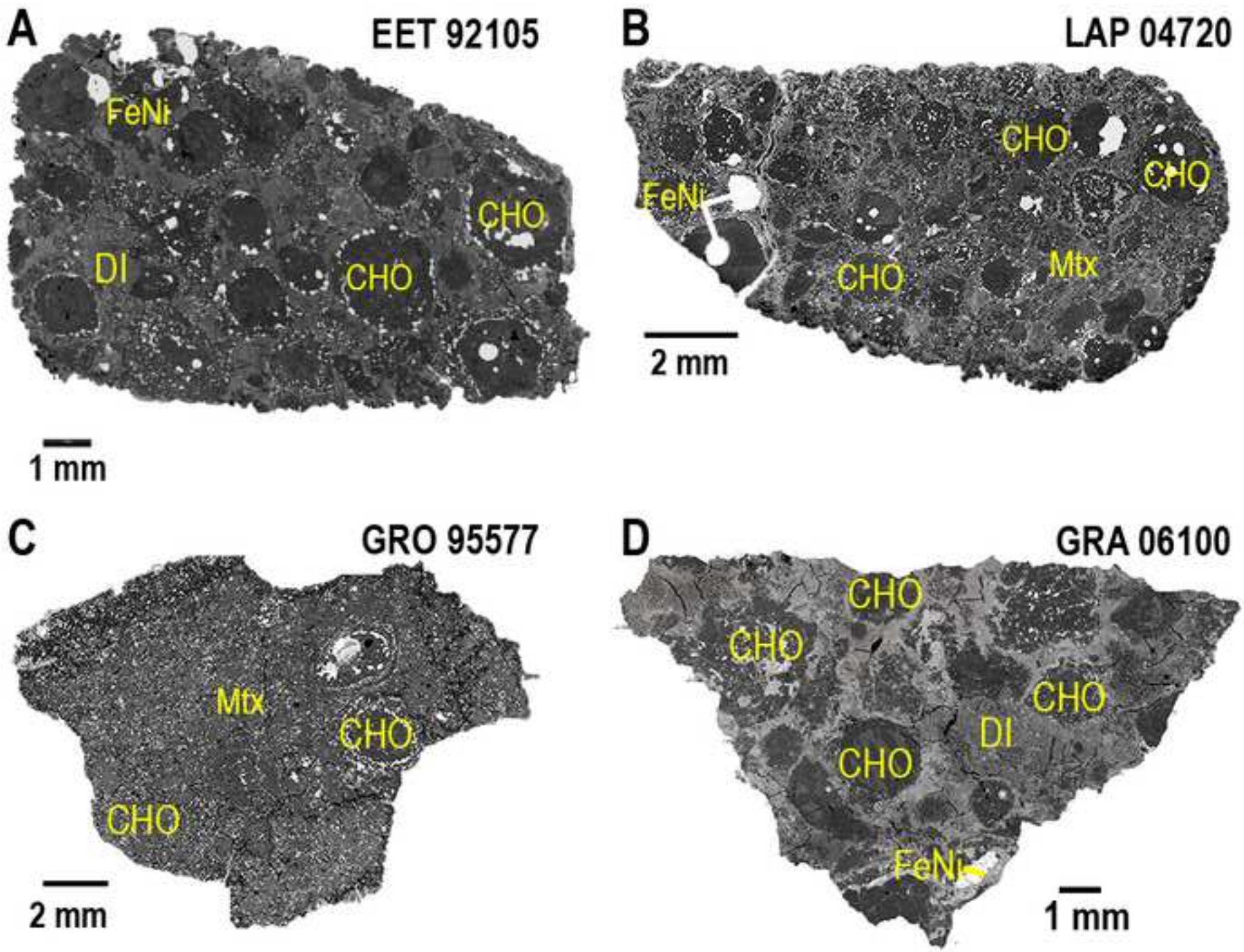

Figure 2

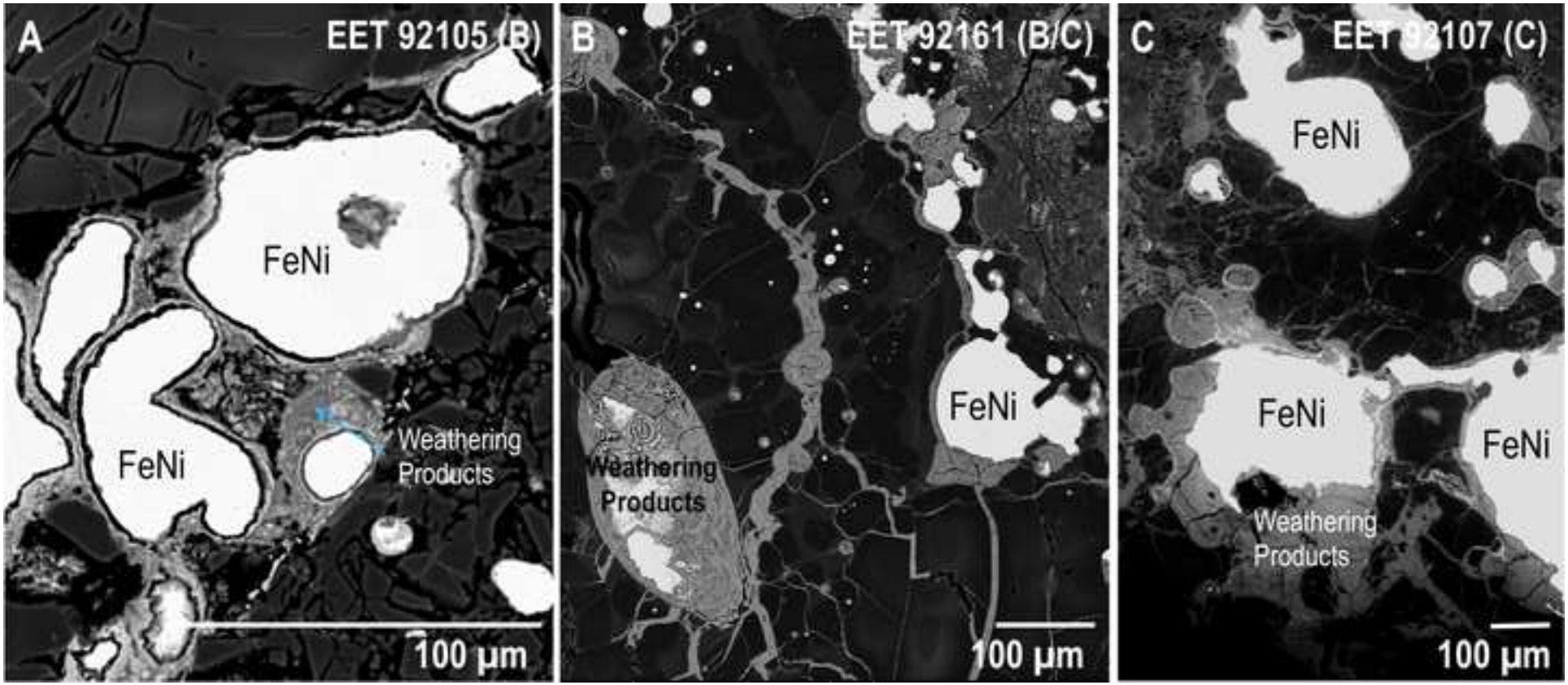

Figure 3

Click here to access/download;Figure;Figure 3 - Oxygen Isotopes.jpg

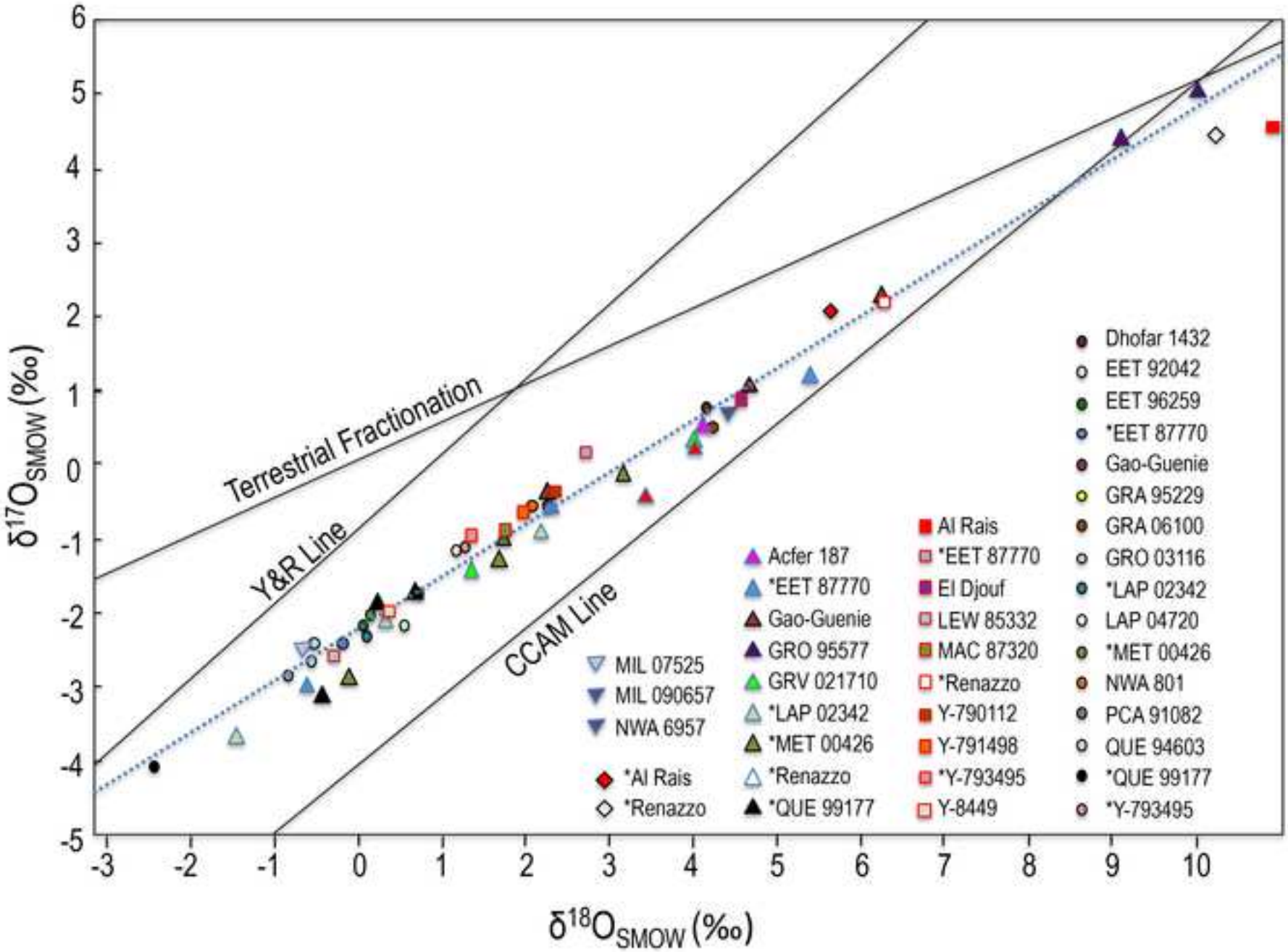

Figure 4

Click here to access/download;Figure;Figure 4 - CR Chondrules redrawn.jpg

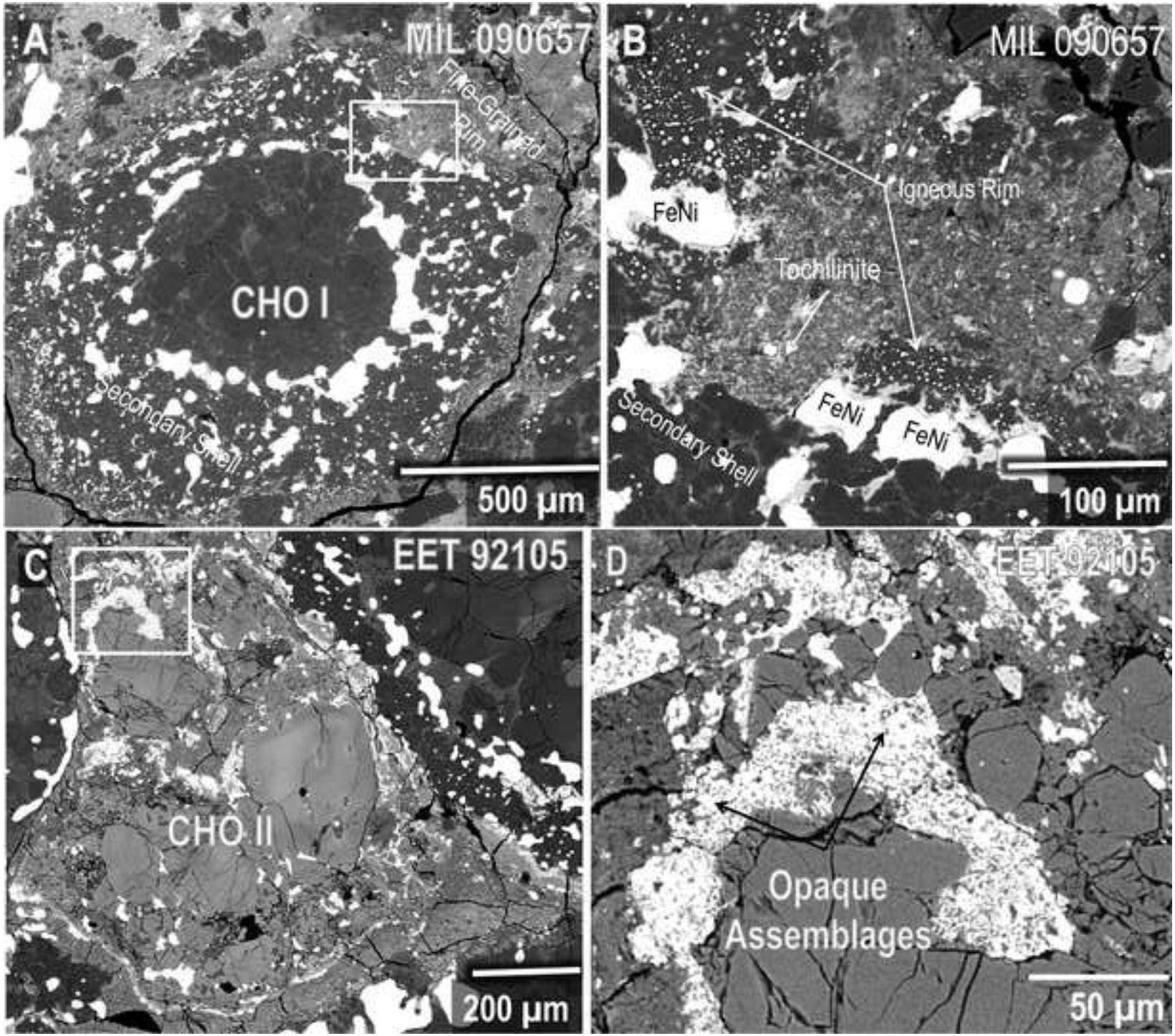

Figure 5

Click here to access/download;Figure;Figure 5 - CR Mesostasis Small.jpg

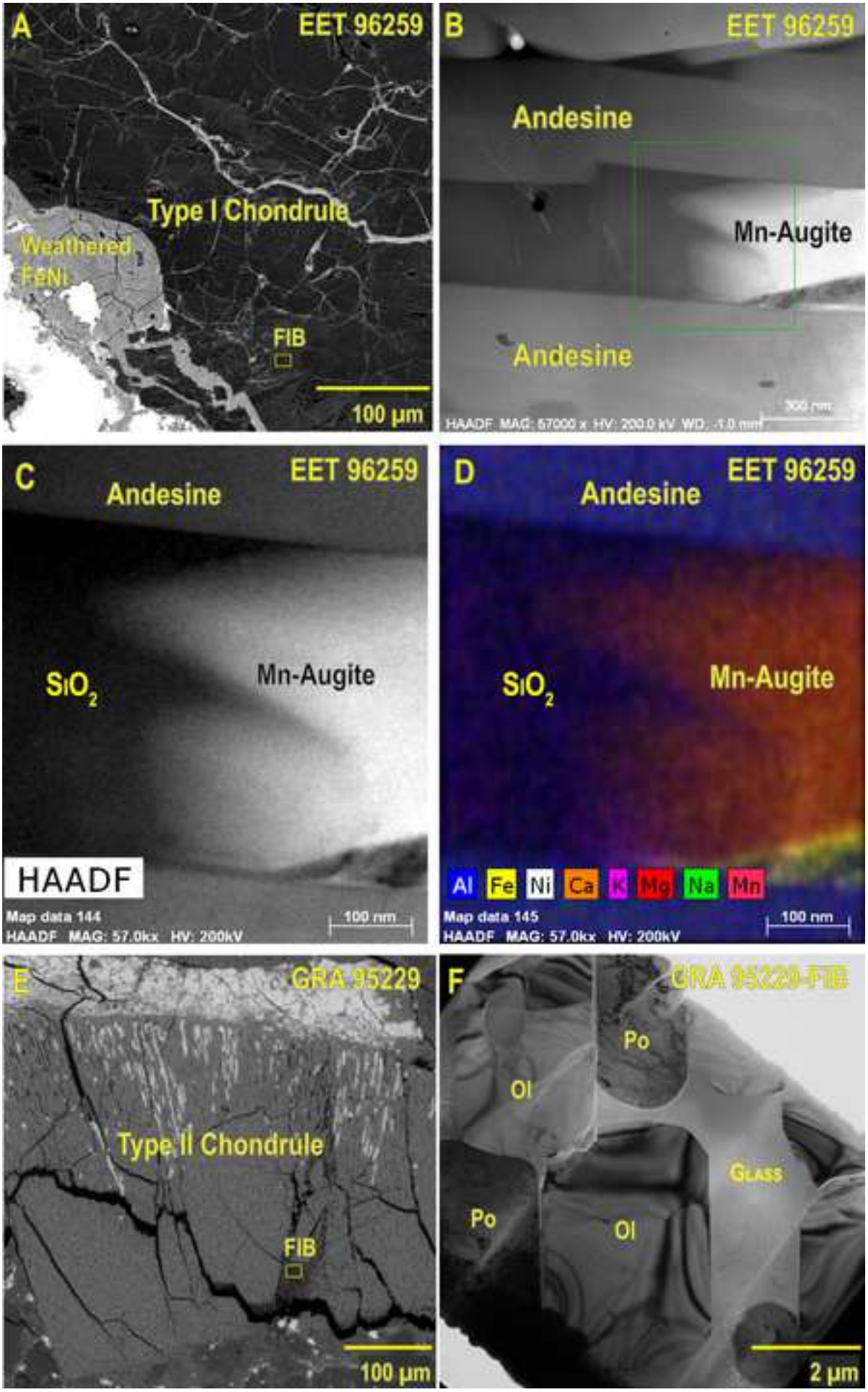

Figure 6

Click here to access/download;Figure;Figure 6 - CR Matrix small.jpg

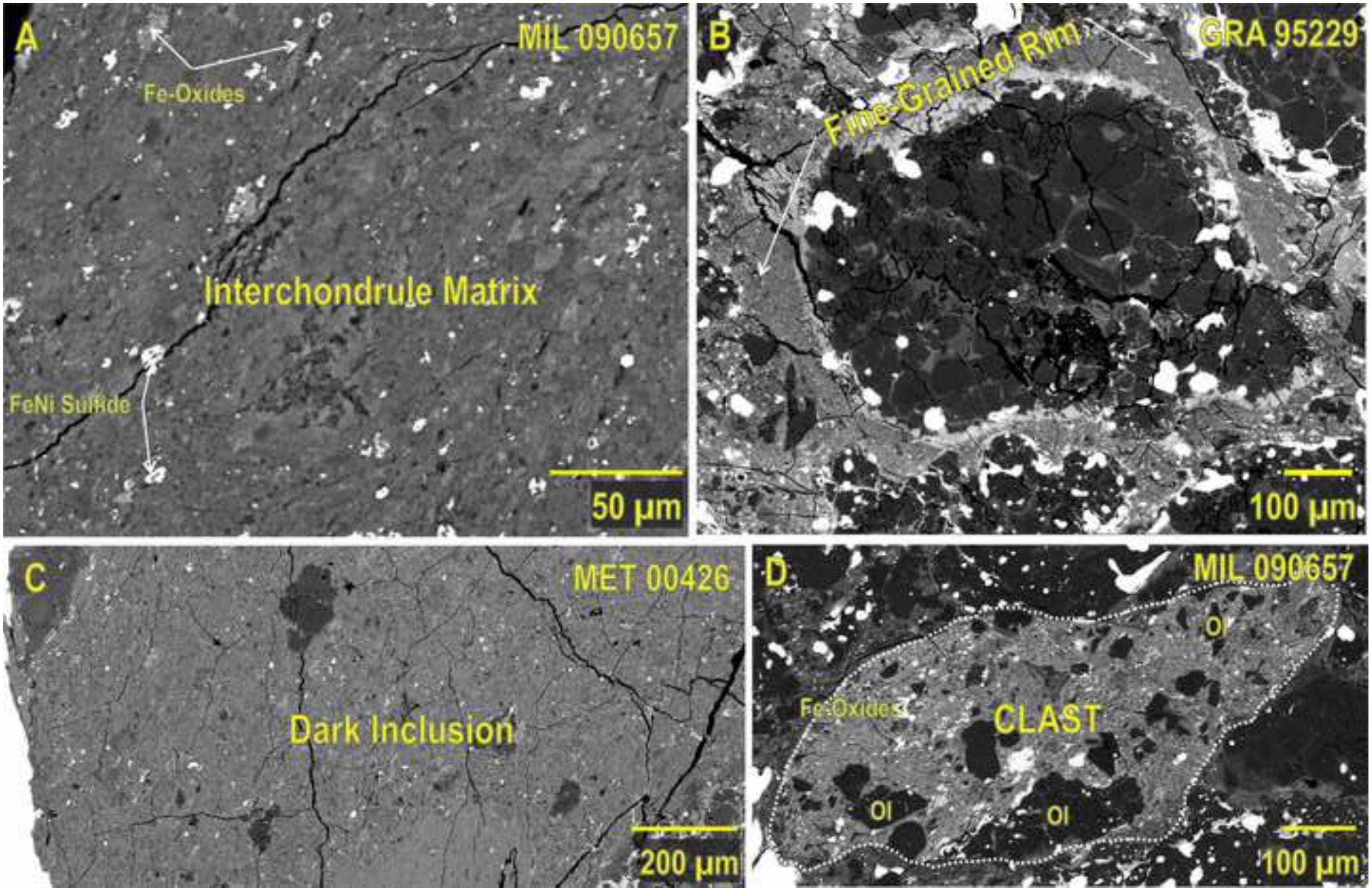

Figure 7

Click here to access/download;Figure;Figure 7 - Matrix Oxygen Isotopes.jpg

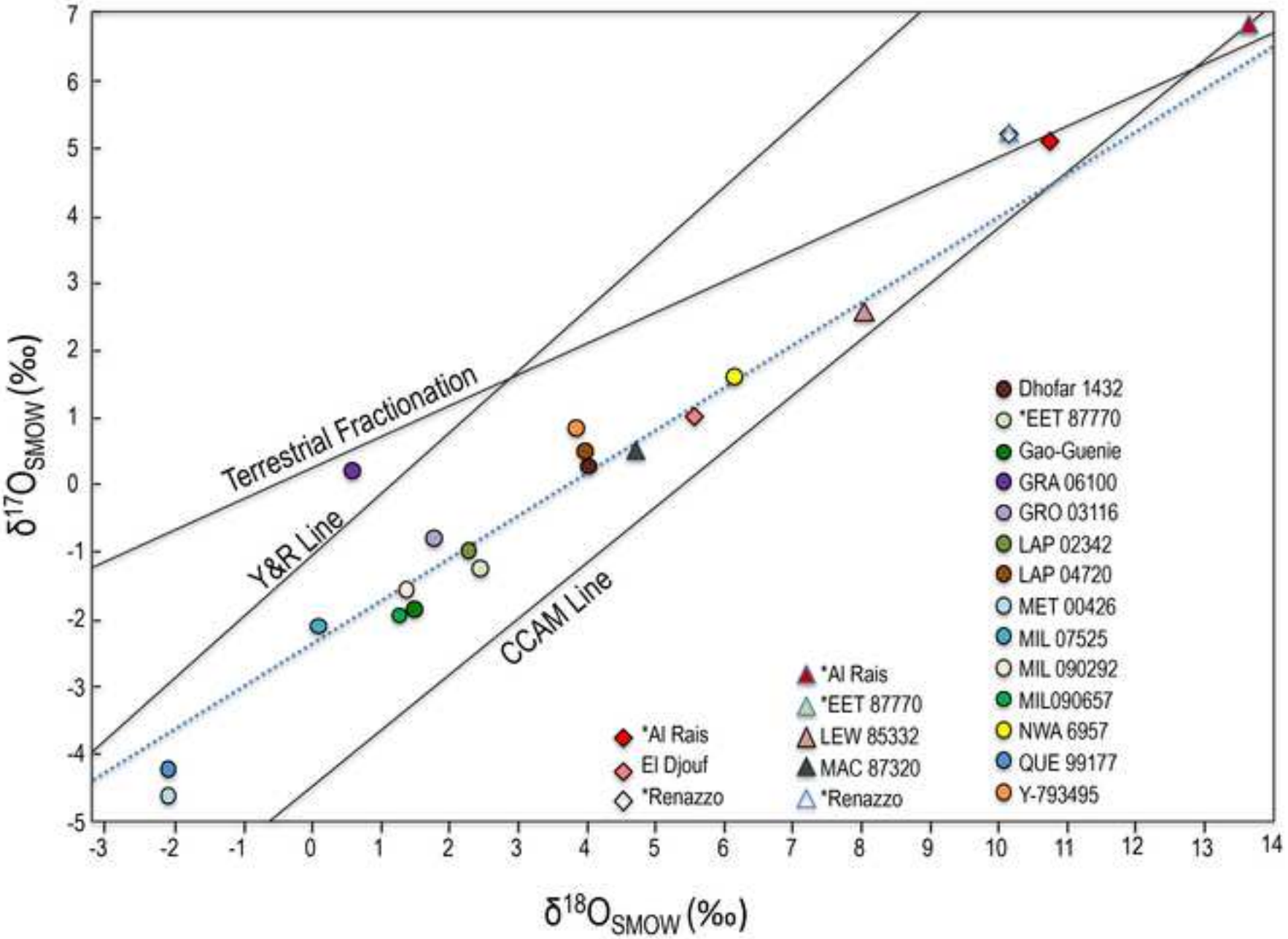

Figure 8

Click here to access/download;Figure;Figure 8 - Matrix.jpg

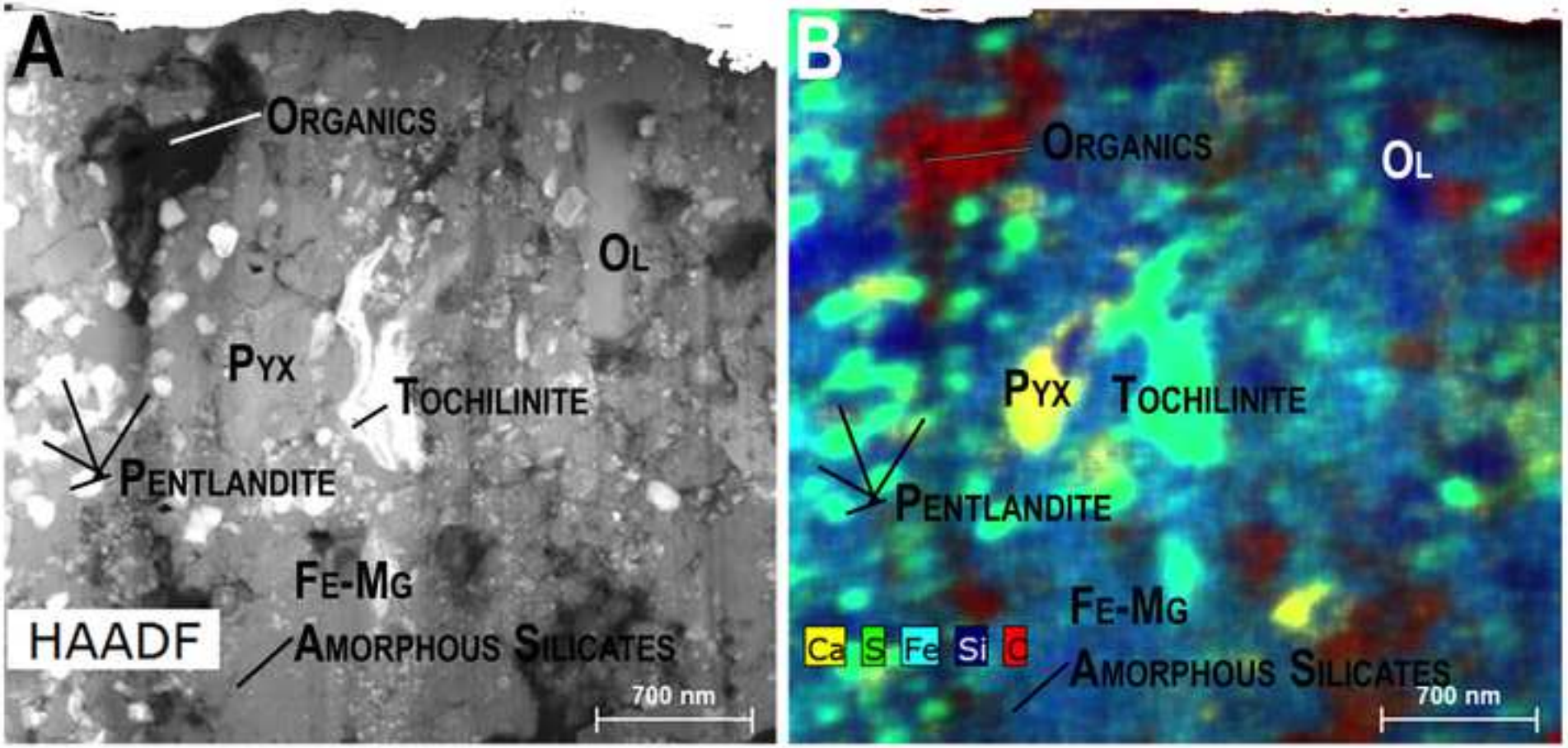

Figure 9

Click here to access/download;Figure;Figure 9 - Matrix of heated CR.jpg

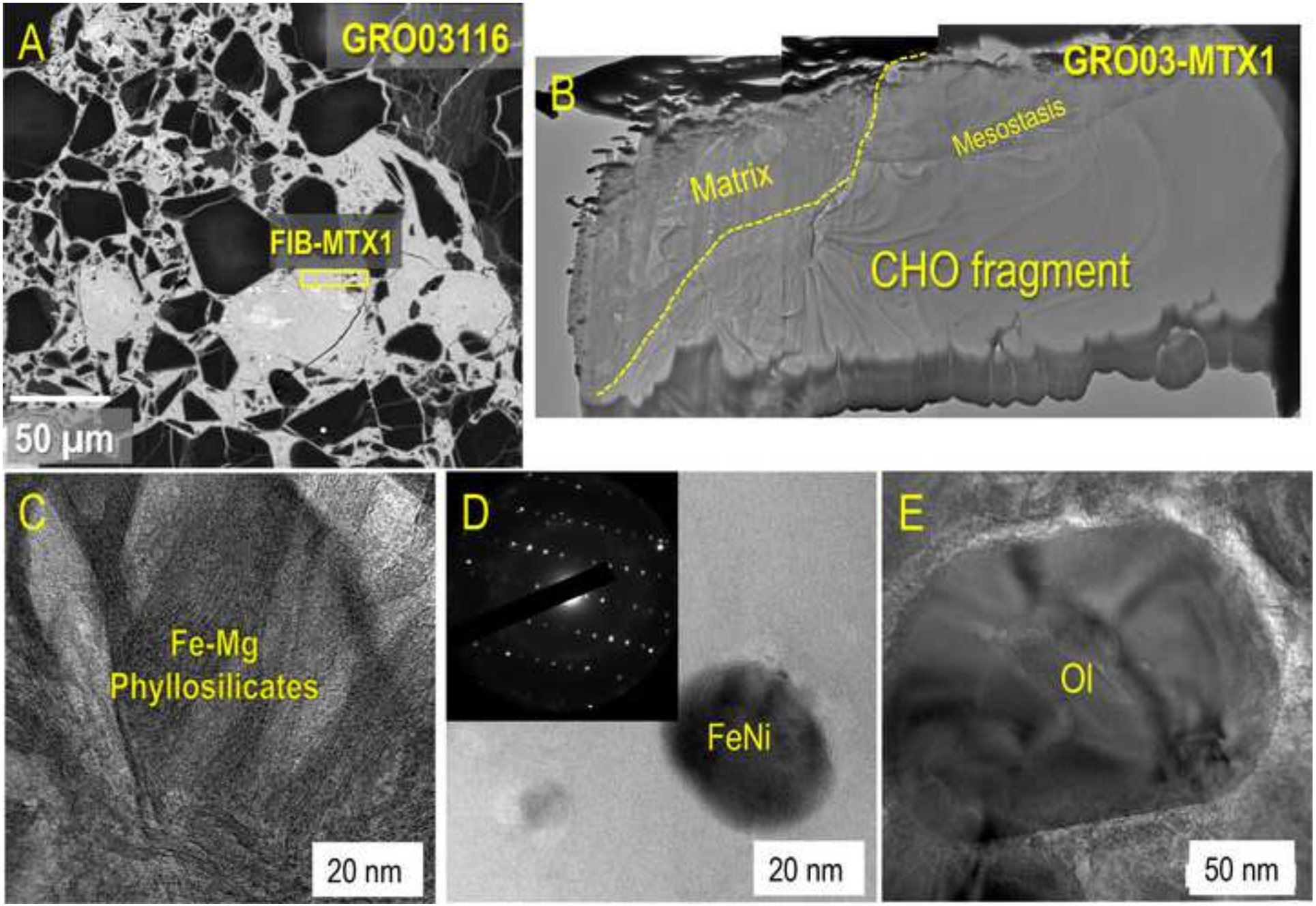

Figure 10

Click here to access/download;Figure;Figure 10 - Presolar Grains.jpg

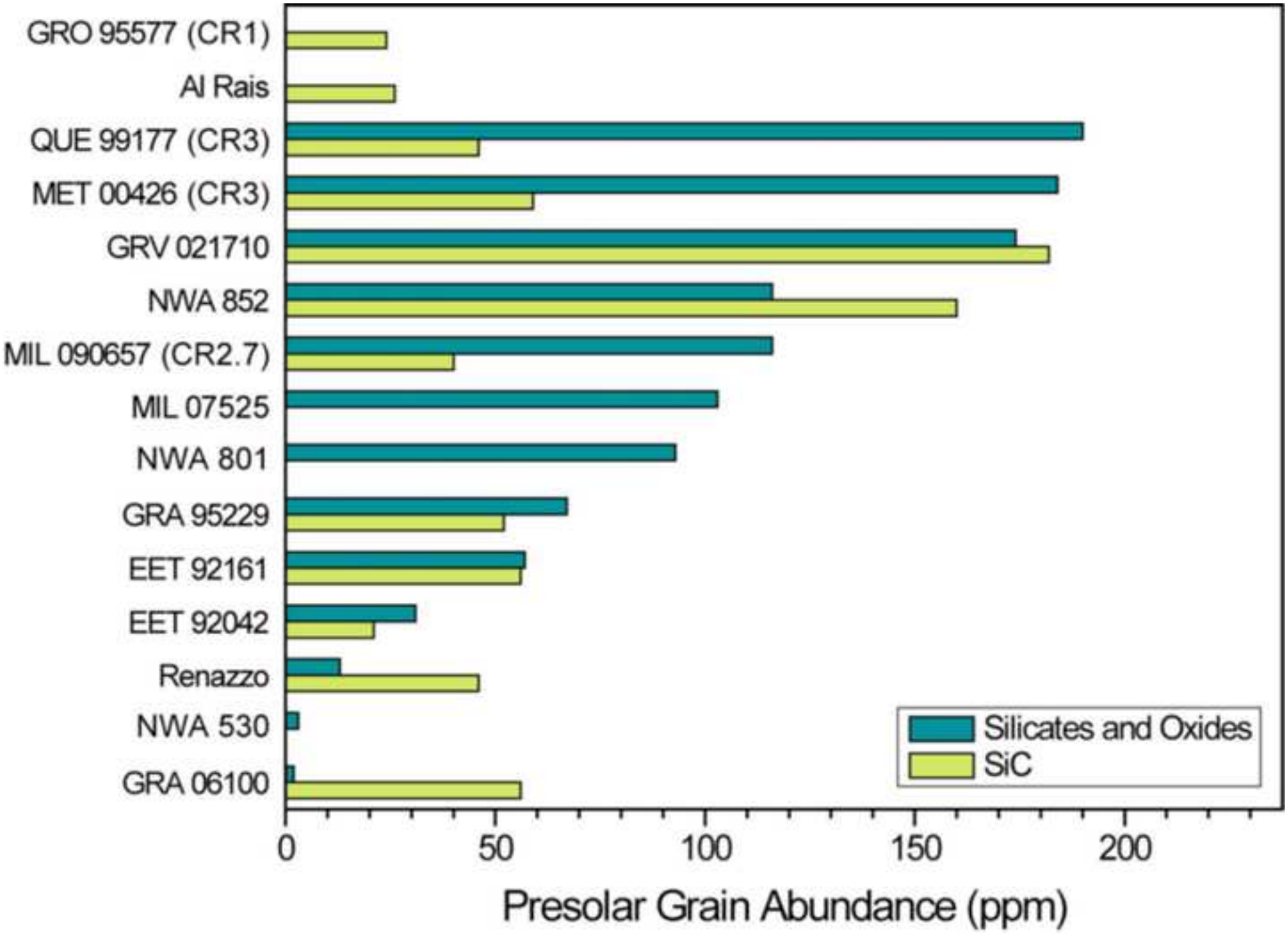

Figure 11

Click here to access/download;Figure;Figure 11 - Aqueous Alteration of CR Chondrites Diagram.jpg

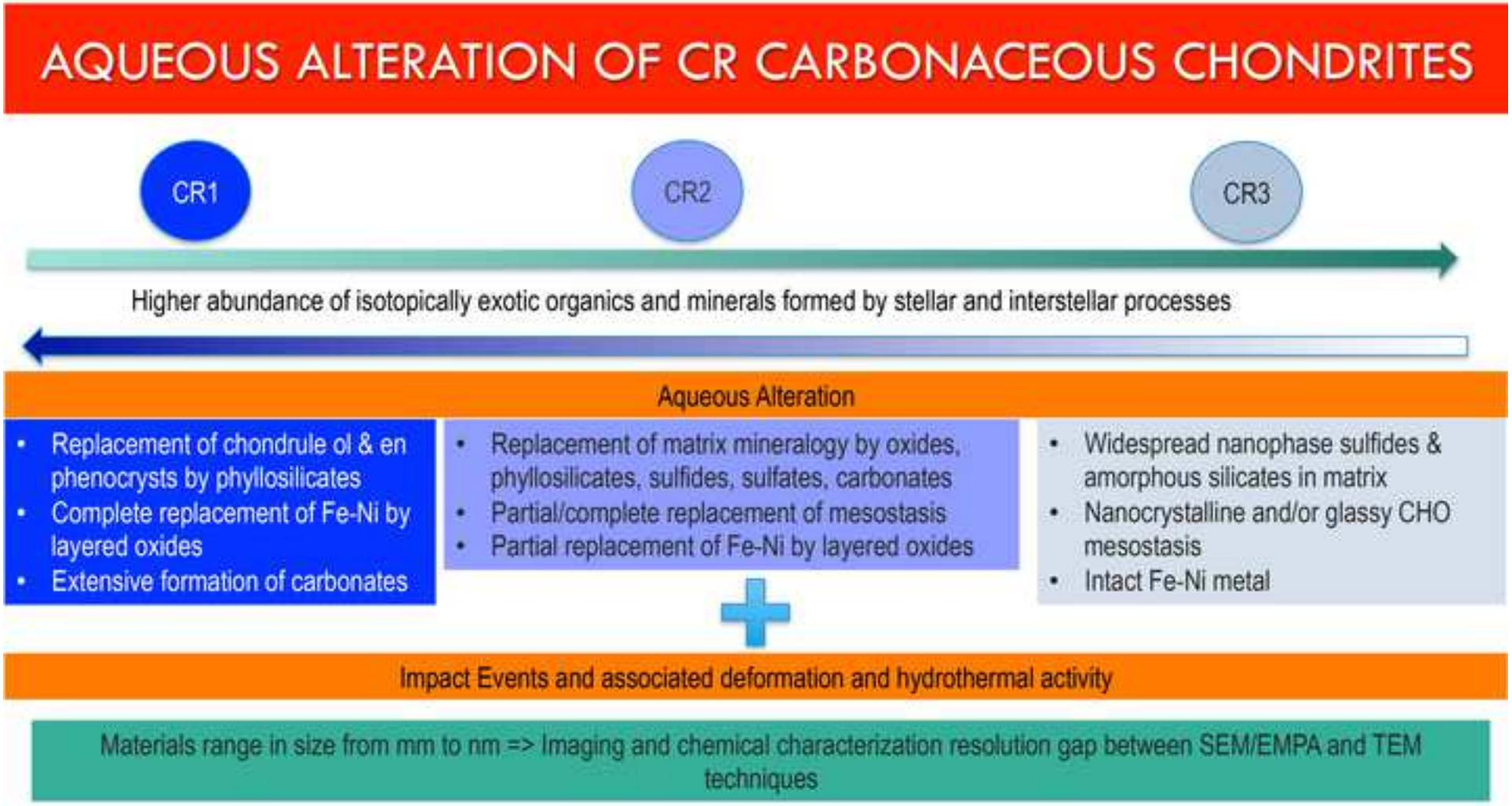

Figure 12

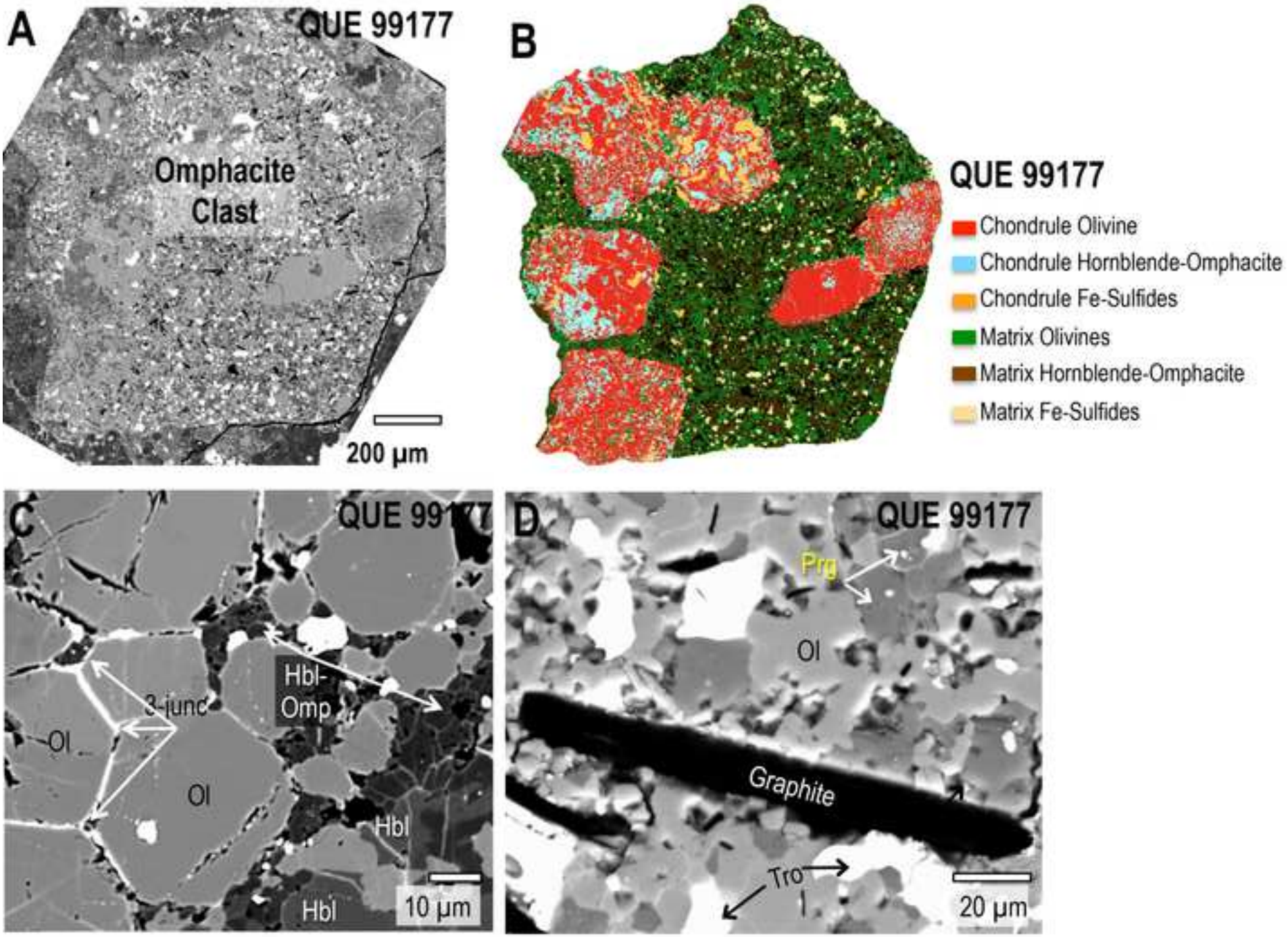

Figure 13